

## **New Zealand Community Fault Model – version 1.0**

H Seebeck	RJ Van Dissen	NJ Litchfield	PM Barnes
A Nicol	RM Langridge	DJA Barrell	P Villamor
SM Ellis	MS Rattenbury	S Bannister	MC Gerstenberger
F Ghisetti	R Sutherland	J Fraser	Nodder SD
MW Stirling	Humphrey J	Bland KJ	(further authors within)

**GNS Science Report 2021/57**  
**May 2022**

## DISCLAIMER

The Institute of Geological and Nuclear Sciences Limited (GNS Science) and its funders give no warranties of any kind concerning the accuracy, completeness, timeliness or fitness for purpose of the contents of this report. GNS Science accepts no responsibility for any actions taken based on, or reliance placed on the contents of this report and GNS Science and its funders exclude to the full extent permitted by law liability for any loss, damage or expense, direct or indirect, and however caused, whether through negligence or otherwise, resulting from any person's or organisation's use of, or reliance on, the contents of this report.

## BIBLIOGRAPHIC REFERENCE

Seebeck H<sup>1</sup>, Van Dissen RJ<sup>1</sup>, Litchfield NJ<sup>1</sup>, Barnes PM<sup>2</sup>, Nicol A<sup>3</sup>, Langridge RM<sup>1</sup>, Barrell DJA<sup>1</sup>, Villamor P<sup>1</sup>, Ellis SM<sup>1</sup>, Rattenbury MS<sup>1</sup>, Bannister S<sup>1</sup>, Gerstenberger MC<sup>1</sup>, Ghisetti F<sup>4</sup>, Sutherland R<sup>5</sup>, Fraser J<sup>6</sup>, Nodder SD<sup>2</sup>, Stirling MW<sup>7</sup>, Humphrey J<sup>3</sup>, Bland KJ<sup>1</sup>, Howell A<sup>1</sup>, Mountjoy JJ<sup>2</sup>, Moon V<sup>8</sup>, Stahl T<sup>3</sup>, Spinardi F<sup>8</sup>, Townsend DB<sup>1</sup>, Clark KJ<sup>1</sup>, Hamling IJ<sup>1</sup>, Cox SC<sup>1</sup>, de Lange W<sup>8</sup>, Wopereis P<sup>9</sup>, Johnston M<sup>1</sup>, Morgenstern R<sup>1</sup>, Coffey GL<sup>1</sup>, Eccles JD<sup>10</sup>, Little TA<sup>5</sup>, Fry B<sup>1</sup>, Griffin J<sup>11</sup>, Townend J<sup>5</sup>, Mortimer N<sup>1</sup>, Alcaraz SA<sup>1</sup>, Massiot C<sup>1</sup>, Rowland J<sup>10</sup>, Muirhead J<sup>10</sup>, Upton P<sup>1</sup>, Hirschberg H<sup>5</sup>, Lee JM<sup>1</sup>. 2022. New Zealand Community Fault Model – version 1.0. Lower Hutt (NZ): GNS Science. 97 p. (GNS Science report; 2021/57). doi:10.21420/GA7S-BS61.

<sup>1</sup> GNS Science, PO Box 30368, Lower Hutt 5040, New Zealand

<sup>2</sup> National Institute of Water & Atmospheric Research (NIWA), Private Bag 14901, Wellington 6241, New Zealand

<sup>3</sup> University of Canterbury, Private Bag 4800, Christchurch 8140, New Zealand

<sup>4</sup> TerraGeoLogica, 60 Brabant Drive, Ruby Bay, Mapua 7005, New Zealand

<sup>5</sup> Victoria University of Wellington, PO Box 600, Wellington 6140, New Zealand

<sup>6</sup> Golder, PO Box 2281, Christchurch 8140, New Zealand

<sup>7</sup> University of Otago, PO Box 56, Dunedin 9054, New Zealand

<sup>8</sup> University of Waikato, Private Bag 3105, Hamilton 3240, New Zealand

<sup>9</sup> Beca, PO Box 242, Nelson 7040, New Zealand

<sup>10</sup> University of Auckland, Private Bag 92019, Auckland 1142, New Zealand

<sup>11</sup> Geoscience Australia, GPO Box 378, Canberra ACT 2601, Australia

## CONTENTS

<b>ABSTRACT</b> .....	<b>IV</b>
<b>KEYWORDS</b> .....	<b>IV</b>
<b>1.0 INTRODUCTION</b> .....	<b>1</b>
<b>2.0 MODEL DESIGN</b> .....	<b>3</b>
<b>3.0 FAULT DEFINITIONS AND PARAMETERS</b> .....	<b>6</b>
3.1 Active Fault Zones .....	6
3.1.1 Definition of Active Fault.....	6
3.1.2 Definition of Active Fault Zone .....	6
3.2 Capable Fault Zones .....	6
3.3 Fault Zone Parameters .....	7
3.3.1 Object ID Number (OBJECTID) .....	7
3.3.2 Fault ID Number (Fault_ID).....	7
3.3.3 Fault Name (Name).....	7
3.3.4 Name Status (Name_stat)* .....	7
3.3.5 Lineage* .....	8
3.3.6 Fault Status (Fault_stat)* .....	10
3.3.7 Neotectonic Domain (DomainName, Domain_No) .....	12
3.3.8 Dip (Dip_pref, Dip_minus, Dip_plus).....	17
3.3.9 Dip Direction (Dip_dir) .....	17
3.3.10 Sense of Movement (Dom_sense, Sub_sense).....	17
3.3.11 Rake .....	19
3.3.12 Slip Rate (SR_pref, SR_min, SR_max) .....	20
3.3.13 Slip Rate Timeframe (SRT)*.....	21
3.3.14 Down-Dip Depth (Depth_D90, Depth_Dfc) .....	22
3.3.15 Up-Dip Depth (UpdDth)* .....	26
3.3.16 Quality Code (QualCode) .....	26
3.3.17 References .....	26
3.3.18 Comments .....	26
3.4 Parameter Uncertainties .....	27
<b>4.0 3D MODEL CONSTRUCTION</b> .....	<b>28</b>
4.1 Fault Representations.....	28
4.2 Fault Segment Linkage.....	30
4.2.1 Scenario 1 .....	31
4.2.2 Scenario 2 .....	31
4.2.3 Scenario 3 .....	31
4.2.4 Examples of Fault Segment Linkage .....	32
4.3 Fault Intersections .....	33
<b>5.0 MODEL COMPARISON</b> .....	<b>38</b>
<b>6.0 TOWARD NZ CFM V2.0</b> .....	<b>44</b>
<b>7.0 ACKNOWLEDGMENTS</b> .....	<b>45</b>
<b>8.0 REFERENCES</b> .....	<b>45</b>

## FIGURES

Figure 1.1	Comparison of New Zealand active fault models .....	2
Figure 2.1	Schedule and extent of the November 2020 New Zealand Community Fault Model workshops..	3
Figure 2.2	Comparison of NZ CFM v1.0 with the New Zealand Active Faults Database.....	5
Figure 3.1	Fault zones in NZ CFM v1.0 colour-coded by Lineage.....	9
Figure 3.2	Fault zones in NZ CFM v1.0 colour-coded by Fault Status. ....	11
Figure 3.3	Neotectonic domains of New Zealand as defined in this report and used in NZ CFM v1.0 .....	13
Figure 3.4	Fault zones in NZ CFM v1.0 colour-coded by dominant sense of movement.....	18
Figure 3.5	Fault zones in NZ CFM v1.0 colour-coded by Slip Rate (preferred).....	21
Figure 3.6	New Zealand Fault-Rupture Depth Model v1.0 .....	23
Figure 3.7	Maximum fault-rupture depth method for NZ CFM v1.0 fault zones.....	24
Figure 3.8	Maximum fault-rupture depth for NZ CFM v1.0 fault zones.....	25
Figure 4.1	Illustration of fault zone segment linkage rules.....	32
Figure 4.2	Example of along-strike fault segmentation.....	33
Figure 4.3	Illustration of intersection relationships of 3D modelled faults .....	34
Figure 4.4	Faults with along-strike and or down-dip intersection geometries .....	36
Figure 4.5	Illustration of oblique-fault intersection rules.....	37
Figure 5.1	NZ CFM v1.0 fault strike azimuth by neotectonic domain .....	40
Figure 5.2	Crustal profile location map .....	41
Figure 5.3	Southern North Island crustal profile .....	42
Figure 5.4	Northeastern South Island crustal profile.....	43

## TABLES

Table 3.1	Neotectonic domain types, names and numbers used in NZ CFM v1.0.....	15
Table 3.2	Rake categories for new and modified fault zones in NZ CFM v1.0.....	19

## APPENDICES

<b>APPENDIX 1</b>	<b>NZ CFM V1.0.....</b>	<b>79</b>
<b>APPENDIX 2</b>	<b>GNS SCIENCE DATASET CATALOGUE METADATA RECORD .....</b>	<b>90</b>
<b>APPENDIX 3</b>	<b>PUYSEGUR.....</b>	<b>93</b>

## APPENDIX FIGURES

Figure A1.1	Map extent showing regions of the New Zealand Community Fault Model .....	79
Figure A1.2	Western North Island.....	80
Figure A1.3	Bay of Plenty .....	81
Figure A1.4	Central North Island .....	82
Figure A1.5	Northern Hikurangi and southern Kermadec margins .....	83
Figure A1.6	Central Hikurangi margin.....	84
Figure A1.7	Southern North Island and northeastern South Island.....	85

Figure A1.8	Western and central South Island .....	86
Figure A1.9	Southeastern South Island .....	87
Figure A1.10	Fiordland margin and southern South Island.....	88
Figure A1.11	Puysegur margin .....	89
Figure A3.1	Puysegur Subduction Margin .....	94
Figure A3.2	Northern Fiordland margin cross-section.....	95
Figure A3.3	Southern Fiordland margin cross-section.....	96
Figure A3.4	Alternative Puysegur–Fiordland subduction interface surface.....	97

## ATTACHMENTS

NZ_CFM_v1_0.xlsx .....	Attached to PDF
------------------------	-----------------

## ABSTRACT

Fault models developed by the scientific community aim to provide a consistent and broadly agreed-upon representation of faults in a region for such societally important endeavours as seismic hazard assessment (e.g. national seismic hazard models), strong ground-motion predictions and physics-based fault systems modelling.

The New Zealand Community Fault Model (NZ CFM) is a two- and three-dimensional representation of fault zones associated with the New Zealand plate boundary for which Quaternary activity has been established (or deemed probable) and are, in the main, considered capable of producing moderate- to large-magnitude earthquakes. The NZ CFM builds on the Active Fault Model of New Zealand (Litchfield et al. 2013, 2014), updates that model through science community engagement and input and extends the updated faults from the surface to seismogenic depths. A nominal compilation scale of 1:500,000–1:1,000,000 was chosen to provide representative surface fault traces consistent with finer-scale representations, such as the New Zealand Active Faults Database. Faults in the model are defined based on criteria that include surface geology, seismicity, seismic reflection profiles, bores and geologic cross-sections.

The first edition of the NZ CFM (v1.0) is populated from 36.0 to 49.8° S and from 163.5° E to 179.0° W and comprises two principal datasets. The first dataset is a two-dimensional (2D) map representation of active (or potentially active) fault zone traces. This 2D fault zone representation contains information on the geometric and kinematic attributes of each fault zone or fault zone segment as expressed on the ground surface. Generalised estimates of geometric (dip and dip direction), kinematic (sense of movement, rake and net slip rate) and slip rate timeframe parameters have been provided for most fault zones, along with assigned uncertainties. In addition, a 'Quality Code' provides an indication of the quantity and type of data available for each fault zone, weighted toward the quality of the slip-rate data. The second dataset is a three-dimensional (3D) triangulated mesh surface representation of the fault zones in the model. However, there are some important differences between the 2D and 3D fault zone models; in particular, major fault zone intersections and subduction plate interfaces.

NZ CFM v1.0 is publicly available from the GNS website. The NZ CFM v1.0 data package includes ArcGIS and QGIS projects and shapefiles of the 2D fault zone model, a MOVE project and triangulated surfaces for the 3D fault zone model, tabulated fault zone parameters and documentation.

## KEYWORDS

Active fault, capable fault, Community Fault Model, New Zealand, sense of movement, dip, dip direction, rake, slip rate, kinematics, plate boundary, tectonic domain

## 1.0 INTRODUCTION

Many of the fundamental aspects of earthquake science, including earthquake nucleation, dynamic rupture, seismic wave propagation and stress triggering, are influenced by geometric properties of the fault zones (e.g. Plesch et al. 2020). The location and geometry of a fault is a key determinant in seismic hazard assessment, whereby the location and magnitudes of past and likely future earthquakes are estimated using geologic, seismologic or geodetic observations (e.g. Stirling et al. [2012] or Field et al. [2014]).

Community Fault Models (CFMs) developed by the scientific community aim to provide consistent and broadly agreed-upon representations of fault structures in a specified region. CFMs are built to provide the basis for further applications that require, for example, a better understanding of the geometric and kinematic characteristics of seismogenic faults in a region. These applications typically relate to studies of active faulting, earthquake phenomena and the improvement of seismic hazard assessment. The most advanced CFM, now into its second decade, is the Southern California Earthquake Center (SCEC) Community Fault Model<sup>1</sup> that comprises a three-dimensional (3D) representation of active faults in southern California and adjacent offshore basins (Plesch et al. 2007, 2016; Nicholson et al. 2017). While there are similar types of earthquake source model used throughout the world (e.g. Japan [Fujiwara et al. 2009] or Taiwan [Chan et al. 2020]), few are explicitly community-driven.

GNS Science has long maintained products such as the active fault earthquake source model for the National Seismic Hazard Model (NSHM; Figure 1.1; e.g. Stirling et al. 2012); New Zealand Active Faults Database (Langridge et al. 2016), Active Fault Model of New Zealand (Figure 1.1; Litchfield et al. 2013, 2014) and national 1:1,000,000- and 1:250,000-scale digital geological maps (e.g. Rattenbury and Isaac 2012; Edbrooke et al. 2014; Heron 2020), which provide a significant amount of basic fault information across onshore and offshore New Zealand. To date, however, a 3D model of active faults that represents New Zealand's collective scientific knowledge that can be easily used or adapted for multiple scientific and practical uses has not been available.

The New Zealand Community Fault Model (NZ CFM) is a multi-organisational project led by GNS Science. The multi-institutional and cross-disciplinary nature of the community input is reflected by the authorship of the report. The NZ CFM builds on the Active Fault Model of New Zealand (Litchfield et al. 2013, 2014), updates that model through scientific community engagement and input and extends the updated faults from the surface to seismogenic depths. The NZ CFM project has developed two- and three-dimensional representations of important fault zones (primarily, but not exclusively, active fault zones) across New Zealand to support downstream applications such as seismic hazard and synthetic seismicity modelling. These two complementary datasets comprise NZ CFM v1.0 (Figure 1.1). These representations consist of fault zone features defined geometrically based on various information sources, including surface expression (traces and fault-related folds), seismicity, seismic reflection profiles, wells and geological maps and cross-sections. Each represented fault zone is described in terms of kinematically relevant properties such as dip, rake and slip rate.

This report outlines the compilation process of NZ CFM v1.0 and explains the geometric and kinematic parameters for the current and future compilations of the model, the fault intersection and linkage rules employed to smoothly 'mesh' the 3D faults at depth and along strike and the software used to build the model in 3D.

---

1 <https://www.scec.org/research/cfm>

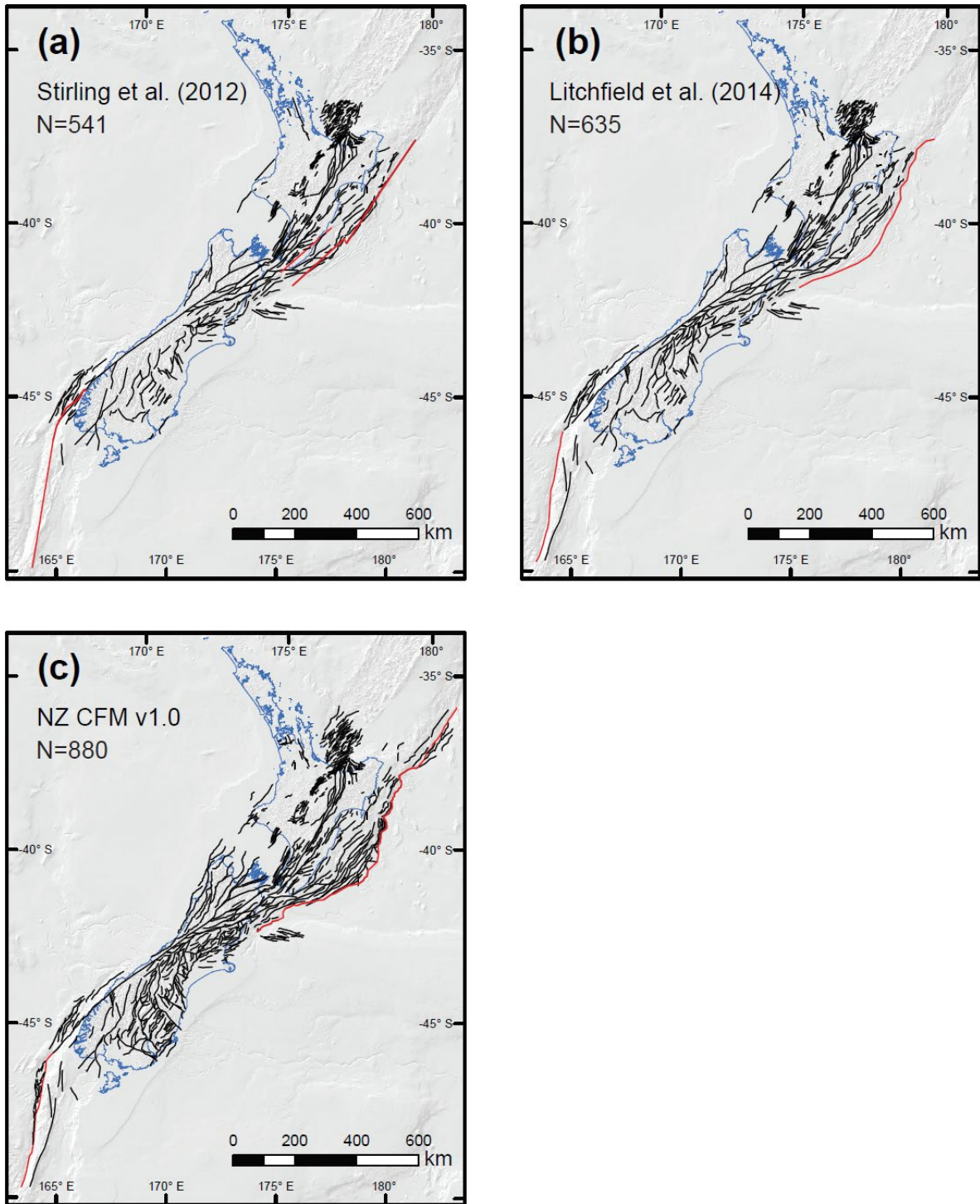


Figure 1.1 Comparison of New Zealand active fault models. Comparison of the active fault representations in the (a) active fault earthquake source model of the 2010 version of the NSHM (Stirling et al. 2012), (b) Active Fault Model of New Zealand (Litchfield et al. 2013, 2014) and (c) NZ CFM v1.0. Fault sections in (a)–(c) are shown as black lines, with the upper edges of the subduction interfaces depicted as red lines. N = number of fault zones and fault zone segments in each model.

## 2.0 MODEL DESIGN

The first edition of the NZ CFM detailed in this report (NZ CFM v1.0) is a 3D representation of 880 fault zones associated with the New Zealand plate boundary for which Quaternary activity has been established (or deemed probable). These fault zones are considered to have the potential to generate moderate- to large-magnitude earthquakes (Figure 1.1c).

Two national-scale New-Zealand-Government-funded seismic hazard research programmes, the NSHM Programme<sup>2</sup> and the Resilience to Nature’s Challenges Earthquake and Tsunami Programme<sup>3</sup>, provided the impetus to embark on the NZ CFM project. Both of these programmes required an up-to-date, widely agreed, national-scale 3D active fault model to underpin their research. The research delivery timelines of those two programmes dictated the need for rapid compilation of NZ CFM v1.0, as described below.

The NZ CFM project held an inaugural all-day workshop hosted at GNS Science, Lower Hutt, on 27 September 2019. About 50 earthquake scientists, engineers and policy makers attended. Details of the workshop, including copies of the presentations given at the workshop, are publicly available.<sup>4</sup> Shortly after the inaugural workshop, a policies and procedures document was commissioned (Rattenbury 2020) to guide compilation and documentation of the NZ CFM and to ensure that it meets FAIR Data Principles; that is, be Findable through ISO19115-compliant metadata stored in a harvestable metadata catalogue; Accessible via a shared server identified by the metadata; Interoperable through common file formats used and wanted by the community; and Reusable, where the terms of use are fully understood and the build history and assumptions of the model are well described.

In late November 2020, eight regionally focused, half-day online review workshops were convened to discuss, debate and evaluate compilation of the NZ CFM (Figure 2.1), including individual fault parameters, intersection relationships and seismogenic potential. An initial fault model was provided to participants to review, and provide modifications for, prior to the workshop. About 40 earth scientists and engineers participated in these workshops, typically 10–20 in any one half-day session.

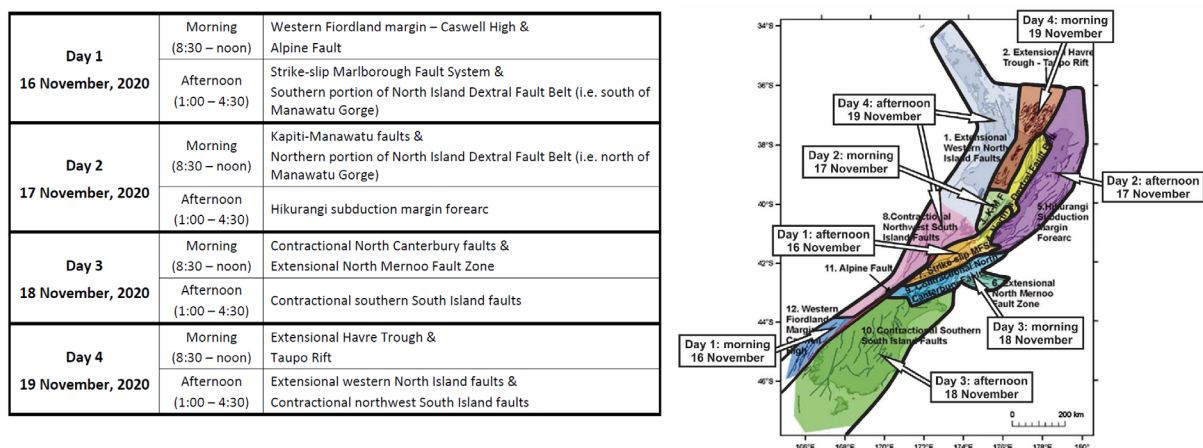


Figure 2.1 Schedule and extent of the November 2020 New Zealand Community Fault Model workshops.

2 <https://www.gns.cri.nz/Home/Our-Science/Natural-Hazards-and-Risks/Earthquakes/National-Seismic-Hazard-Model-Programme>

3 <https://resiliencechallenge.nz/scienceprogrammes/earthquake-and-tsunami/>

4 <https://www.gns.cri.nz/Home/Our-Science/Natural-Hazards-and-Risks/Earthquakes/Community-Fault-Model/CFM-workshops>

These NZ CFM workshops established the two-dimensional (2D) model inventory, building on the Active Fault Model of New Zealand (Litchfield et al. 2013, 2014; Figure 1.1) and updates to the NSHM since the 2016 Kaikōura earthquake (e.g. Goded et al. 2018a). The model contains a full spectrum of fault types, including steeply dipping strike-slip faults and moderately to steeply dipping dip-slip and oblique-slip normal and reverse faults, along with large variably dipping subduction interfaces. As the present model builds upon Litchfield et al. (2013, 2014), the reader is referred to these previous publications for background context relevant to the development and parameterisation of New Zealand fault models.

The NZ CFM is populated from 36.0 to 49.8° S and from 163.5° E to 179.0° W and comprises two principal datasets. The first dataset is a 2D map representation of active (or potentially active) faults developed in New Zealand Transverse Mercator projection (Figure 1.1c). This 2D fault representation was compiled using ArcGIS mapping software and contains information on the geometric and kinematic attributes of each fault or fault segment (see Section 3). The second dataset is a 3D representation of the fault zones developed from the geometric attributes detailed in the 2D representation. There are some important differences between the 2D and 3D fault models; in particular, major fault intersections. The construction of the 3D model and the differences with the 2D model are described in Section 4 of this report.

NZ CFM v1.0 is supplied in two digital formats: a 2D ESRI shapefile GIS format of fault zone traces with embedded fault zone parameter attributes and as a 3D GOCAD ASCII triangulated surface (t-surf) format that can be imported into many 3D modelling software products. The t-surf format does not support attributes but can be linked to an accompanying table of parameters via the unique identifier of Fault name. An excel table of fault attributes is also included.

Representative fault zones in NZ CFM v1.0 were compiled at a nominal compilation scale of 1:500,000–1:1,000,000. This scale range equates to a spatial resolution of approximately 1–2 km along individual fault zones. These fault zone representations are more detailed than those presented in Litchfield et al. (2013, 2014) and are more closely allied with detailed fault trace representations in the 1:250,000-scale (QMAP) geological map database (Rattenbury and Isaac 2012; Heron 2020) and 1:250,000-scale version of the New Zealand Active Faults Database (NZAFD; Langridge et al. 2016; Heron 2020) through the sharing of common locations (vertices) (Figure 2.2). The fault zone representations in NZ CFM v1.0, as well as those of the QMAP and NZAFD datasets, are simplified and should not be used in isolation for any purposes relating to local land-use or site-specific engineering development.

As with previous fault models (Litchfield et al. 2013, 2014), some fault zones in NZ CFM v1.0 are segmented. Segmented fault zones have continuous trace representations that incorporate along-strike changes in geometry or slip rate. Fault zone segments in NZ CFM v1.0 are defined by dip or slip-rate changes along strike relative to adjacent segments. The location of boundaries between segments is consistent with Litchfield (2013, 2014), with the exception of the Alpine Fault. In this model, the southern offshore trace of the Alpine Fault has been redefined to better honour the available data.

A tabulation of all fault zones compiled into the 2D dataset of NZ CFM v1.0 is provided in Appendix 1, along with a series of overlapping maps that show all of the faults. Metadata relating to NZ CFM v1.0 are set out in Appendix 2.

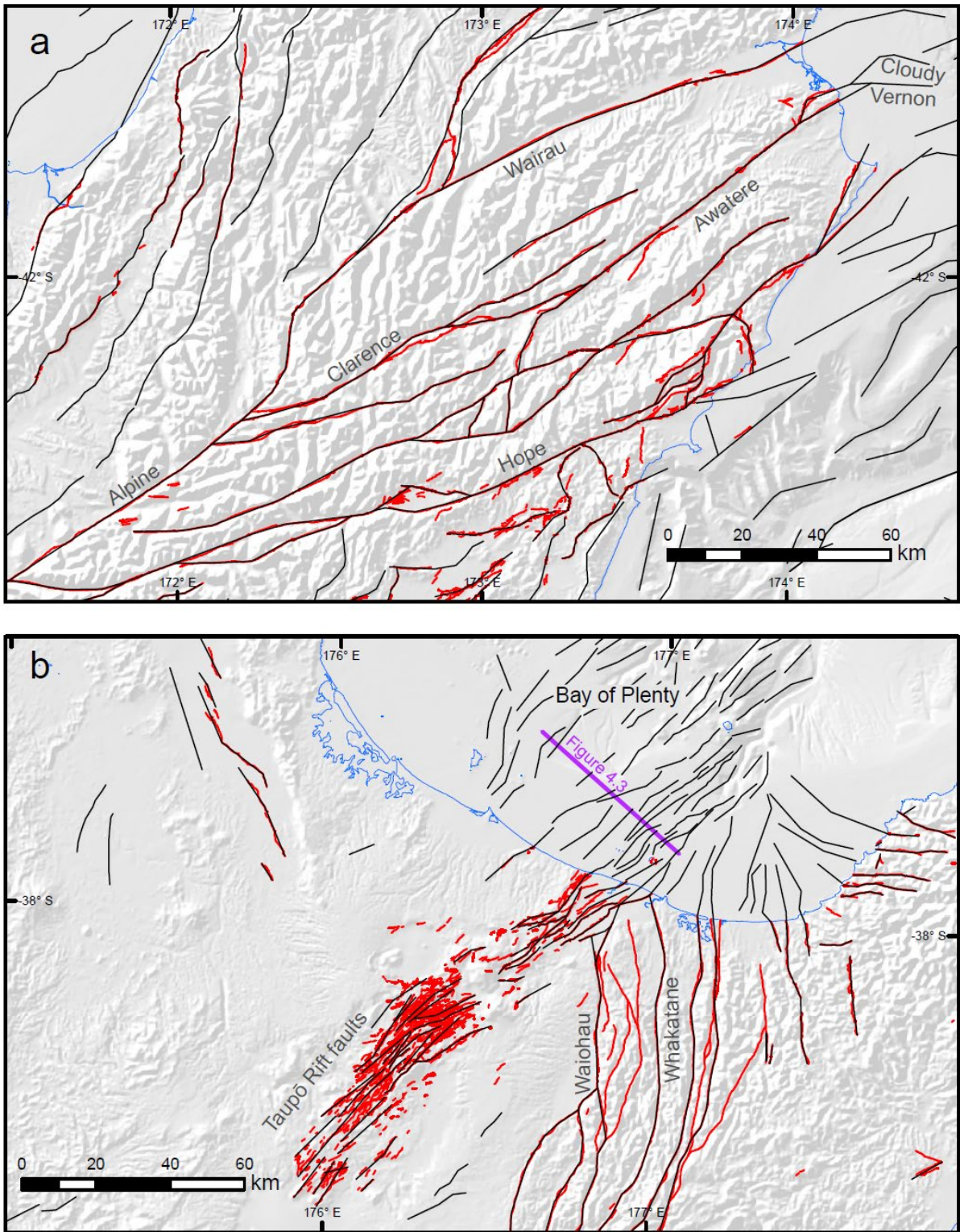


Figure 2.2 Comparison of NZ CFM v1.0 with the New Zealand Active Faults Database (NZAFD). Comparison of fault zone traces of the generalised NZ CFM v1.0 (black lines) and the more detailed NZAFD (red lines; Langridge et al. 2016) for (a) the northeastern South Island and (b) the central North Island and Bay of Plenty. The profile of Gase et al. (2019) is shown in Figure 4.3. The blue line marks the coastline and lower reaches of major rivers.

## 3.0 FAULT DEFINITIONS AND PARAMETERS

### 3.1 Active Fault Zones

#### 3.1.1 Definition of Active Fault

A fault is classified as active if there is evidence for ground-surface displacement/deformation in the past 125,000 years (i.e. since the peak sea-level highstand of the last interglacial period, marine isotope stage 5e; Langridge et al. 2016). A different age criterion is used for the Taupō Rift, which is evolving so rapidly (especially narrowing its locus of activity) that faults there are classified as active if there is evidence for displacement/deformation in the past 25,000 years (Vandergoes et al. 2013; Villamor et al. 2017).

#### 3.1.2 Definition of Active Fault Zone

We follow the definition of Litchfield et al. (2014) in describing this compilation as a model rather than a database due to the highly generalised representation of fault traces with a single set of fault characterisation parameters. Each fault represented in the model is therefore referred to as a 'fault zone', emphasising the distinction between the simplified fault zones in this model and the more detailed active fault traces and parameters of the source data. In this sense, an active fault zone in NZ CFM v1.0 comprises a series of one or more active faults represented by a single trace (i.e. surface position or projected surface position) compiled at a nominal scale of 1:500,000–1:1,000,000. As such, fault zones in this model are often a simplification of multiple fault traces in databases such as the New Zealand Active Faults Database (Langridge et al. 2016<sup>5</sup>) or on published maps such as the QMAP 1:250,000 series (Rattenbury and Isaac 2012) and their combined GIS dataset equivalent (Heron 2020). Active fault zones are identified with a Fault Status of A-LS (Section 3.3.6).

Generally, each linear map trace that represents a fault zone in NZ CFM v1.0 approximates a previously named and published active fault. In such circumstances, the published name is used. Other fault zones are identified here for the first time or are groupings of one or more published active faults; these have given informal names. Each delineated fault zone has a unique identification number and name (refer to Appendix 1 for details).

### 3.2 Capable Fault Zones

About half of all shallow large earthquakes (<25 km,  $M_w \geq 7.0$ ) in New Zealand since c. 1850 occurred on faults that, based on today's state of knowledge of active-fault location, would not have been identified as active prior to the earthquake (Nicol et al. 2016). This leads to the conclusion that, just because a fault is not yet proven as active, this does not necessarily mean that it is not capable of producing large earthquakes. As one of the primary goals of NZ CFM v1.0 is to facilitate seismic hazard applications, we consider it prudent to include fault zones that are considered potentially capable of producing large earthquakes ( $>M_w 6$ ), even if they have not been proven to be active. These are classified in NZ CFM v1.0 as 'capable fault zones' with a Fault Status denoted as N-PS (see Section 3.3.6).

The criteria for inclusion of capable fault zones in NZ CFM v1.0 has not yet been formally standardised across the New Zealand region, nor has an attempt been made to systematically identify all faults that could be interpreted as capable. Rather, inclusion has been based on

---

5 <http://data.gns.cri.nz/af/>

a case-by-case assessment, evaluating such factors as: (i) geometric and kinematic similarity of the fault zone to nearby zones that are known or inferred to be active; (ii) distinctness of the geomorphic expression of the fault zone, including the topography it has produced or influenced; and (iii) proximity of the fault zone to historical – though commonly poorly located – moderate to large earthquakes.

As with active faults, a capable fault zone in NZ CFM v1.0 includes a series of one or more faults that are represented by a single trace (i.e. surface position or projected surface position) and compiled at a scale detailed in Section 3.1.2.

Generally, each mapped linear trace that represents a capable fault zone approximates a previously named and published fault. In such circumstances, the published name is used. Other capable fault zones are identified here for the first time or are groupings of one or more published faults; these have been given informal names. Each capable fault zone has a unique identification number and name.

### **3.3 Fault Zone Parameters**

Fault parameters defined in NZ CFM v1.0 are: (i) Object ID, (ii) Fault ID number, (iii) Name, (iv) Name status\*, (v) Lineage\*, (vi) Fault status\*, (vii) Neotectonic domain, (viii) Dip, (ix) Dip-direction, (x) Sense of movement, (xi) Rake, (xii) Net slip rate, (xiii) Slip-rate timeframe\*, (xiv) Down-dip depth\*, (xv) Up-dip depth\*, (xvi) Quality Code, (xvii) References and (xviii) Comments. These parameters are defined below and uncertainties in parameters are discussed in Section 3.4. Those denoted by an ‘\*’ are new parameters relative to Litchfield et al. (2013, 2014). Parameter definitions carried through from Litchfield et al. (2013, 2014) remain largely unchanged, with the exception of Rake, which has been changed to the Aki and Richards (2002) convention. In the subsection headings below, the code name for the parameter in the ArcGIS attribute field is given in parentheses. The fault zone parameters for each fault zone in NZ CFM v1.0 can be found in the attached Appendix 1 table.

#### **3.3.1 Object ID Number (OBJECTID)**

This is an automatically generated ArcGIS field.

#### **3.3.2 Fault ID Number (Fault\_ID)**

Each fault or fault segment in NZ CFM v1.0 has been assigned a unique fault identification number, shown in Figures A1.2–A1.11.

#### **3.3.3 Fault Name (Name)**

Each fault or fault segment in NZ CFM v1.0 has been assigned a unique name based on its formal published name, a variant on that name or an informal name based on representative geographic feature.

#### **3.3.4 Name Status (Name\_stat)\***

- Published: Name of fault zone and its general location, as approximated by the relevant NZ CFM v1.0 linework; has appeared previously in publicly available reference documents (e.g. scientific papers, reports, maps).

- Informal: Name of fault zone and/or its general location, as approximated by the relevant NZ CFM v1.0 linework; has not appeared previously in publicly available reference documents.

### 3.3.5 Lineage\*

The active fault model of Litchfield et al. (2013, 2014) is the main starting point of NZ CFM v1.0. The lineage term attempts to track the relation between specific fault zones in the former and those now in the latter.

- Unmodified: The fault zone in NZ CFM v1.0 is unmodified (or with minor modifications) from that represented in Litchfield et al. (2013, 2014). Minor modifications include small adjustments to the mapped fault zone position of Litchfield et al. (2013, 2014) to accord better with the representation in NZAFD or small changes in slip rate resulting from, for example, the adoption of a larger rake uncertainty range (see Section 3.3.1).
- Modified: This denotes that significant changes have been made to the geometric and/or kinematic characterisation of a fault zone represented in Litchfield et al. (2013, 2014). This also includes cases where a new (or different) name has been given to a fault zone already included in Litchfield et al. (2013, 2014).
- New: A new fault zone not previously represented in Litchfield et al. (2013, 2014).

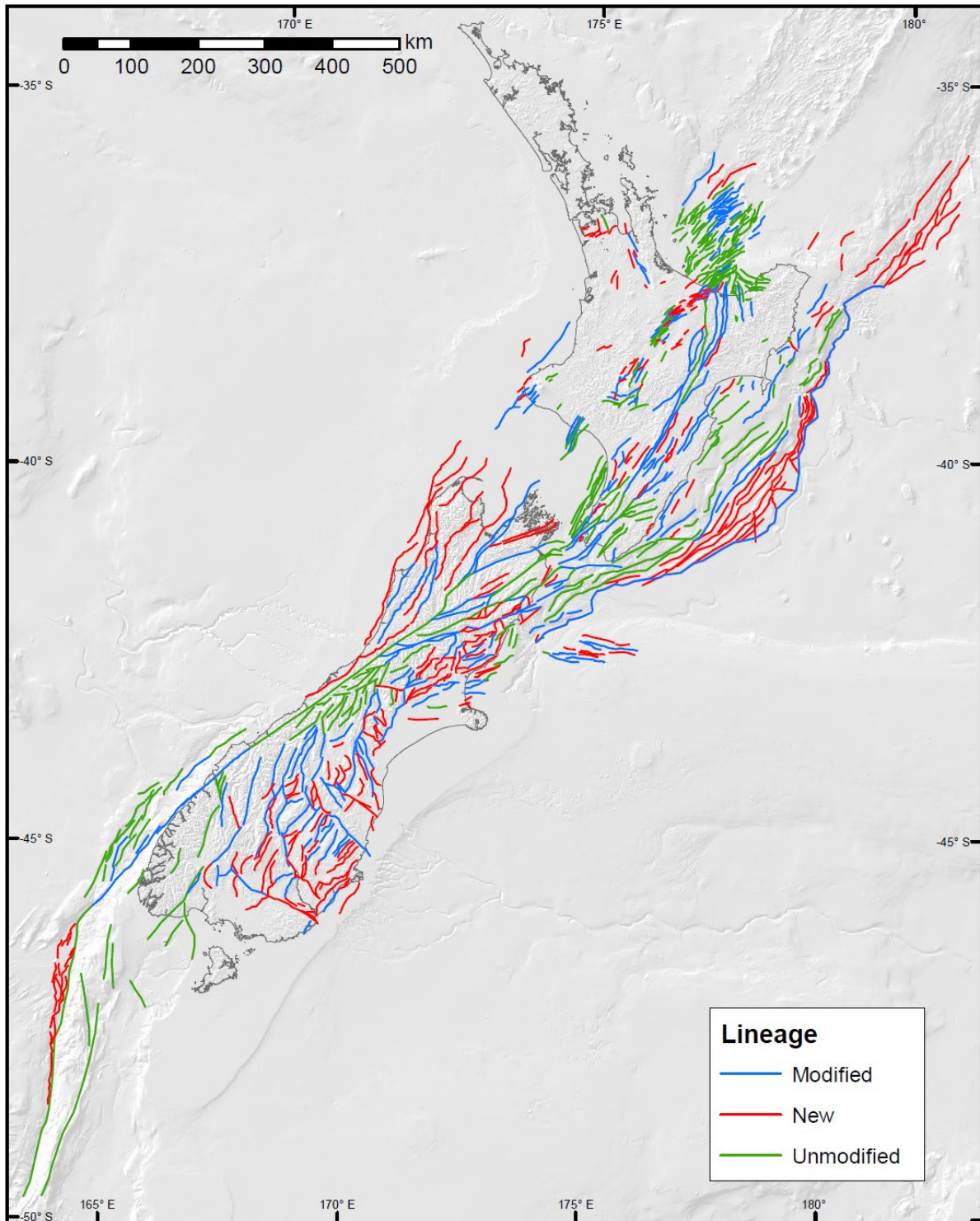


Figure 3.1 Fault zones in NZ CFM v1.0 colour-coded by Lineage.

### 3.3.6 Fault Status (Fault\_stat)\*

Using the categorisation listed below (A-LS, A-US, N-PS), fault zones are identified as either active or capable (Figure 3.2; see Sections 3.1 and 3.2, respectively), and, for active fault zones, Fault Status is used to differentiate those that are considered seismogenic from those that are considered not.

- **A-LS: Active and likely to be seismogenic.**  
The majority of NZ CFM v1.0 fault zones are in this category.
- **A-US: Active but unlikely to be seismogenic.**  
Examples include offshore fault zones near the eastern edge of the Hikurangi Subduction Margin that almost certainly have moved within the last 125,000 years but are shallow, propagating through unconsolidated strata, and thus unlikely to generate large earthquakes. In addition, a few fault zones in the eastern South Island are considered too short for independent rupture but are rather interpreted as splays off nearby longer faults with a shared rupture history. Such fault zones may not pose an independent ground shaking hazard but may be subject to surface displacement relevant to tsunami hazard (offshore) or ground displacement hazard (on land).
- **N-PS: Not proven active but considered potentially capable of being seismogenic.**  
These are termed 'capable fault zones' (see Section 3.2). Examples of fault zones within this category include those in the central Southern Alps and some of the range-bounding reverse faults in eastern South Island and northwest Nelson that have no definitive recent activity but substantial past displacement (e.g. on million-year-plus timeframes). Other examples include many of the offshore faults in deeper water where markers of 125,000 years or younger age have yet to be identified (or are not present); therefore the faults cannot be conclusively proven as active.

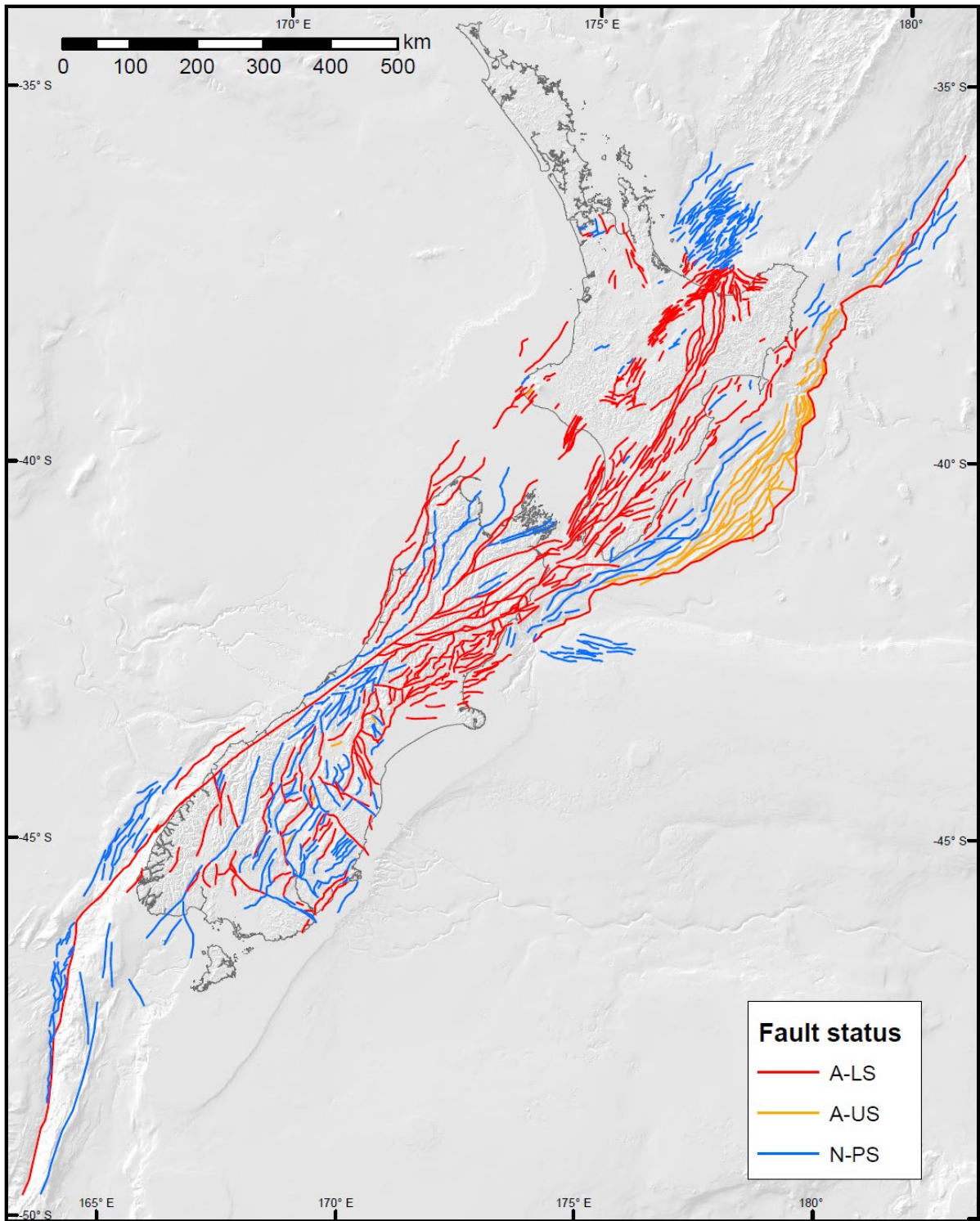


Figure 3.2 Fault zones in NZ CFM v1.0 colour-coded by Fault Status.

### 3.3.7 Neotectonic Domain (DomainName, Domain\_No)

To give context to the active faults of New Zealand, a tectonic domain map was developed by Litchfield et al. (2014) (Figure 2.1). As part of the NZ CFM project, this domain map has been updated and modified (Figure 3.3) based on commonality across an area of fault orientation, sense of movement and slip rate and, to a lesser extent, on fault distribution, bedrock geology, regional strain rate and heat flow.

Changes to the tectonic domains of Litchfield et al. (2014) include: (a) domains are now referred to as 'neotectonic domains'; (b) 16 new neotectonic domains have been added, including four peripheral platform domains, two crustal block domains and two outer-rise extensional domains; and (c) several domains of Litchfield et al. (2014) have been subdivided. For example, the large 'extensional western North Island fault zones' tectonic domain of Litchfield et al. (2014) has been subdivided into a southern 'western North Island' neotectonic domain and a northern 'North Waikato – South Auckland' neotectonic domain, and the large 'contractional south eastern South Island fault zones' tectonic domain has been subdivided into several domains, including the Southern Alps, Central Canterbury, Otago and Southern South Island neotectonic domains. These and other changes are outlined in more detail in Table 3.1, along with a listing of NZ CFM v1.0 neotectonic domain names (DomainName), numbers (Domain\_No) and types. Figure 3.3 shows neotectonics domains coloured by Domain Type that are defined by the dominant style of fault movement defined in Table 3.1.

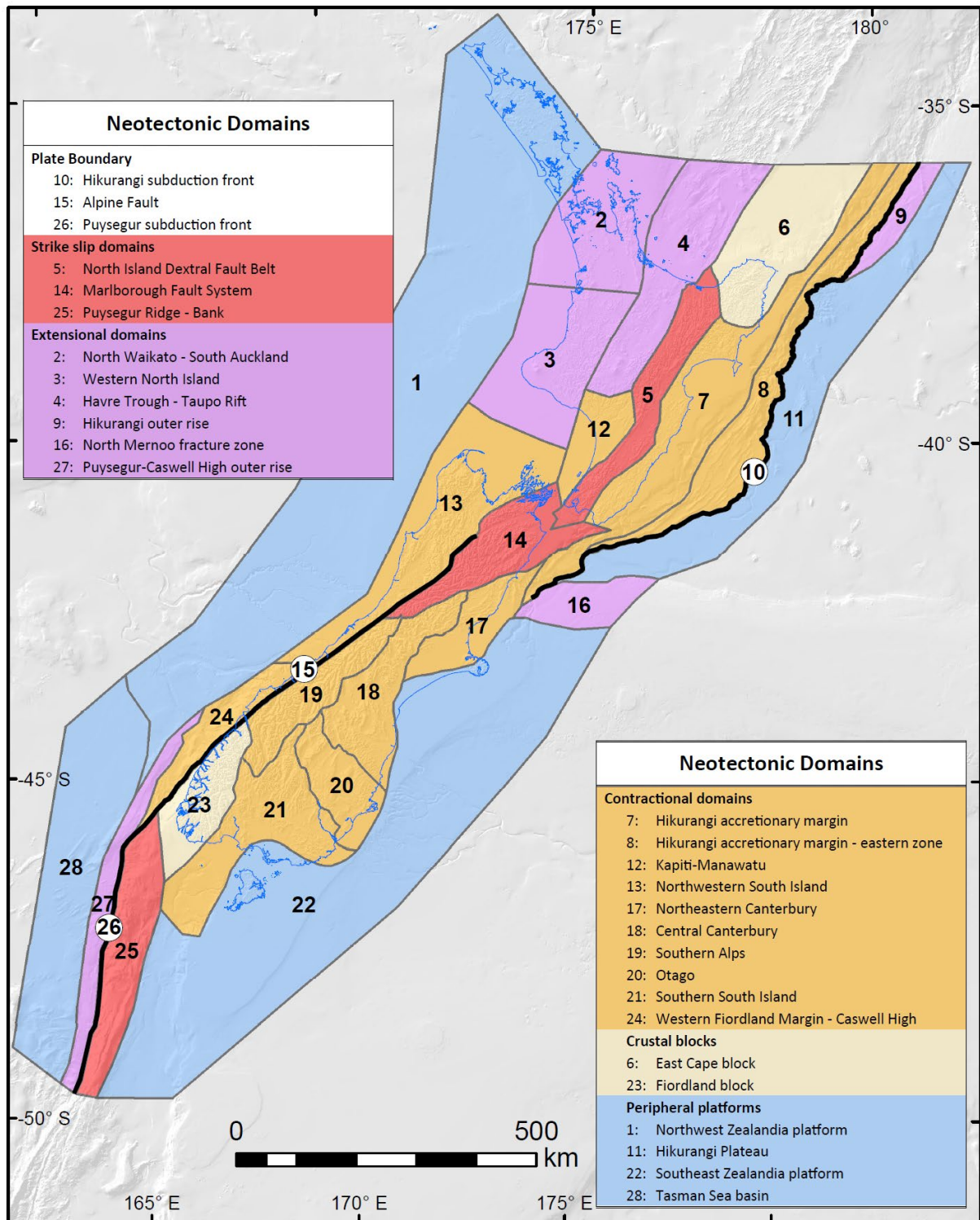


Figure 3.3 Neotectonic domains of New Zealand as defined in this report and used in NZ CFM v1.0. See Table 3.1 for further detail.

This page left intentionally blank.

Table 3.1 Neotectonic domain types, names and numbers used in NZ CFM v1.0. See Figure 3.3 for location of domains. Also listed are predominant styles of neotectonic fault movement within each domain and relation to tectonic domains of Litchfield et al. (2014). Colours shown in Domain Type relate to those in Figure 3.3.

Domain Type	Domain Name	Domain Number	Neotectonic Character	Style of Neotectonic Fault Movement	Relation to Tectonic Domains of Litchfield et al. (2014)
Plate Boundary	Hikurangi subduction front	10	Contractional	Predominantly reverse dip-slip	Hikurangi subduction thrust domain
	Alpine Fault	15	Transpressive	Predominantly dextral strike-slip, subordinate reverse dip-slip	Alpine Fault domain
	Puysegur subduction front	26	Contractional	Predominantly reverse dip-slip	Puysegur subduction thrust domain
Strike-Slip	Marlborough Fault System	14	Strike-slip	Predominantly dextral strike-slip, subordinate reverse dip-slip	Strike-slip Marlborough Fault System domain
	Puysegur Ridge – Bank	25	Strike-slip	Predominantly dextral strike-slip	Puysegur Ridge – Bank strike-slip fault zones domain
	North Island Dextral Fault Belt	5	Strike-slip	Predominantly dextral strike-slip, subordinate reverse dip-slip	North Island Dextral Fault Belt domain of Litchfield et al. (2014)
Contractional	Southern Alps	19	Contractional	Predominantly reverse dip-slip	New: Formerly the northwestern portion of the contractional southeastern South Island fault zones domain and the western-most portion of the contractional North Canterbury fault zones domain
	Hikurangi accretionary margin	7	Contractional	Predominantly reverse dip-slip, possible subordinate dextral strike-slip	Hikurangi subduction margin forearc domain of Litchfield et al. (2014)
	Hikurangi accretionary margin – eastern zone	8	Contractional	Predominantly reverse dip-slip	New
	Western Fiordland Margin – Caswell High	24	Contractional	Predominantly reverse dip-slip, possible subordinate dextral strike-slip	Western Fiordland Margin – Caswell High fault zones domain
	Kāpiti–Manawatu	12	Contractional	Predominantly reverse dip-slip, possible subordinate dextral strike-slip	Contractional Kāpiti–Manawatu fault zones domain
	Northwestern South Island	13	Contractional	Predominantly reverse dip-slip	Contractional northwestern South Island fault zones domain and northern portion of western Fiordland Margin – Caswell High fault zones domain
	Northeastern Canterbury	17	Contractional	Predominantly reverse dip-slip, subordinate dextral strike-slip	New: Formerly the eastern portion of the contractional North Canterbury fault zones domain and the northeastern-most portion of the contractional southeastern South Island fault zones domain
	Central Canterbury	18	Contractional	Predominantly reverse dip-slip, subordinate dextral strike-slip	New: Formerly the central portion of the contractional North Canterbury fault zones domain and the north-central portion of the contractional southeastern South Island fault zones domain
	Otago	20	Contractional	Predominantly reverse dip-slip	New: Formerly the east-central portion of the contractional southeastern South Island fault zones domain
Southern South Island	21	Contractional	Predominantly reverse dip-slip (assumed)	New: Formerly the southern portion of the contractional southeastern South Island fault zones domain	
Extensional	Havre Trough – Taupō Rift	4	Extensional	Predominantly normal dip-slip	Extensional Havre Trough – Taupō Rift fault zones domain
	Puysegur–Caswell High outer rise	27	Extensional	Predominantly normal dip-slip	New
	Hikurangi outer rise	9	Extensional	Predominantly normal dip-slip	New
	Western North Island	3	Extensional	Predominantly normal dip-slip	New: Formerly the central portion of the extensional western North Island fault zones domain
	North Mernoo fracture zone	16	Extensional	Predominantly normal dip-slip	Extensional North Mernoo fault zones domain
	North Waikato – South Auckland	2	Extensional	Predominantly normal dip-slip	New: Formerly the southern portion of the extensional western North Island fault zones domain
Crustal Block	East Cape block	6	Neotectonic character poorly understood	-	New: Formerly the northern portion of the Hikurangi subduction margin forearc domain
	Fiordland block	23	Neotectonic character poorly understood	-	New: Formerly the southwestern portion of the contractional southeastern South Island fault zones domain
Peripheral Platform	Northwest Zealandia platform	1	Little or no identified neotectonism	-	New: Encompasses the northwestern (i.e. Northland) portion of the extensional western North Island fault zones domain
	Southeast Zealandia platform	22	Little or no identified neotectonism	-	New: Encompasses the southern (i.e. southern-most Southland and Stewart Island) portion of the contractional southeastern South Island fault zones domain
	Hikurangi Plateau	11	Little or no identified neotectonism	-	New
	Tasman Sea basin	28	Little or no identified neotectonism	-	New

This page left intentionally blank.

### 3.3.8 Dip (Dip\_pref, Dip\_minus, Dip\_plus)

Dip is the downward inclination of a fault plane from the horizontal (0–90°). Overall dip of a fault structure is rarely known with confidence and assigned dip values are usually representative estimates based on a range of geological or geometric considerations (Litchfield et al. 2014). Estimates of average fault dip parameter in NZ CFM v1.0 are quantified in three attribute fields: the value considered most likely ('best' or 'preferred' dip – Dip\_pref); a minimum likely value (Dip\_min) and maximum likely value (Dip\_max).

All crustal faults in NZ CFM v1.0 are modelled as having a constant dip with depth, for which the 'preferred' estimate is used. The minimum and maximum values provide a general indication of dip-angle uncertainty and, in most cases, lie between 10° and 15° either side of the preferred value. In contrast, the three subduction interfaces in the 3D model of NZ CFM v1.0 (Hikurangi, Kermadec Trench and Puysegur) have dips that increase with depth (see Section 4.1).

### 3.3.9 Dip Direction (Dip\_dir)

A one- or two-letter code giving the overall geographic octant towards which a fault zone dips. An attribute of 'subvertical and variable' is used for the relatively few instances where a fault zone has a subvertical dip and its dip direction is variable.

- N = north
- S = south
- W = west
- E = east
- NW = northwest
- NE = northeast
- SW = southwest
- SE = southeast.

### 3.3.10 Sense of Movement (Dom\_sense, Sub\_sense)

Two attribute fields quantify the dominant and, where applicable, subordinate sense (type) of relative movement (slip or displacement) on the fault plane. The sense is generally restricted to normal, reverse, sinistral (left lateral) or dextral (right lateral), although a combination of a dip-slip and strike-slip sense may apply when they have a similar contribution to oblique slip, e.g. 'dextral and reverse'. In many cases, the subordinate sense (if any) is not known with confidence and has been inferred based on fault strike in relation to consideration of regional stress directions. For a small number of faults with strike-slip movement, the sense is not known and is given simply as strike-slip.

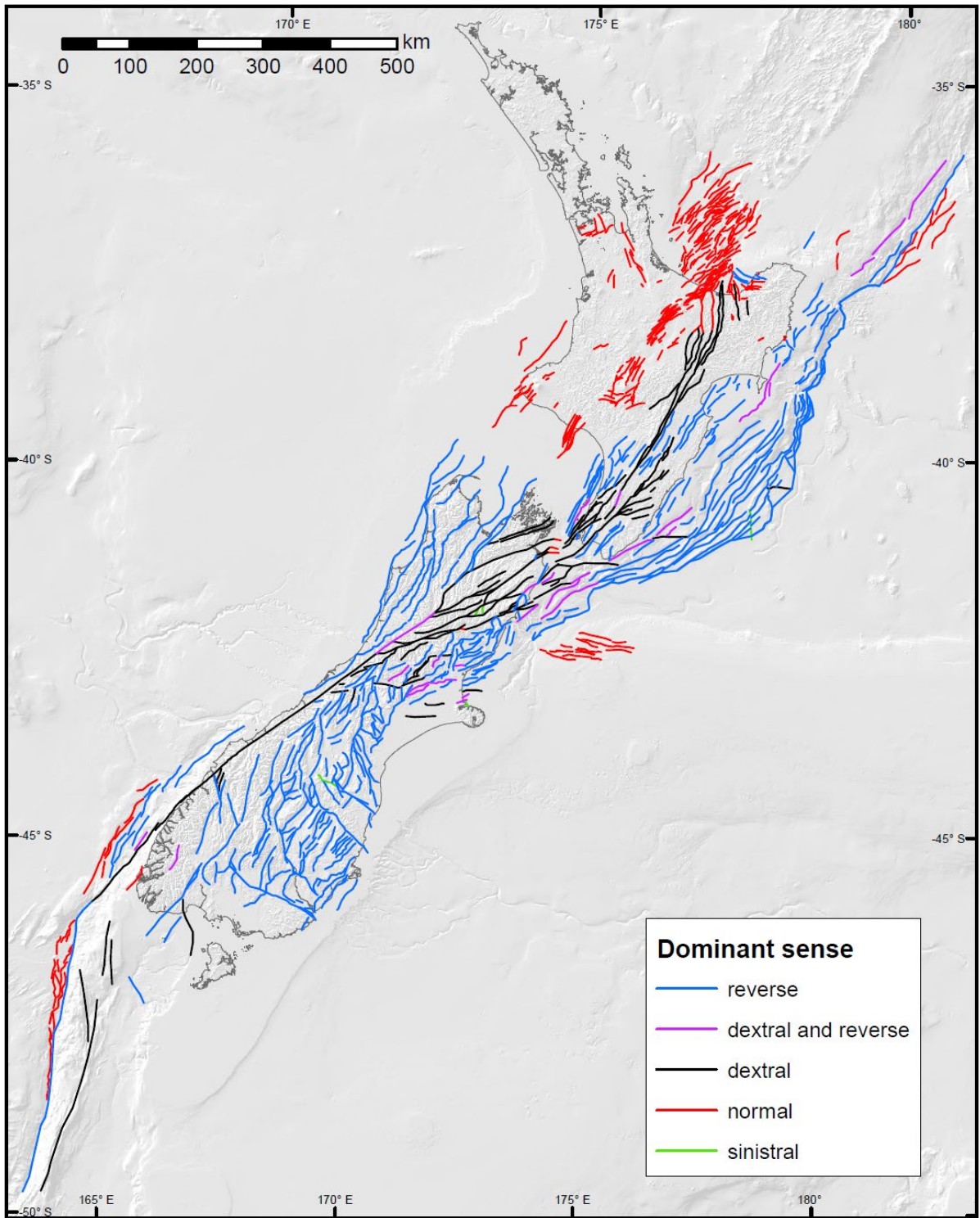


Figure 3.4 Fault zones in NZ CFM v1.0 colour-coded by dominant sense of movement.

### 3.3.11 Rake

The direction of hanging-wall slip relative to a horizontal line on the fault plane. Rake in NZ CFM v1.0 adopts the convention of Aki and Richards (2002) and is expressed as an angle from 0° to ±180°, whereby:

- 180° = -180° = dextral
- 90° = reverse
- -0° = sinistral
- -90° = normal.

Note: the rake convention of Aki and Richards (2002) differs from that used in Litchfield et al. (2013, 2014), where rake was expressed as an angle from 0° to 360°. The reason for changing rake convention in NZ CFM v1.0 is for consistency with several commonly used hazard, risk and earthquake simulator applications – e.g. OpenSHA (Field et al. 2003), OpenQuake (Silva et al. 2014), RSQSim (Richards-Dinger and Dieterich 2012). Therefore, to facilitate compatibility between NZ CFM v1.0 and those (and similar) applications, we have adopted the Aki and Richards (2002) rake convention.

Table 3.2 Rake categories for new and modified fault zones in NZ CFM v1.0.

Description	Sense of Slip		Rake (°)		
			Preferred	Uncertainty Range (±20°)	
	Dominant	Subordinate			-20°
Pure dextral strike-slip	Dextral	None	180	160	-160
Dextral with some reverse	Dextral	Reverse	160	140	180
Equal parts dextral and reverse	Dextral and reverse		135	115	155
Reverse with some dextral	Reverse	Dextral	110	90	130
Pure reverse dip-slip	Reverse	None	90	70	110
Reverse with some sinistral	Reverse	Sinistral	70	50	90
Equal parts reverse and sinistral	Reverse and sinistral		45	25	65
Sinistral with some reverse	Sinistral	Reverse	20	0	40
Pure sinistral strike-slip	Sinistral	None	0	-20	20
Sinistral with some normal	Sinistral	Normal	-20	-40	0
Equal parts sinistral and normal	Sinistral and normal		-45	-65	-25
Normal with some sinistral	Normal	Sinistral	-70	-90	-50
Pure normal dip-slip	Normal	None	-90	-110	-70
Normal with some dextral	Normal	Dextral	-110	-130	-90
Equal parts normal and dextral	Normal and dextral		-135	-155	-115
Dextral with some normal	Dextral	Normal	-160	-180	-140

For consistency, and considering uncertainties in rake estimation, fault zones in Litchfield et al. (2013, 2014) with documented rake estimates (converted to the Aki and Richards [2002] convention) have been changed to the closest preferred rake value (Rake\_pref) in Table 3.2, with rake uncertainty increased from  $\pm 10^\circ$  to  $\pm 20^\circ$  (Rake\_minus, Rake\_plus). For new and modified fault zones, rake and uncertainty is generally ascribed according to the categories listed in Table 3.2.

### **3.3.12 Slip Rate (SR\_pref, SR\_min, SR\_max)**

The slip rate parameter represents the net (rake-parallel) rate of movement of a fault zone in mm/yr, averaged over a specified time period (see Section 3.3.13). Estimates of slip rate in NZ CFM v1.0 are quantified in three attribute fields: the value considered most likely ('best' or 'preferred' dip – SR\_pref); a minimum likely value (SR\_min) and maximum likely value (SR\_max). Slip rate is generally calculated from the displacement of a marker of known or inferred age, but it can also be estimated based on, for example, geodetic observations and modelling. Where fault zones have associated folds, the net slip rate usually includes displacement accommodated by folding. Slip rates in NZ CFM v1.0 have been reconciled with the New Zealand Paleoseismic Site Database, a national database of paleoseismic data collected at sites, including slip rates on 189, mainly onshore, NZ CFM faults throughout New Zealand (Litchfield et al., forthcoming 2022).

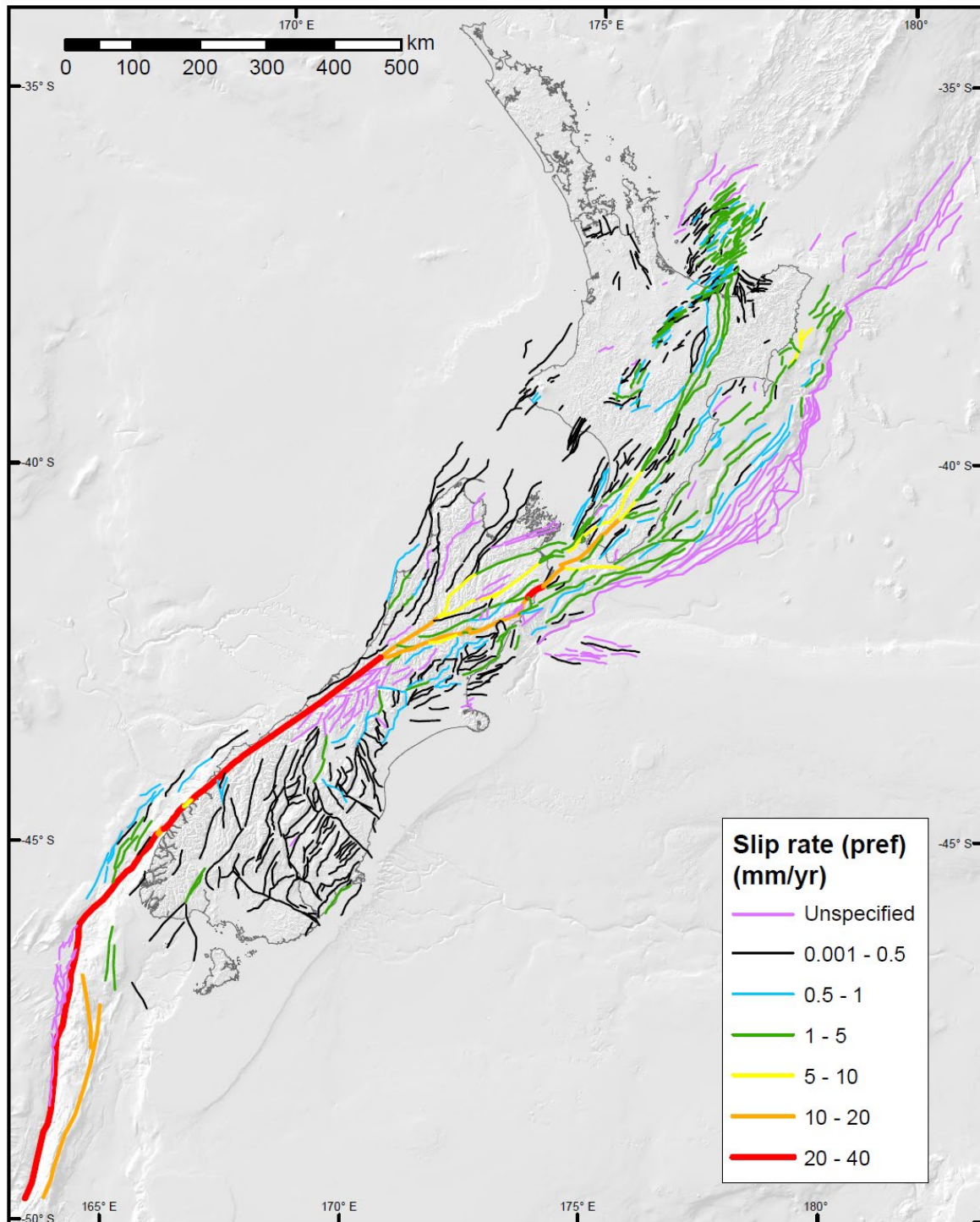


Figure 3.5 Fault zones in NZ CFM v1.0 colour-coded by Slip Rate (preferred).

### 3.3.13 Slip Rate Timeframe (SRT)\*

This parameter describes the timeframe (stepping back from the present) over which the slip rates listed in NZ CFM v1.0 are determined. The field has not been populated for all faults in NZ CFM v1.0; in general, it has been provided for only the better-studied faults. There are two methods provided for recording this parameter.

Four attribute fields are available for quantifying the slip rate timeframe parameter. The first three fields relate to the specific age of the offset marker from which the preferred, minimum and maximum slip rates were determined (respectively, SRT\_pref, SRT\_min and SRT\_max).

Where possible, this option is used. However, that level of age detail is not always available, nor, in some cases, even meaningful to apply. The fourth attribute field (SRT\_gen) provides an alternative option for the slip rate timeframe to be characterised in a more general way using the age range categories listed below. If the timeframe spans more than one category, the category that encompasses most of the timeframe is the one that is listed.

- Yrs: Slip rate estimated from information that spans the last few years (i.e. the last 100 years). Such estimates are typically based on geodetic observations and modelling.
- 10s yrs: Slip rate estimated from information that spans the last tens of years (i.e. the last  $10^1$  years). Such estimates are typically based on geodetic observations and modelling.
- 100s yrs: Slip rate estimated from information that spans the last hundreds of years (i.e. the last  $10^2$  years).
- 1000s yrs: Estimated from information that spans the last thousands of years (i.e. the last  $10^3$  years).
- 10,000s yrs: Estimated from information that spans the last tens of thousands of years (i.e. the last  $10^4$  years).
- 100,000s yrs: Estimated from information that spans the last hundreds of the thousands of years (i.e. the last  $10^5$  years).
- $\geq 1$  Ma: Slip rate determined (or inferred) based on observation that spans the last million years or more (i.e. the last  $\geq 10^6$  years).

### 3.3.14 Down-Dip Depth (Depth\_D90, Depth\_Dfc)

The depths to the base of fault zones in the NZ CFM (down-dip depth) are from a combination of sources. Approximately two-thirds of the faults in the NZ CFM have down-dip depths constrained by the methods detailed in Ellis et al. (2021) discussed below. The remaining third of fault zones have down-dip depths estimated from a combination of factors, including crustal thickness (e.g. outer-rise faults), consistency with depths from Ellis et al. (2021) but outside their region of analysis (e.g. northern Bay of Plenty), down-dip fault intersection with major structures (e.g. Hikurangi subduction interface, Alpine Fault) or depths based on geological considerations (e.g. Waverley and North Mernoo faults).

The two fault depth estimates used from Ellis et al. (2021) are seismogenic depth (D90) and maximum fault-rupture depth (Dfcomb; abbreviated here to 'Dfc'). Ellis et al. (2021) employ a combination of two independent models to estimate the down-dip depths of fault zones. Model 1 uses the distribution of regional seismicity derived from a relocated earthquake catalogue to calculate the 90% seismicity cut-off depth (D90) for crustal earthquakes. Model 2 uses surface heat-flow and rock type to compute depths to the 450°C isotherm, which is regarded as the thermal stability limit for seismogenic faults and is equivalent to the seismogenic depth limit (D90). Both models have overshoot factors applied ( $\times 1.25$ ) to account for rupture into the conditional stability zone. These thermal stability limits (i.e. the depths to the 450°C isotherm) are combined with the seismogenic D90 estimates (including overshoot factors) to produce a preferred maximum rupture depth, the New Zealand Fault-Depth Rupture Model v1.0 (Figure 3.6). Both models have depth cut-offs at the Moho and the Hikurangi slab interface. Using a weighting scheme based on the relative uncertainties of the two models, estimates of D90 and Dfc (Dfcomb; Figure 3.6) – including uncertainties – are derived; these depth estimates are used in NZ CFM v1.0 for the majority of faults.

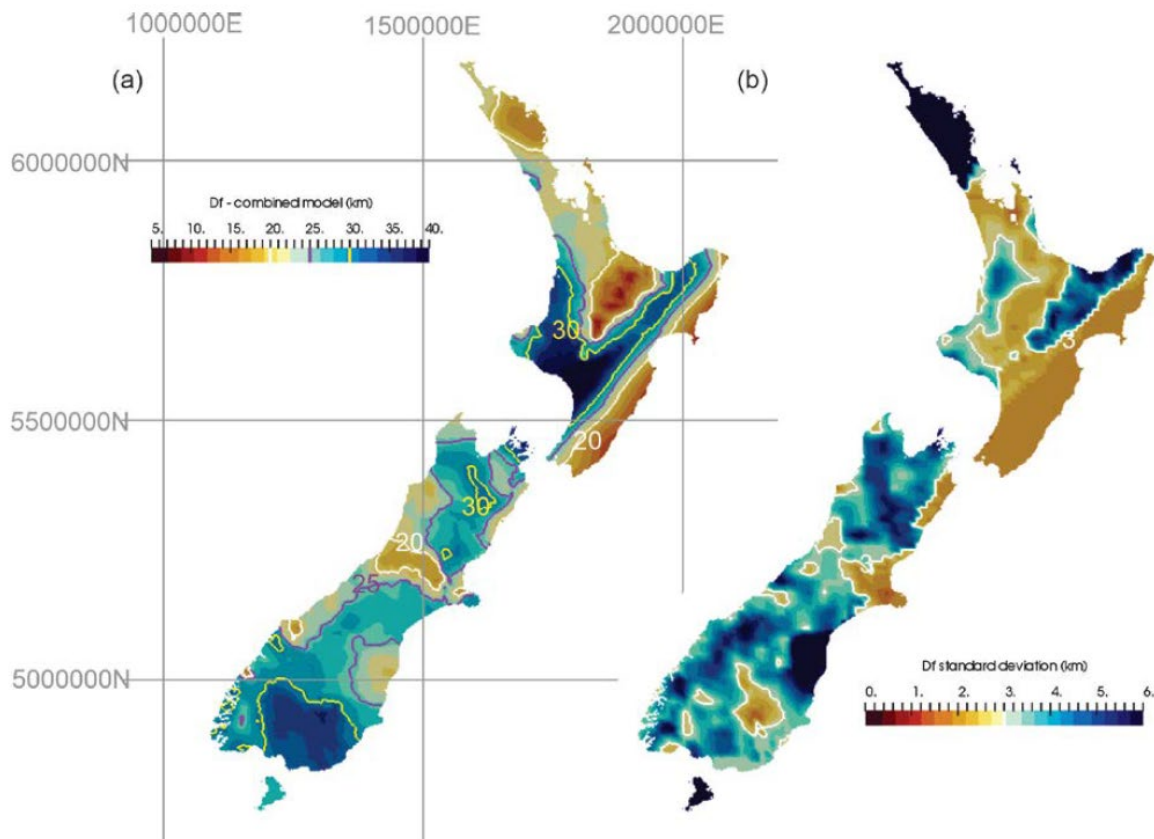


Figure 3.6 New Zealand Fault-Rupture Depth Model v1.0. (a) Combined estimate of maximum fault-rupture depth ( $D_{fcomb}$ ) of Ellis et al. (2021). Depth contours are shown for 20 km (white), 25 km (purple) and 30 km (yellow). (b) Estimated uncertainty (standard deviation) for the combined model. Uncertainty contour of 3 km in white. From Figure 2.7 of Ellis et al. (2021).

The `Depth_D90` and `Depth_Dfc` values listed in the NZ CFM v1.0 parameter table are the vertical elevation below sea-level in kilometres, averaged along the length of the fault zone, where the down-dip portion of the fault plane intersects, respectively, either `D90` or `Dfcomb` of Ellis et al. (2021). The base-of-fault-zone depth used in the 3D build of NZ CFM v1.0 is, generally, `Dfc` (maximum fault-rupture depth).

Because only two thirds of the faults in the NZ CFM have a modelled seismogenic depth (`D90`) or maximum fault-rupture depth (`Dfc`), the attributes `Depth_D90` and `Depth_Dfc` have an associated attributes detailing the source of the depth estimate. The attributes `Method_D90` and `Method_Dfc` use numbers 1 to 3 to denote the source of the depth estimate (Figure 3.7):

1. Average fault depth from Ellis et al. (2021).
2. Default depths based on geological considerations of crustal thickness, fault length or consistency with Ellis et al. (2021).
3. Maximum depth of down-dip fault intersection.

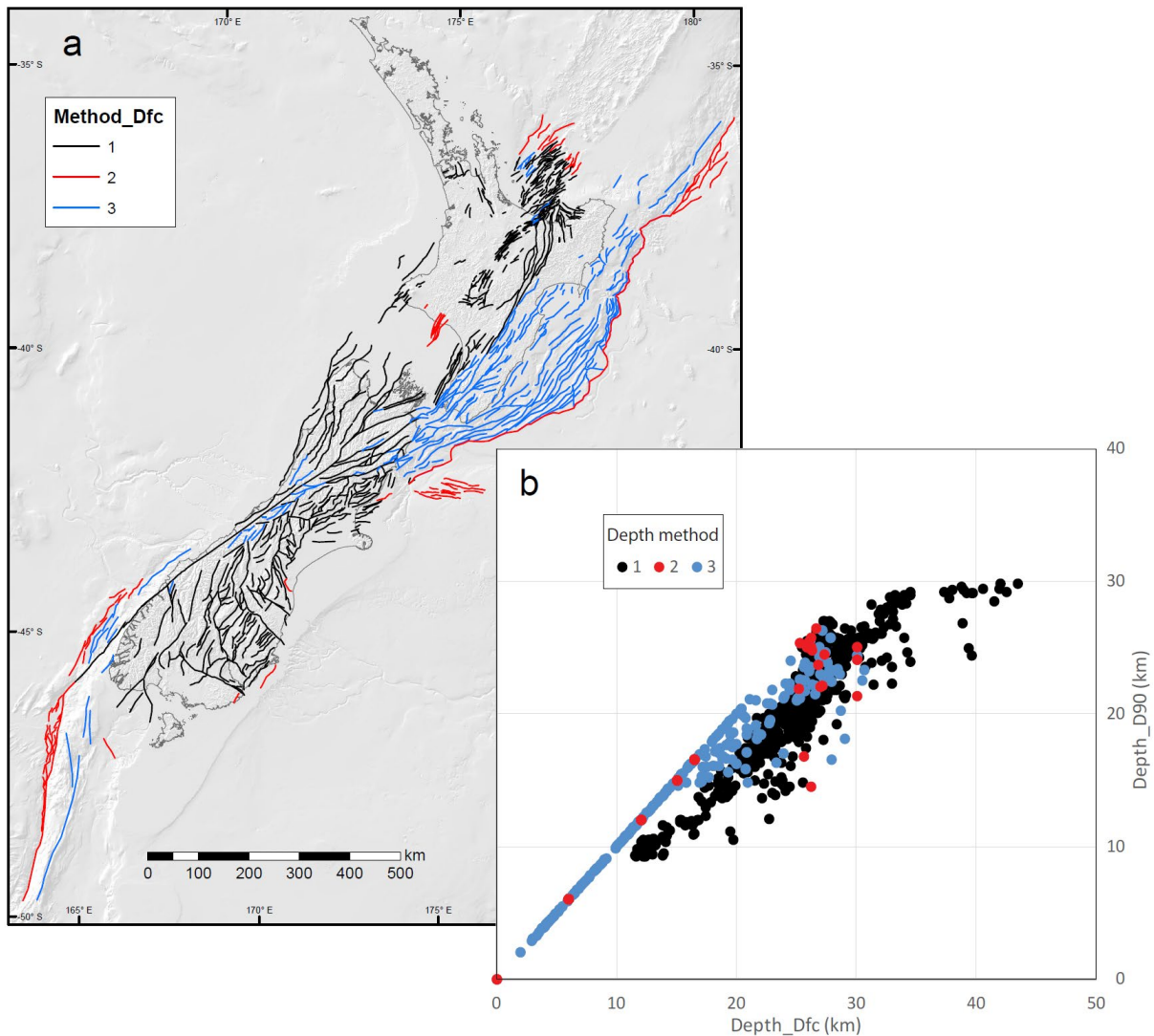


Figure 3.7 Maximum fault-rupture depth method for NZ CFM v1.0 fault zones (Method\_Dfc). (a) Depth estimates for maximum fault-rupture depth estimated from 1 = Dfcomb of Ellis et al. (2021); 2 = default depths based on geological considerations of crustal thickness, fault length or consistency with Ellis et al. (2021); or 3 = maximum depth of down-dip fault intersection. (b) Maximum fault-rupture (Depth\_Dfc) versus seismogenic (Depth\_D90) depth. The depth method key is the same as for the main map.

Depending on specific downstream applications of NZ CFM v1.0, differing fault-depth estimates may be required. That is, no single depth estimate will satisfy the requirements of all ensuing applications. In NZ CFM v1.0, two down-dip fault depth estimates are provided: D90 (seismogenic depth) and Dfc (maximum fault-rupture depth). It is the responsibility of users of NZ CFM v1.0 to decide which of these two – perhaps neither – is most appropriate to use for their specific application. At present, the 3D version of the model has been developed using Depth\_Dfc (Figure 3.8).

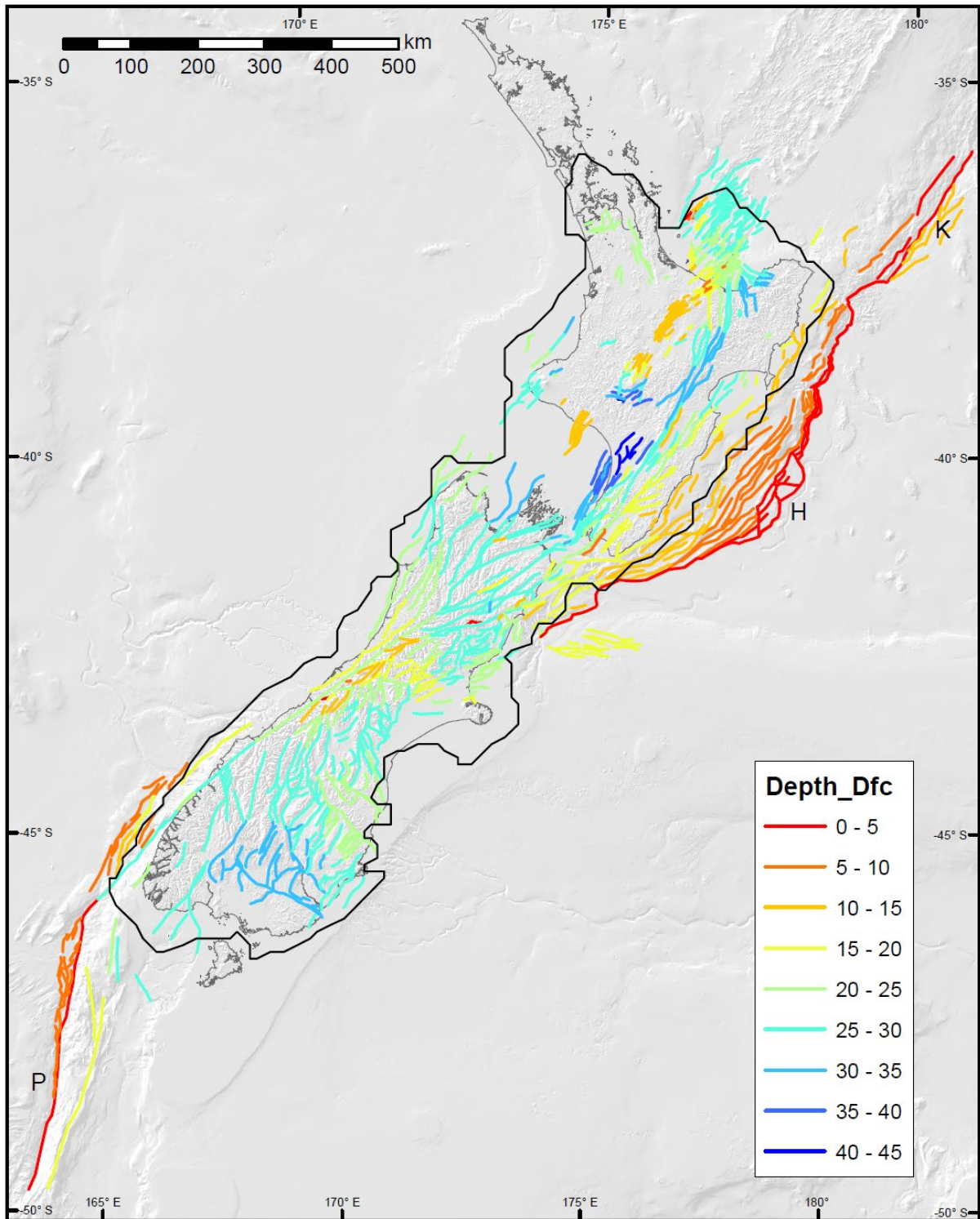


Figure 3.8 Maximum fault-rupture depth for NZ CFM v1.0 fault zones (Depth\_Dfc). See Figure 3.7 for location of depth estimate method. Black outline shows the analysis region of Ellis et al. (2021) for depth estimates based on seismogenic (D90) and maximum fault-rupture (Dfc). The Kermadec (K), Hikurangi (H) and Puysegur (P) subduction interface fault traces have been set to a default zero elevation due to their variably increasing depths to 75 km. Two-thirds of the faults use depth estimates from Ellis et al. (2021). The remainder are based on depths of down-dip intersections with major faults, crustal thickness and fault length estimates or that are consistent with Ellis et al. (2021).

### 3.3.15 Up-Dip Depth (UpDth)\*

The depth, in kilometres, of the up-dip edge of the fault zone's fault plane. Most fault zones in NZ CFM v1.0 reach the ground surface and, accordingly, have an up-dip depth of 0 km. For the relatively few blind faults in NZ CFM v1.0, preferred (UpDth\_prf), minimum (UpDth\_min) and maximum (UpDth\_max) up-dip depth is recorded as a positive value below the ground (or seabed) surface.

### 3.3.16 Quality Code (QualCode)

A five-tier ranking system is used to provide an indication of the quantity and type of geological data available for each fault zone. The Quality Code is most influenced by the robustness of the slip-rate data/determination. Several of these Quality Code categories have been modified and re-ordered comparable to those in Litchfield et al. (2013, 2014).

- **1:** Fault zone with high-quality fault-specific field (e.g. trench, dated displaced markers) or marine (e.g. swath, markers with well-constrained ages) data. This Quality Code number and definition is unchanged from that in Litchfield et al. (2013, 2014).
- **2:** Fault zone with some fault-specific constraints from field or marine data and, typically, further evaluated based on comparisons with nearby better-characterised fault zones and considerations given to regional slip-rate budgets. This Quality Code definition is slightly modified compared to Quality Code 2 in Litchfield et al. (2013, 2014) but encompasses the majority of their Quality Code 2 fault zones.
- **3:** Fault zone that has geometric parameters but few, if any, fault-specific data, and slip rates have been mainly inferred from geomorphic expression (e.g. scarp height and morphology as an indicator of age) and/or comparisons with nearby better-characterised fault zones. This Quality Code definition is similar to, but slightly modified from, Quality Code 4 in Litchfield et al. (2013, 2014).
- **4:** Fault zone that has geometric parameters but slip rate has been ascribed based largely on geodetic and/or instrumental seismicity considerations. This Quality Code definition differs from any used in Litchfield et al. (2013, 2014) but encompasses their Quality Code 3.
- **5:** Fault zone that has geometric parameters but slip rate has not been derived or inferred. This is a modified, more general Quality Code definition than is found in Litchfield et al. (2013, 2014), but it does encompass their Quality Code 5.

### 3.3.17 References

Key references that inform/define various parameters for each fault zone described in NZ CFM v1.0.

### 3.3.18 Comments

Additional comments that help inform the derivation of various parameter values listed in NZ CFM v1.0. These include documenting changes to the name or surface fault trace of the fault relative to Litchfield et al. (2013, 2014) and justification of slip rates.

### **3.4 Parameter Uncertainties**

For the numerical parameters dip, rake and net slip rate, uncertainties are quantified by providing three values for each: a minimum value, a maximum value and what is considered to be the most likely ('preferred' or 'best') value. The minimum and maximum values are inferred to approximate 95% confidence bounds, though in a qualitative rather than statistically rigorous way. The preferred value may in some cases be the mean of several site-specific measurements or be the median between maximum and minimum values. In other cases, the parameters are calculated from the best-constrained site-specific offset and age data and may result in a value anywhere between the maximum and minimum (e.g. for a particular fault zone, a value towards the maximum may be considered most likely). As a result, there is not necessarily a symmetrical distribution of uncertainty between maximum and minimum values.

## 4.0 3D MODEL CONSTRUCTION

Faults in the 2D map component of NZ CFM v1.0 are represented in the 3D model component as triangulated mesh surfaces (t-surf), which consist of nodes or points (with coordinates x, y and z) associated with one another as triangular elements. The 3D geometry of faults in NZ CFM v1.0 were built with MOVE geological modelling software from Petroleum Experts Ltd (formerly Midland Valley), using the GIS-referenced fault zone traces as initial constraints. MOVE software uses a mix of implicit mathematical fitting of surfaces between constraining points and user-defined settings to create an explicit, coordinate-based triangulated mesh.<sup>6</sup>

Triangular meshes are better suited to describing complex fault surface geometries and topologies, as well as their intersections, than rectangular meshes (Meade 2007). In NZ CFM v1.0 the node (point) spacing is allowed to vary as a function of fault shape but has a general spatial resolution of c. 1–2 km for crustal faults (7–10 km for the subduction interfaces), similar to the compilation scale of fault-trace representations. Unlike the SCEC CFM, NZ CFM v1.0 is a single, preferred, explicit model representation of active and potentially seismogenic faults and does not yet incorporate alternative interpretations. The present 3D model uses the maximum depth of fault rupture (Depth\_Dfc), detailed in Section 3.3.14, for lower depth extent of the fault surfaces. The modelled zone fault surfaces are provided in GOCAD ACSII t-surf format in New Zealand Transverse Mercator projection. In addition, a comma-delimited ascii (.csv) file containing the location for the centre of each triangle face comprising a fault zone surface along with the dip angle, strike and normal (azimuth) directions of each face is also available.

### 4.1 Fault Representations

3D fault representations in NZ CFM v1.0 are constrained by many sources of information, including surface traces (e.g. Langridge et al. 2016), earthquake focal mechanisms and hypocentre distributions (e.g. Williams et al. 2013), geodetic inversions (Beavan et al. 2011), seismic reflection profiles (e.g. Lamarche and Barnes 2005; Barnes and Ghisetti 2016; Seebeck et al. 2021), geologic cross-sections (e.g. Ghisetti et al. 2016b) and combinations thereof (Williams et al. 2013). Information from cross-sections was treated cautiously, as they commonly contain inference with limited sub-surface data control, and some may have been drawn with the intent to illustrate a particular tectonic concept or model.

While the surface locations of active fault zones in New Zealand are generally well known, their down-dip geometry and associated variations with depth are poorly constrained. Given these limitations, all isolated crustal faults (excluding the Hikurangi, Kermadec and Puysegur subduction interfaces) have been modelled with constant dip to depth (e.g. Plesch et al. 2007). Fault zones are projected from mean sea-level (0 m elevation) perpendicular to their average strike. Projection of faults from 0 m elevation was a requirement of downstream applications such as the NSHM and RSQSim. This requirement introduces a horizontal positioning error into geometries for dipping faults that outcrop at elevations significantly different from mean sea-level. In the NZ CFM, this mainly affects faults of the Hikurangi accretionary margin – eastern zone domain on the outer continental slope, where water depths reach 2–3 km.

The modelling used the intermediate ‘preferred’ dip estimate for each fault zone or fault zone segment (refer to Section 3.3.8). Subsequent versions of the NZ CFM may use, where applicable, more complex portrayals of fault shape with depth, such as listric geometries.

---

6 <https://www.petex.com/products/move-suite/>

In contrast to the projection of upper plate faults from a mean sea-level elevation, the Hikurangi, Kermadec and Puysegur subduction interface surfaces are projected from their true elevation, typically 3–6 km below sea level.

The Hikurangi subduction interface is based on Williams et al. (2013) and has a variable, downwardly increasing dip to a depth of 75 km. While a lower fault tip depth of 75 km is well below crustal seismogenic depths, slow slip events on the plate interface in the southern part of the subduction zone occur to these depths (Wallace 2020). For consistency, both the Kermadec and Puysegur subduction interfaces are truncated at 75 km depth.

The Kermadec subduction interface is contiguous with the Hikurangi subduction interface from about the latitude of East Cape northward. The Kermadec subduction interface is a 200 km along-strike projection of the northern Hikurangi subduction interface of Williams et al. (2013) and has a variable and increasing dip with depth. While a previously published interface geometry for the Kermadec segment was available (Hayes 2018), the along-strike continuity of the subduction interface between the Hikurangi and Kermadec segments of the margin was a key consideration. The Hayes (2018) Hikurangi–Kermadec subduction interface was sufficiently different from the Williams et al. (2013) geometry to warrant generating separate Hikurangi and Kermadec segments for this model.

A re-interpreted Puysegur subduction interface has been generated for this model based on a compilation of published sources (see Appendix 3 for more information). The sparse, and sometimes contradictory, data coverage for the Puysegur subduction margin, along with the complicated tectonic setting, result in large uncertainties for any plate interface interpretation for this area. Cross-sections (Lebrun et al. 2000; Reyners et al. 2002; Stratford et al. 2020; Shuck et al. 2021) and plate interface geometries (Wallace et al. 2007; Hayes and Furlong 2010; Hayes 2018) were compared to the relocated earthquake catalogue of Reyners et al. (2011). The new representative plate interface surface retains the ‘ploughshare’ geometry of Reyners et al. (2002) and has similarities to previous representations, such as Hayes and Furlong (2010). Reconciling the steeply dipping plate interface geometry beneath the Fiordland sector of the subduction margin with the apparent shallow dips of the interface along the Puysegur sector remains a challenge, and resolution will likely depend on a catalogue of more accurately located earthquakes than currently exist. Based on the distribution of relocated earthquakes, we have adopted the Lebrun et al. (2000) model for the intersection of the Puysegur subduction interface with the Alpine Fault. In this model, the Puysegur subduction interface is truncated by the Alpine Fault. To the west of the Alpine Fault, the subduction interface is represented by low-angle reverse faults of the western Fiordland margin – Caswell High domain (Figure 3.3). An alternate interpretation of a continuous plate interface that initiates along the Fiordland margin deformation front and curves smoothly to depth is also provided. Further information on the re-interpretation of the Puysegur subduction interface, alternative interpretation and constraints used to develop the model surfaces can be found in Appendix 3.

Excluding the subduction interfaces, the vast majority of the 3D-modelled fault zones in NZ CFM v1.0 extend to their regionally determined maximum seismogenic rupture depth ( $D_{fc}$ ; see Section 3.3.14) (Ellis et al. 2021). For long fault zones, the base-of-fault-zone depths can vary along strike dependent on the local elevation of the maximum seismogenic rupture depth estimate.

Several groups of faults within the 3D model do not persist to the maximum seismogenic rupture depth determined by Ellis et al. (2021) (Figure 3.7). The first group of faults with maximum depths differing from  $D_{fc}$  typically intersect subduction interfaces at depths less

than c. 30 km. In these instances, these upper plate faults are truncated at the subduction interface. The second group of faults with maximum depths differing from  $D_{fc}$  are located outside of the region constrained by the analysis of Ellis et al. (2021). In these regions, typically toward the outer, peripheral margins of active faulting, the depth to the lower limit of fault rupture is estimated and poorly constrained. For normal faults on the subducting Australian plate west of the Puysegur subduction front (Puysegur–Caswell High outer-rise domain), a lower depth of 6 km was estimated from the age and thickness of Cretaceous to Oligocene oceanic crust (Van Avendonk et al. 2017). The depth of normal faults in the Hikurangi outer-rise domain, east of the Hikurangi subduction front, was estimated as 15 km based on GeoNet Earthquake Centroid Moment Tensor focal mechanisms (Ristau 2008) and the 12–15 km thickness of the Cretaceous Hikurangi Plateau (Davy et al. 2008) that they dissect. Normal faults in the North Mernoo fracture zone domain (Figure 3.3) were extended to depths of 16.5 km based on fault length and width scaling relationships from Thingbaijam et al. (2017). Normal faults imaged by seismic reflection profiles in the Whanganui Basin (e.g. Waverley faults, in Western North Island domain) are interpreted to be related to the collapse above an underlying reverse fault and are not thought to extend to significant depth. These bending- or collapse-related faults have been assigned a nominal depth of 12 km.

## 4.2 Fault Segment Linkage

Rules for fault zone intersections and linkages in the model have been developed to ensure segmented fault zones have a common segment boundary intersection to depth. While the majority of fault zones in the model are isolated and modelled with a constant dip perpendicular to strike, many of the major fault zones, particularly those accommodating strike-slip motion, comprise of multiple segments. Where adjacent fault zone segments have differing dips, projection of fault zone dip to depth creates a discontinuity in the fault surface that needs to be smoothed.

The boundary between adjacent fault zone segments is defined by a change in the kinematic or geometric parameters defining that fault segment. The Alpine and Hope faults are examples of long fault zones comprising multiple segments that incorporate slip rate and dip changes along strike.

Along-strike changes in the dip of a segmented fault zone were accommodated by creating a buffer zone on each side of a segment boundary (Figure 4.1a). The maximum width of these buffer zones is typically on the order of 10 km, 5 km each side of a segment boundary, and approximately half the seismogenic thickness. The fault zone surface is interpolated through the buffer zone between fault segments to create a continuous fault surface along strike. The original segmentation of this continuous fault surface was preserved by cutting the constructed surface along the segment boundary along an orientation bisecting the angle between the adjacent fault zone segments. The result is a common segment boundary from the surface to depth that smoothly varies between adjacent fault zone segments.

Three main geometric relationships (or scenarios) encompass the general possibilities for linkage between fault zone segments, as described in the following subsections. The constructed geometric linkages are not meant to imply anything about fault kinematics, such as whether individual ruptures may propagate, or be arrested, across a fault zone segment boundary.

#### **4.2.1 Scenario 1**

Scenario 1 represents the linking of adjacent fault zone segments with the same strike but differing dips (Figure 4.1). The two fault zone segments are connected across a buffer zone either side of the segment boundary, initiating at the fault zone trace junction and progressively broadening down to the base-of-fault depth. This buffer zone thus has a triangular geometry, with a strike that differs from the fault zone trace at the surface. The buffer zone is a geometric construction created to link two differently dipping fault surfaces and does not necessarily reflect the true geometry of the fault zone connection.

#### **4.2.2 Scenario 2**

Scenario 2 involves two fault zone segments (or fault zones that are considered to be contiguous) of the same assigned dip angle with fault traces that form a reflex angle (an angle  $>180^\circ$ ) as measured on the side of the fault trace that faces the dip direction (Figure 4.1). The buffer is initiated at the surface trace junction and progressively broadens down to the base-of-fault. The triangular zone gap that is created at the segment boundary separating the two fault surfaces is interpolated through to form a continuous fault surface. The segment boundary is re-instated by cutting the surfaces along the angle bisecting the boundaries of the triangular zone.

#### **4.2.3 Scenario 3**

Scenario 3 involves two fault segments (or faults that are considered to be contiguous) of the same assigned dip angle but fault traces that form an obtuse angle (an angle  $<180^\circ$ ) as measured on the side of the fault trace that faces the dip direction (Figure 4.1). The buffer is initiated at the surface trace junction and progressively broadens down to the base-of-fault. The overlapping triangular zones projecting past the common intersection line are removed. The segment boundary is re-instated by cutting their surfaces along the common intersection line.

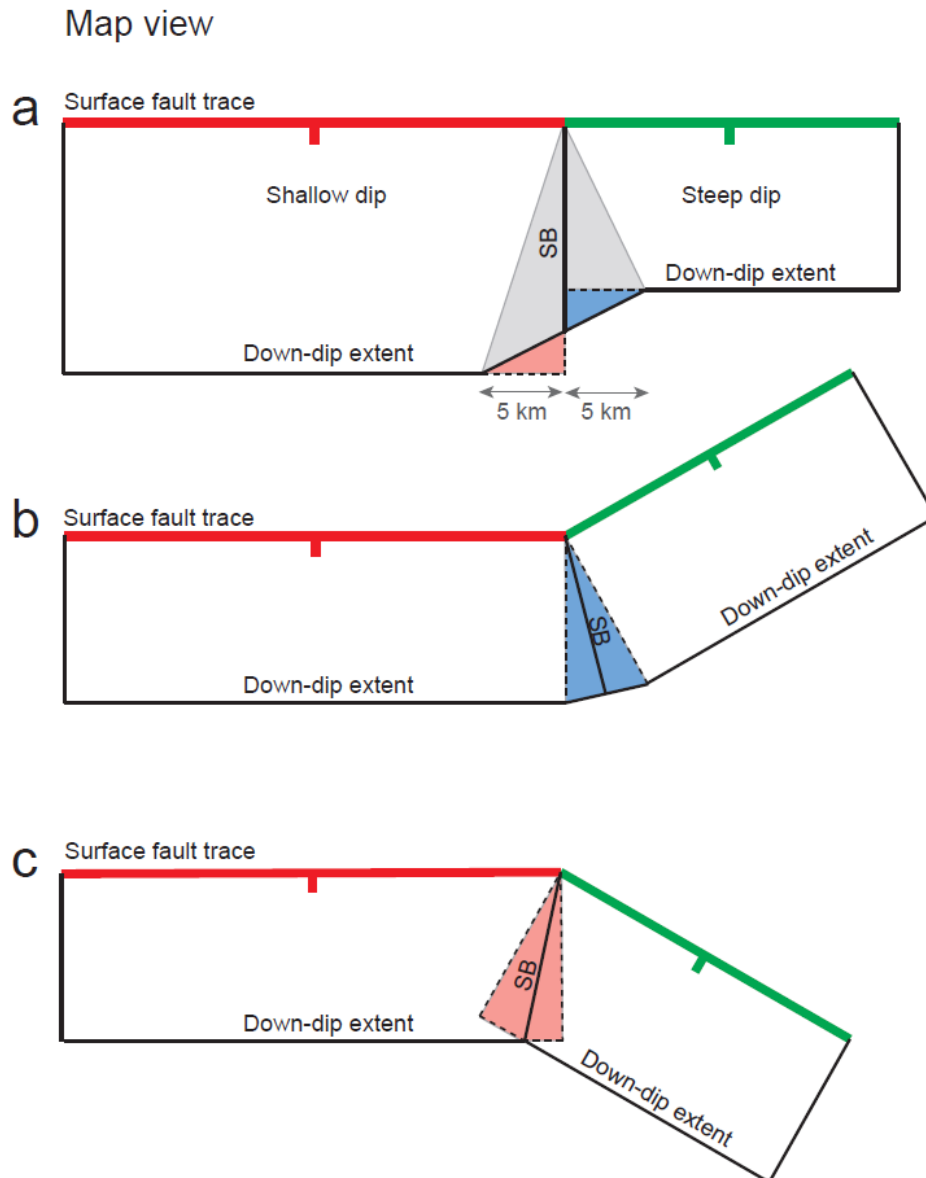


Figure 4.1 Illustration of fault zone segment linkage rules. Schematic map view of linkage rules used to join adjacent fault zone segments to form fault surfaces with a common segment boundary; SB = segment boundary. (a) Scenario 1: fault zone segments of same strike but differing dip. (b) Scenario 2: fault zone segments of same dip and reflex angle between strikes. (c) Scenario 3: fault zone segments of same dip and obtuse angle between strikes. Areas added or subtracted from the fault zone are indicated by blue and red triangles, respectively. The segment boundary bisecting the angle between the two fault zones is cut through a continuous surface to re-instate the original segmentation.

#### 4.2.4 Examples of Fault Segment Linkage

These three scenarios are type examples of the kinds of geometric relationships found between fault segments and contiguous faults within the 3D model. Combinations of these scenarios form a spectrum of relationships, whereby dip and strike changes between segments are modelled using the above approaches (e.g. Figure 4.2). Overall, the inclusion of smoothly varying interpolated zones between fault zone segments has little impact on the average dip of a 3D model fault zone, generally remaining within a few degrees of its 2D parameterisation and well within the estimated uncertainties, represented by the minimum and maximum dip values.

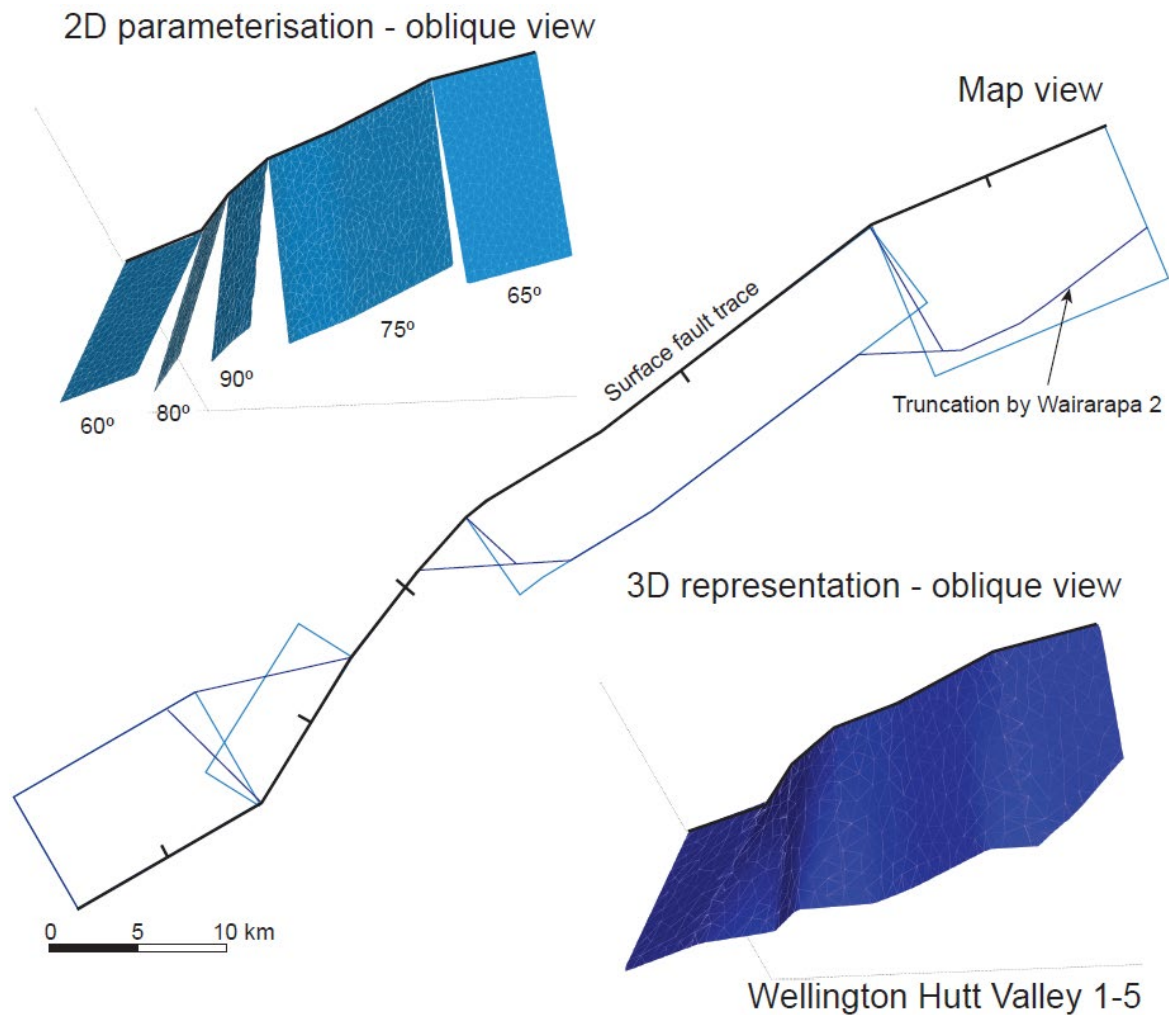


Figure 4.2 Example of along-strike fault segmentation. The southern part of the Wellington Hutt Valley fault zone (North Island Dextral Fault Belt domain) comprises five segments with differing dips along a sinuous fault trace. The 2D parameterisation (light-blue polygons and lines) results in discontinuous fault zone segments at depth. The 3D representation (dark-blue polygons and lines) interpolates between fault zone segments to produce a smoothly varying fault with common segment boundary intersections.

In a few cases, the segmentation of curved faults in map view, combined with dip changes along strike, results in the deviation of fault dip in the 3D surface away from the 2D parameterisation of the fault (e.g. Cloudy and Vernon faults; northeastern end of Marlborough Fault system domain). Here, the down-dip geometry specified by the 2D parameterisation was inconsistent with a smoothly varying or 'realistic' fault surface. This inconsistency was resolved by projecting the average preferred dip of the fault zone segments to depth in a direction perpendicular to the average fault zone segment trend.

### 4.3 Fault Intersections

Fault intersections are an important consideration for any 3D representation of a fault network. Due to the number and complexity of the faults in NZ CFM v1.0, fault intersections for only the largest and tectonically important faults have been addressed. Fault intersections within the model consist of two general types, either along-strike or down-dip.

Initial attempts at developing a down-dip fault zone intersection criteria that could be universally applied proved unworkable due to the number and complexity of these types of intersections throughout the model. Due to the opposing dips of closely spaced faults in several parts of the New Zealand plate boundary zone, such as in the Havre Trough – Taupō Rift, Central

Canterbury and Otago neotectonic domains (Figure 3.3), the lack of information on intersection geometries and the uncertainty of how to partition slip rates onto intersecting faults or portions of faults, it is envisaged that resolving the down-dip intersections for cross-cutting faults will be a focus of future iterations of the model. At present in NZ CFM v1.0, these closely spaced oppositely dipping faults are retained as mutually intersecting. In some cases, such as normal faults within Havre Trough – Taupō Rift domain, mutually cross-cutting faults may be valid.

As the present model endeavours to generate a representative fault network suitable for future physics-based earthquake and deformation modelling, there is a large degree of uncertainty as to how the fault zone geometry changes with depth. Therefore the actual fault and intersection geometries represented in the present model may not be representative of the actual geometry of faults at seismogenic depths. One of the only locations we have with which to compare NZ CFM v1.0 to faults imaged at depth is a recent crustal-scale depth-converted seismic reflection line collected in the Bay of Plenty (Gase et al. 2019). Figure 4.3 shows the geometry of the model faults relative to the geometry of faults interpreted on the seismic line. For some faults, there is good agreement between model and interpreted fault dips (e.g. White Island 1); in other cases, it is apparent that the model faults differ from the lower-angle dips observed in the seismic reflection profile (e.g. Tarawera 5). In the centre of Figure 4.3, a number of faults intersect a large low-angle fault at depth, the geometry of which is not represented in the current model.

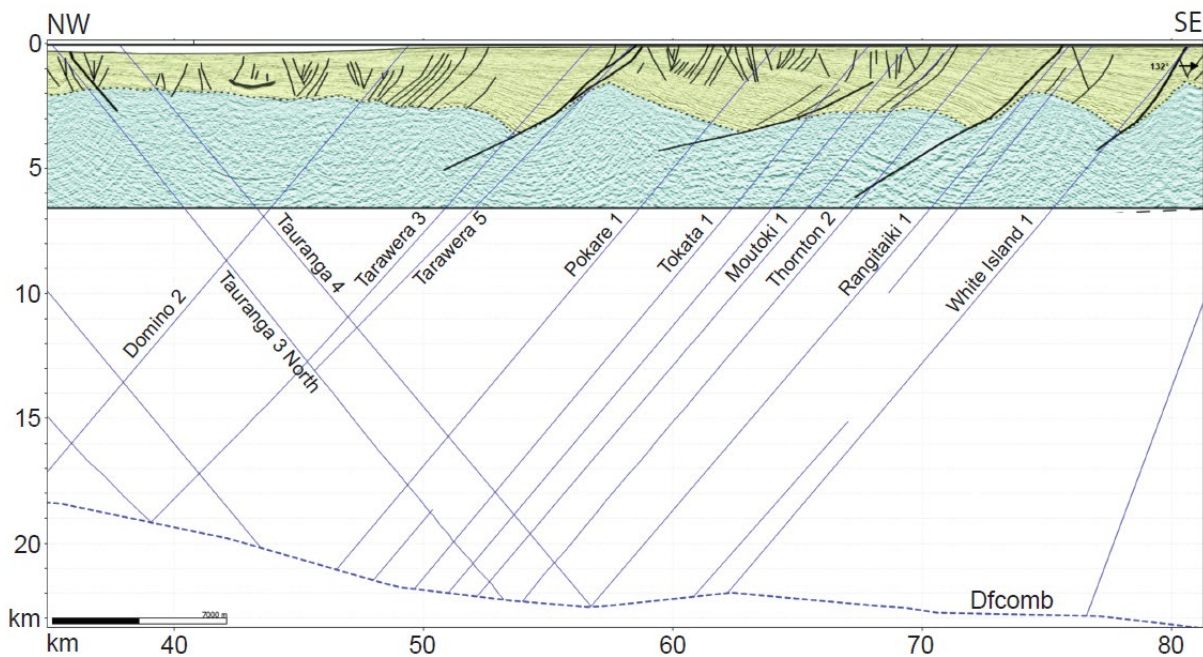


Figure 4.3 Illustration of intersection relationships of 3D modelled faults across the Havre Trough – Taupō Rift domain, Bay of Plenty. Planar representations of the 3D component of NZ CFM v1.0 (solid blue lines) and Dfc (dashed blue line; Dfcomb of Ellis et al. 2021) in relation to the interpreted, depth-converted seismic reflection profile of Gase et al. (2019). The profile location is shown in Figure 2.2.

This comparison highlights the limitations of using surface or near-surface data to constrain fault geometry and intersection relationships at depth. For some purposes, the difference between a representative and actual fault geometry may have little influence on results derived from these different fault representations. For example, Seebeck et al. (2021) demonstrate that using a planar or listric fault representation in low-frequency spectral element earthquake simulations has little influence on the resulting distribution of ground motions.

While the majority of down-dip intersections associated with individual cross-cutting fault zones have not been addressed in this model, down-dip intersections with fault zones intersecting large plate boundary faults have been truncated. Figure 4.4 shows fault zones that truncate both at depth and along-strike of all other intersecting fault zones. These fault zones are predominantly associated with the long strike-slip fault systems of the North and South Islands. Specifically, no fault cross-cuts the plate boundary Alpine–Wairau faults either along strike or down dip. Toward the south, reverse faults within the Fiordland accretionary wedge (e.g. South Wedge 1–10 and Central Wedge 1, 2 and 3) are truncated by the Alpine Fault and do not project down to the regional maximum seismogenic depth determined by Ellis et al. (2021).

Similarly, no faults cross-cut the major faults of the Marlborough Fault System or North Island Dextral Fault Belt. Boundaries have been introduced to the extensional faults of eastern and western Bay of Plenty to avoid minor faults cross-cutting rift margins. At the eastern Bay of Plenty coastline, normal faults of the Taupō Rift and strike-slip faults of the North Island Dextral Fault Belt intersect and cross-cut at oblique angles. In this location, the Edgecumbe – White Island 1 faults are considered the boundary across which no other normal fault cross-cuts toward the east.

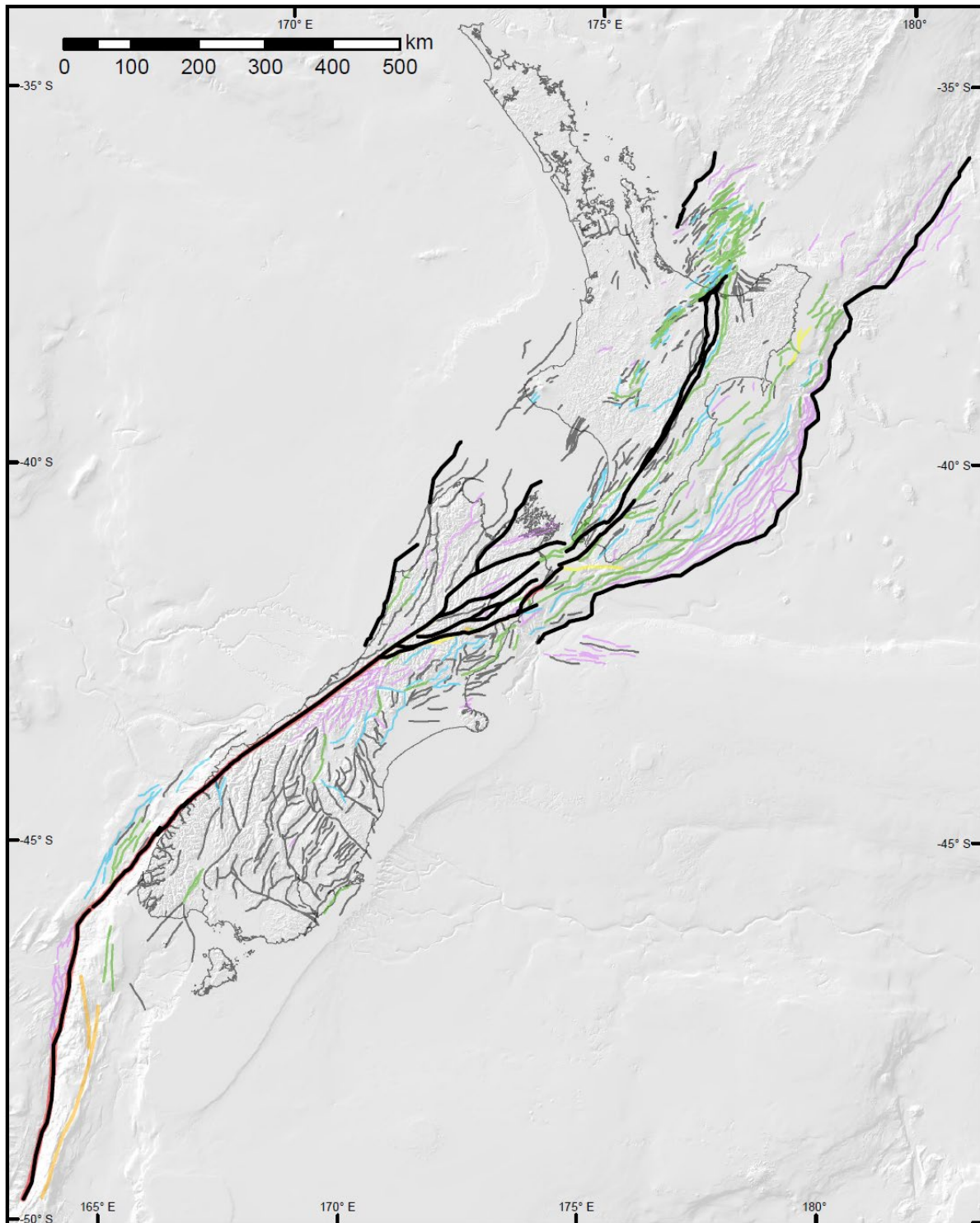


Figure 4.4 Faults with along-strike and or down-dip intersection geometries. Black lines represent major faults that truncate any intersecting fault. All other faults coloured by slip rate as in Figure 3.5. Plate interfaces (Puysegur, Hikurangi and Kermadec Trench) extend beneath upper-plate faults shown by surface trace. Faults with down-dip intersections shown in Figure 3.7.

At oblique fault zone intersections where one fault zone dips in a similar direction and angle to an intersecting fault zone, faults below the surface do not connect (Figure 4.5). At these intersection locations, kinematic coherence between the intersecting faults is assumed (e.g. Mouslopoulou et al. 2008) and therefore hard-linked connections between faults are formed. Strike-slip fault zones of the North Island Dextral Fault Belt at the intersection with the Taupō Rift are projected along strike at depth to form a common intersection line with the boundary fault zones of the Taupō Rift. Similarly, in the southern North Island, strike-slip fault zones intersecting obliquely with the Wairarapa Fault (Masterton, Carterton and Mokonui Southwest faults) are also projected along strike to form a common intersection at depth. This along-strike projection results in the fault zone dimensions differing from the 2D line representation.

The oblique intersection of the Marlborough Fault System with the Alpine Fault has the opposing geometric relationship (Figure 4.5). Here, the Alpine Fault dips toward the Marlborough Fault System, thereby resulting in cross-cutting relationships at depth, with Marlborough fault planes terminating at abutting junctions on the Alpine Fault plane. In this case, the down-dip dimensions of faults intersecting the Alpine Fault are smaller than their 2D line representation due to truncation against the plate boundary structure. In most cases, with the exception of the intersection between fault zones of the Taupō Rift and the fault zones of North Island Dextral Fault Belt, high slip-rate faults truncate lower slip-rate faults.

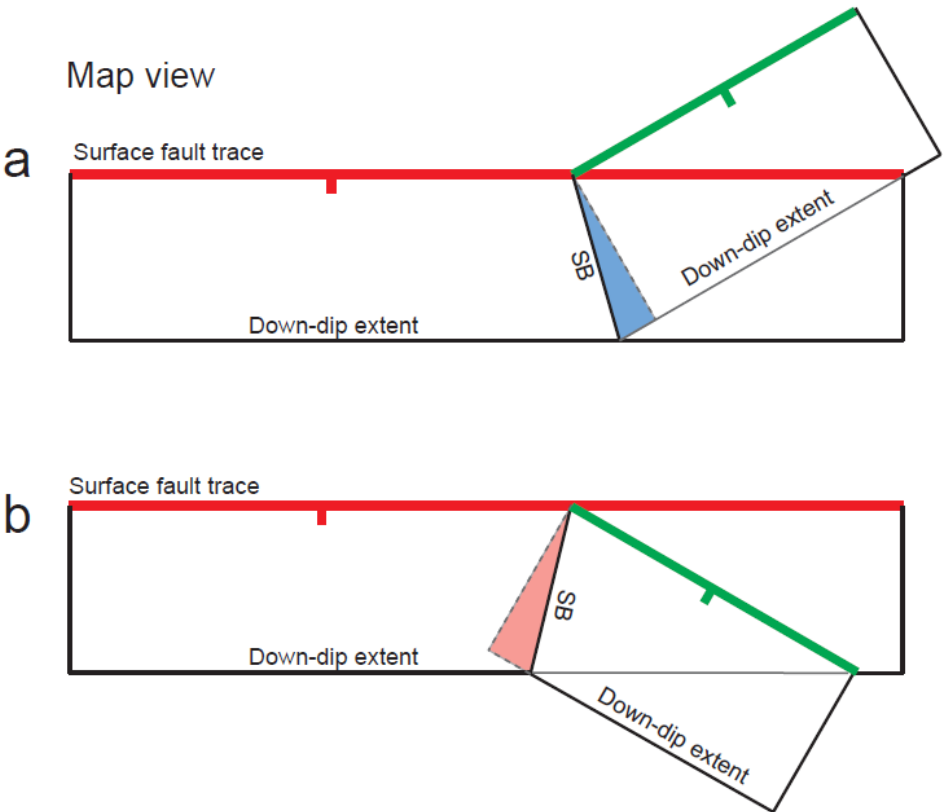


Figure 4.5 Illustration of oblique-fault intersection rules. Schematic map view of linkage rules associated with obliquely intersecting fault segments. (a) Extension of minor fault (green line) at depth to form seamless intersection with major fault (red line). (b) Truncation of minor fault (green line) at depth to form seamless intersection with major fault (red line). Areas added or subtracted are indicated by blue and red triangles, respectively. Segment boundaries (SB) are formed at the mutual intersection of the two faults.

## 5.0 MODEL COMPARISON

NZ CFM v1.0 describes a complex system of fault zones that define the Australian–Pacific plate boundary deformation zone through New Zealand. The model extent includes the offshore Puysegur and Hikurangi subduction zones, the Alpine Fault and various on- and offshore fault zones of the North and South Islands.

A major addition to the 3D representation of NZ CFM v1.0 compared to previous fault models are the plate boundary subduction structures. Delineated at the surface by the Puysegur, Hikurangi and Kermadec Trench subduction fronts, these are modelled as single, continuous fault surfaces to depths of 75 km. The Hope and Alpine faults, which accommodate substantial proportions of the plate motion through the continental collision section of the plate boundary, are each divided into 10 and 12 segments, respectively, and connect between the Puysegur and Hikurangi subduction zones. These major fault zones are contiguous from the surface to the maximum seismogenic rupture depth along their length. NZ CFM v1.0 contains a simple representation of the Alpine Fault incorporating dip-changes along strike, which is modelled as forming a smoothly varying structure with the Wairau Fault through to Cook Strait.

Fault zone intersections for major structures have been developed. The 3D representation of NZ CFM v1.0 includes the seamless intersection of crustal faults with subduction interfaces, the Alpine and Hope faults and North Island Dextral Fault Belt, for example. This improves upon the cross-cutting relationships of previous models. Regions with the highest degree of fault complexity include the northeastern South Island, where reverse fault zones intersect with strike-slip faults of the Marlborough Fault System, and the Bay of Plenty coastline where normal fault zones of the Havre Trough – Taupō Rift intersect with the strike-slip fault zones of the North Island Dextral Fault Belt.

The down-dip limits of fault zones are better constrained than previous compilations (e.g. Stirling et al. 2012) with two estimates provided from analysis and modelling of seismicity and crustal heat flow (Ellis et al. 2021). Depending on requirements, either a maximum estimate of fault rupture or the depth to the base of the seismogenic zone can be utilised.

Fault zone geometries have been modified from Litchfield et al. (2013, 2014) in the Marlborough Fault System domain in accordance with rupture patterns associated with the 2016  $M_w$  7.8 Kaikōura earthquake (Goded et al. 2018a). Fault zone geometries in the region of the Kaikōura earthquake are complex, containing a series of shallowly dipping reverse faults that intersect with major steeply dipping strike-slip faults, all overlying the southern termination of the Hikurangi subduction interface at depths of c. 22–25 km.

The number of fault zones in the Northwestern South Island domain has increased relative to previous 2D models, with additions including both active and capable faults (e.g. Figure 1.1). Earthquakes in this region comprise some of the largest recorded historical events (post-1840 AD) though are sparse. Kinematic data for a number of these fault zones are not well constrained for current activity. Active and capable fault zones in the Auckland and Waikato regions are also newly included.

Compared to previous 2D models, many more faults have been incorporated in the eastern to southern South Island. These include the main range-bounding faults that have experienced major late Cenozoic throw but with insufficient surface evidence to support classification as active. The addition of these numerous fault zones, classified as ‘capable’, provides a much more complete picture of tectonic development though the eastern to southern South Island related to the plate boundary.

Normal fault zones outboard of the Puysegur and northern Hikurangi subduction fronts have been classified as 'capable fault zones'. These outer-rise fault zones have clear bathymetric offsets but do not necessarily meet criteria for classification as active. This situation also applies to the offshore reverse faults along the Fiordland and southern Hikurangi subduction margins, where near-surface folds delineate underlying fault zones but where recent activity has not been demonstrated. Outer-rise faults, particularly along the Fiordland margin, have been assigned shallower depths than in previous compilations due to the relative thinness of the oceanic crust.

The fault zones in the Southern Alps domain are not proven active (i.e. lack of Quaternary sediments hinders evaluation of recent activity) but are located in a region of high strain adjacent to the Alpine Fault. Southern Alps fault zones have orientations compatible with movement within that strain field and therefore are considered potentially capable of being seismogenic.

The neotectonic domains have more uniform areas and spatial distribution compared with previous models. The domains have been developed to better characterise the fault zone style and trend in a given region. A summary of fault zone strike orientation highlights the principal azimuth of fault zones in each neotectonic domain (Figure 5.1; Rattenbury 2022). Fault and fault segment strikes were sampled at lengths of 1 km or less to provide an average azimuth per sample. The fault strike azimuths for every sample were divided into 10° bins to generate fault-orientation statistics for each neotectonic domain. The intent of the analysis was to capture the along-strike variability of fault azimuth through a meaningful level of sampling relative to the compilation scale. These data are shown as rose diagrams in Figure 5.1.

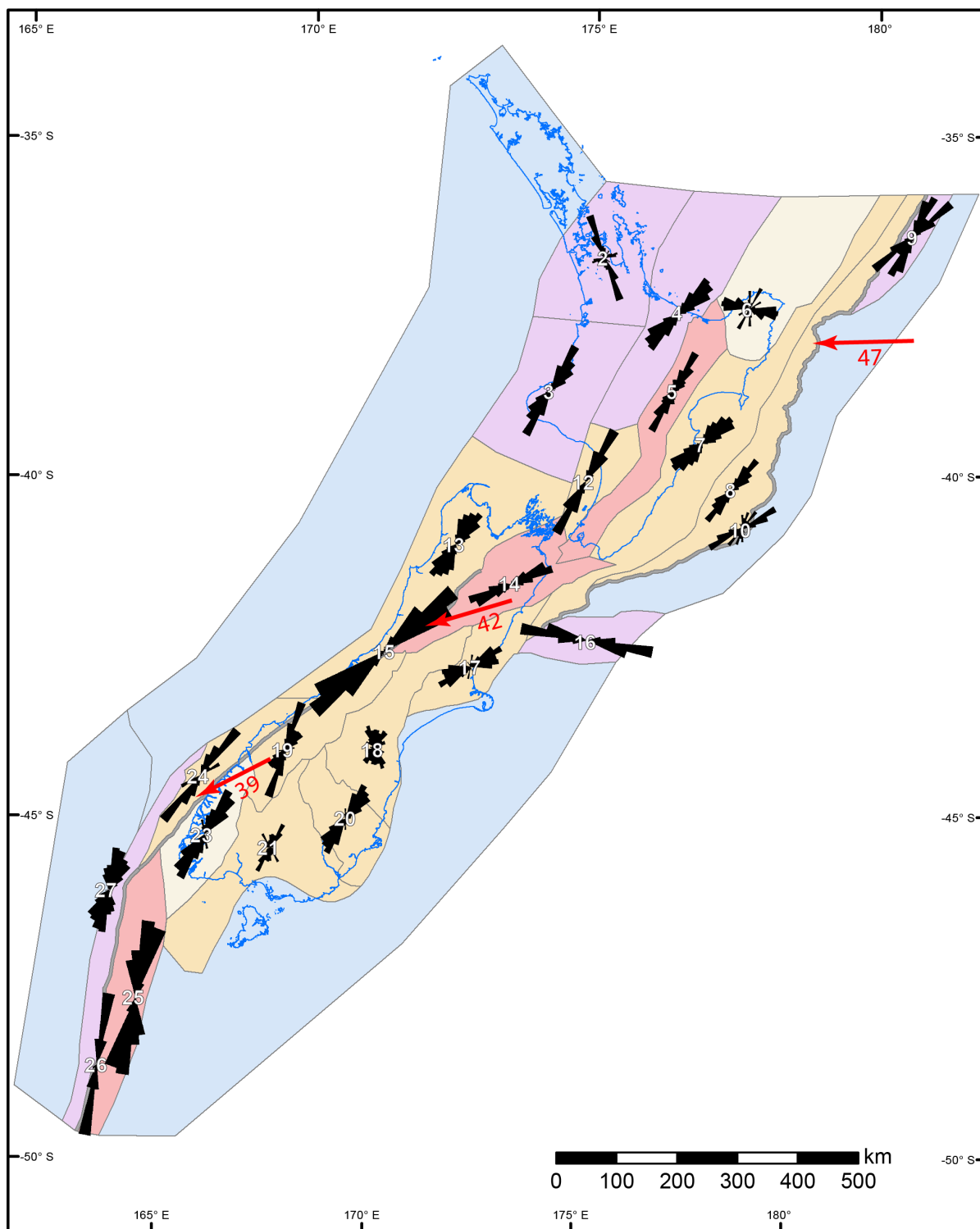


Figure 5.1 NZ CFM v1.0 fault strike azimuth by neotectonic domain, after Rattenbury (2022). The rose diagrams are in 10° increments, scaled according to maximum percentage per domain. The name, number (shown with the associated rose diagram) and fault style for each neotectonic domain are shown in Figure 3.3 and detailed in Table 3.1. Motion vectors of the Pacific Plate relative to the Australian Plate (red arrows with rates in mm/yr) from Beavan et al. (2002) are shown for reference.

The fault zone azimuth data in Figure 5.1 shows the predominant N–NE trend of the majority of active or capable fault zones within the New Zealand plate boundary. The notable exceptions to this trend are the North Waikato – South Auckland (3), North Meroo fracture zone (16) and Central Canterbury (18) domains (Figure 5.1). These domains contain a significant proportion of fault zones or basement fabrics inherited from previous deformation episodes that have been re-activated in the present-day tectonic regime.

Two crustal profiles through NZ CFM v1.0 in the southern North Island and northeastern South Island (locations shown in Figure 5.2) show the down-dip geometry of faults with respect to independent earthquake- and active-source-derived data (Figures 5.3 and 5.4).

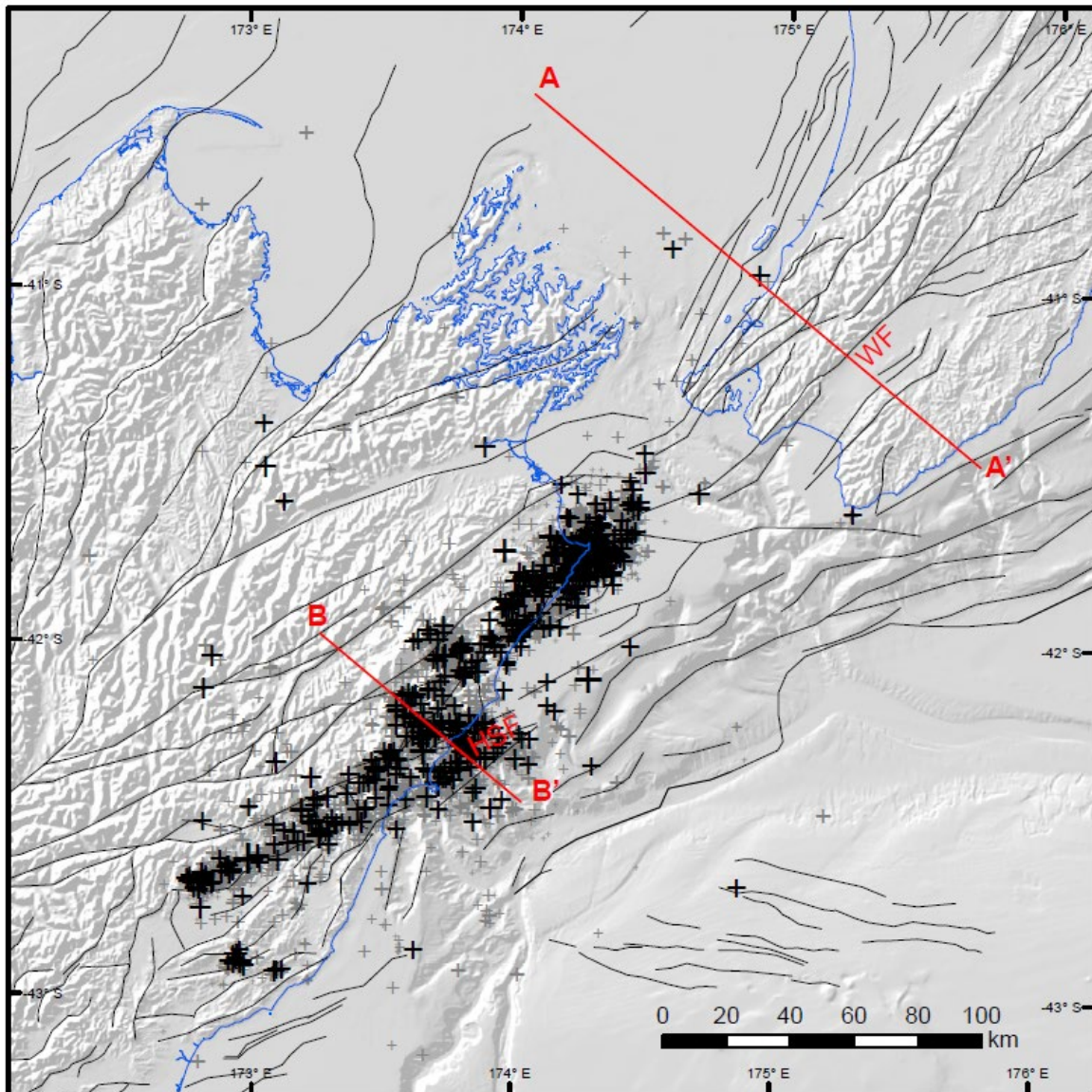


Figure 5.2 Crustal profile location map. Location of crustal profiles depicted in Figures 5.3 (A–A') and 5.4 (B–B') shown by red lines. Relocated earthquakes (black and grey crosses) associated with the Kaikōura earthquake (Chamberlain et al. 2021) shown with respect to NZ CFM v1.0 (black lines). Abbreviations: WF = Wairarapa Fault; HSF = Hope Seaward Fault.

A profile through the southern North Island along the deep geophysical SAHKE transect (Henry et al. 2013) allows comparison of the fault model representation to P-wave velocity ( $V_p$ ) and attenuation ( $Q_p$ ) inversions (Eberhart-Phillips et al. 2020; Figure 5.3). At depths of 10–20 km, higher P-wave velocities in the hanging walls of major strike-slip and reverse slip faults indicate that the down-dip projection of these faults appears appropriate (Figure 5.3a).

We note that the maximum depth of faulting represented by Dfc, the combined seismogenic and thermal model of Ellis et al. (2021), is deeper in this region than the Moho determined by active-source studies (Henrys et al. 2013) and a Moho proxy estimated by the 7.5 km/s isovelocity surface (Reyners et al. 2006; Eberhart-Phillips et al. 2020; Figure 5.3a). Regions of localised high attenuation appear at the intersections of crustal faults with the subduction interface. The coincidence of high attenuation regions at the intersection of faults with the plate interface, potentially associated with fluids, support the geometry of faults in this location. A strong, near-vertical, attenuation contrast is also coincident with the projection of the Wairarapa Fault to depth. The Wairarapa Fault in this location appears to separate regions of low attenuation to the west (high Qp) from high attenuation to the east (low Qp). The steep planar geometry of the Wairarapa Fault represented in NZ CFM v1.0 differs significantly from the interpretation of Henrys et al. (2013), which shows a listric fault that does not intersect with the plate interface.

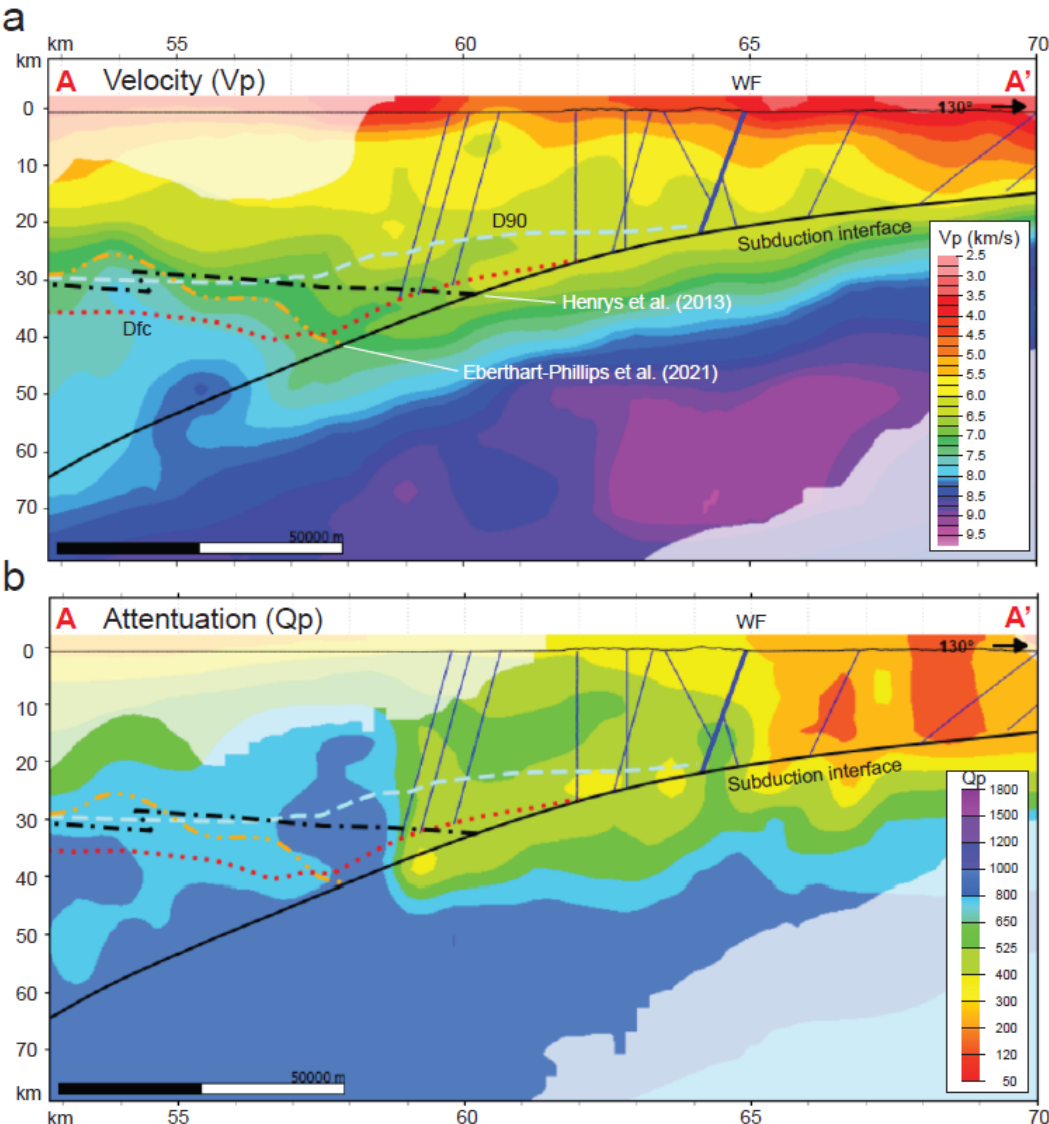


Figure 5.3 Southern North Island crustal profile. Faults of NZ CFM v1.0 superimposed on the P-wave velocity (Vp) and attenuation (Qp) of Eberhart-Phillips et al. (2020) (y-model -173 km). See Figure 5.2 for location. Maximum fault depths (Dfc – red dotted line) and seismologically determined D90 (light-blue dashed line) of Ellis et al. (2021) shown with respect to Moho estimates from an active-source velocity model of Henrys et al. (2013) (black dash-dot line) and the 7.5 km/s isovelocity surface of Eberhart-Phillips et al. (2020) (orange dash-dot line).

A profile through the northeastern South Island through the region of the  $M_w$  7.8 Kaikōura earthquake aftershock sequence (Chamberlain et al. 2021) allows comparison between the location of relocated earthquakes and NZ CFM v1.0. (Figure 5.4). Similar to the previous profile, the P-wave attenuation ( $Q_p$ ) and the  $V_p/V_s$  ratio (Eberhart-Phillips et al. 2020) provide context to both the fault model and earthquake distribution. It is noted that there are no strong dipping alignments of earthquakes from which to delineate major faults at depth. Relocated earthquakes typically form clusters that may represent zones of distributed deformation surrounding fault zones, or their intersections, at depth. Similar to the Wairarapa Fault, the Hope Seward Fault has high attenuation in the hanging wall of this predominantly strike-slip fault (Figure 5.4a). Few relocated earthquakes occur on or near the plate interface, and D90 of Ellis et al. (2021) coincides well with the bulk of the aftershock seismicity.

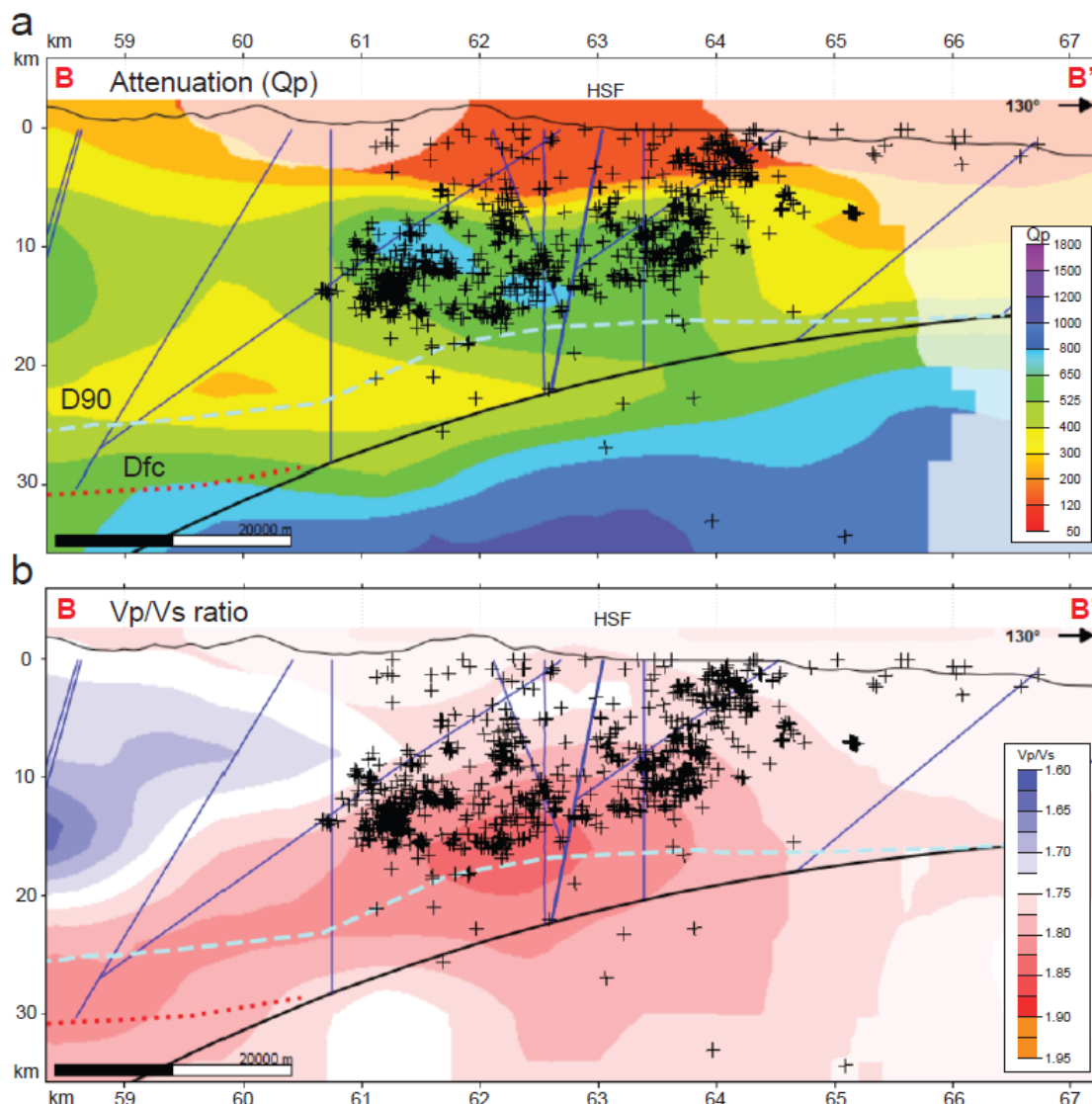


Figure 5.4 Northeastern South Island crustal profile. Faults of NZ CFM v1.0 superimposed on the P-wave attenuation ( $Q_p$ ) and  $V_p/V_s$  ratio of Eberhart-Phillips et al. (2020) (y-model 0 km). See Figure 5.2 for location. Relocated earthquakes (black crosses) highlight the distributed nature of deformation after the 2016  $M_w$  7.8 Kaikōura earthquake. Relocated earthquakes within 5 km of the profile location shown in Figure 5.2 are projected normal to the trend of the section. Maximum fault depths (Dfc – red dotted line) and seismologically determined D90 (light-blue dashed line) of Ellis et al. (2021) are shown for reference.

As the examples demonstrate, the combination of independent geological and geophysical data with NZ CFM v1.0 will allow further refinement and understanding of earthquake-generating faults along the New Zealand plate boundary zone for future iterations of the fault model.

## 6.0 TOWARD NZ CFM V2.0

Data described within NZ CFM v1.0 are a key component for seismic hazard analysis in New Zealand. For example, NZ CFM v1.0 and its predecessors and successors form the foundation for the geological deformation model within the New Zealand NSHM. In addition, within the current update of the NSHM, the geodetic deformation model (Johnson et al., forthcoming 2022) will utilise the geometry described in NZ CFM v1.0 and, in some cases, slip rate also.

It is envisaged that NZ CFM v1.0 will provide the starting point for future fault-model updates by the scientific community and, ideally, the community as a whole will provide the input and impetus for these updates. While new versions of the fault model will be contingent on appropriate funding, it is envisioned that periodic review and update of the NZ CFM would be undertaken on a frequency similar to that proposed for updates of the NSHM (i.e. every c. 5 years) and dependent on regions with new or improved constraints. Below is a list of processes and features that could be part of, or related to, the ongoing development of the NZ CFM.

- Regular update of the current fault source model, including checking consistency with other databases, such as the New Zealand Paleoseismic Site Database.
- Development of practitioner-oriented web interface to facilitate viewing and uptake of the NZ CFM (perhaps similar to what has been developed for the SCEC CFM<sup>7</sup>).
- Development of kinematically optimised fault intersection and linkage rules.
- Development of tools to:
  - Enable automated meshing of the model.
  - Generate (and automate?) alternative fault geometries (i.e. differing fault dips, including changing, non-planar dips with depth).
  - Quantify geometric uncertainties.
  - Domain by domain upgrade of the model at more detailed scale(s) compared to NZ CFM v1.0 and explicit incorporation of relevant 3D data such as topography, bathymetry, seismic lines, well logs, etc.
- Develop methodologies/workflows that ensure increased integration, compatibility and usability between:
  - New Zealand Community Fault Model
  - New Zealand Active Faults Database
  - Geological maps of New Zealand, and
  - National Seismic Hazard Model fault source model.

---

7 <https://www.scec.org/research/cfm-viewer/>

## 7.0 ACKNOWLEDGMENTS

Funding was provided for this project by the New Zealand Ministry of Business, Innovation & Employment to GNS Science via the National Seismic Hazard Model Programme (contract 2020-BD101), Strategic Science Investment Fund and Capability Development Fund; and to the National Science Challenges via the Resilience to Nature's Challenges Earthquake and Tsunami Programme (contract C05X1901). J Griffin published with the permission of the CEO, Geoscience Australia.

## 8.0 REFERENCES

- Abbott ER, Villamor P, Langridge RM, Perrin ND, McVerry GH. 2017. Seismic design spectra for Matahina Dam. Lower Hutt (NZ): GNS Science. 86 p. Consultancy Report 2017/13. Prepared for Trustpower Ltd.
- Aki K, Richards PG. 2002. Quantitative seismology. 2<sup>nd</sup> ed. Sausalito (CA): University Science Books. 700 p.
- Amos CB, Burbank DW, Nobes DC, Read SAL. 2007. Geomorphic constraints on listric thrust faulting: implications for active deformation in the Mackenzie Basin, South Island, New Zealand. *Journal of Geophysical Research: Solid Earth*. 112(B3):B03S11. doi:10.1029/2006JB004291.
- Amos CB, Burbank DW, Read SAL. 2010. Along-strike growth of the Ostler fault, New Zealand: consequences for drainage deflection above active thrusts. *Tectonics*. 29(4):TC4021. doi:10.1029/2009TC002613.
- Amos CB, Lapwood JJ, Nobes DC, Burbank DW, Rieser U, Wade A. 2011. Palaeoseismic constraints on Holocene surface ruptures along the Ostler Fault, southern New Zealand. *New Zealand Journal of Geology and Geophysics*. 54(4):367–378. doi:10.1080/00288306.2011.601746.
- Anderson H, Beanland S, Blick G, Darby DJ, Downes GL, Haines AJ, Jackson J, Robinson R, Webb TH. 1994. The 1968 May 23 Inangahua, New Zealand, earthquake: an integrated geological, geodetic, and seismological source model. *New Zealand Journal of Geology and Geophysics*. 37(1):59–86. doi:10.1080/00288306.1994.9514601.
- Armstrong MJ. 2000. Geomorphological and geophysical investigation of the effects of active tectonic deformation on the hydrogeology of North Culverden Basin, North Canterbury [PhD thesis]. Christchurch (NZ): University of Canterbury. 211 p. + appendices.
- Ballard HR. 1989. Permian arc volcanism and aspects of the general geology of the Skippers Range, NW Otago [PhD thesis]. Dunedin (NZ): University of Otago. 1 vol.
- Bannister S, Gledhill K. 2012. Evolution of the 2010–2012 Canterbury earthquake sequence. *New Zealand Journal of Geology and Geophysics*. 55(3):295–304. doi:10.1080/00288306.2012.680475.
- Barker DHN, Henrys S, Caratori Tontini F, Barnes PM, Bassett D, Todd E, Wallace L. 2018. Geophysical constraints on the relationship between seamount subduction, slow slip, and tremor at the North Hikurangi Subduction Zone, New Zealand. *Geophysical Research Letters*. 45(23):12804–12813. doi:10.1029/2018gl080259.
- Barker DHN, Sutherland R, Henrys S, Bannister S. 2009. Geometry of the Hikurangi subduction thrust and upper plate, North Island, New Zealand. *Geochemistry, Geophysics, Geosystems*. 10(2):Q02007. doi:10.1029/2008gc002153.
- Barnes PM. 1994a. Continental extension of the Pacific Plate at the southern termination of the Hikurangi subduction zone: the North Mernoo Fault Zone, offshore New Zealand. *Tectonics*. 13(4):735–754. doi:10.1029/94TC00798.

- Barnes PM. 1994b. Inherited structural control from repeated Cretaceous to Recent extension in the North Mernoo Fault Zone, western Chatham Rise, New Zealand. *Tectonophysics*. 237(1–2):27–46. doi:10.1016/0040-1951(94)90157-0.
- Barnes PM. 1994c. Pliocene-Pleistocene depositional units on the continental slope off central New Zealand: control by slope currents and global climate cycles. *Marine Geology*. 117(1–4):155–175. doi:10.1016/0025-3227(94)90012-4.
- Barnes PM. 1996. Active folding of Pleistocene unconformities on the edge of the Australian-Pacific plate boundary zone, offshore North Canterbury, New Zealand. *Tectonics*. 15(3):623–640. doi:10.1029/95TC03249.
- Barnes PM. 2009. Postglacial (after 20 ka) dextral slip rate of the offshore Alpine fault, New Zealand. *Geology*. 37(1):3–6. doi:10.1130/g24764a.1.
- Barnes PM, Audru J-C. 1999a. Quaternary faulting in the offshore Flaxbourne and Wairarapa Basins, southern Cook Strait, New Zealand. *New Zealand Journal of Geology and Geophysics*. 42(3):349–367. doi:10.1080/00288306.1999.9514851.
- Barnes PM, Audru J-C. 1999b. Recognition of active strike-slip faulting from high-resolution marine seismic reflection profiles: Eastern Marlborough fault system, New Zealand. *Geological Society of America Bulletin*. 111(4):538–559. doi:10.1130/0016-7606(1999)111<0538:ROASSF>2.3.CO;2.
- Barnes PM, Bostock HC, Neil HL, Strachan LJ, Gosling M. 2013. A 2300-year paleoearthquake record of the Southern Alpine Fault and Fiordland Subduction Zone, New Zealand, based on stacked turbidites. *Bulletin of the Seismological Society of America*. 103(4):2424–2446. doi:10.1785/0120120314.
- Barnes PM, Davy B, Sutherland R, Delteil J. 2002a. Frontal accretion and thrust wedge evolution under very oblique plate convergence: Fiordland Basin, New Zealand. *Basin Research*. 14(4):439–466. doi:10.1046/j.1365-2117.2002.00178.x.
- Barnes PM, de Lépinay BM. 1997. Rates and mechanics of rapid frontal accretion along the very obliquely convergent southern Hikurangi margin, New Zealand. *Journal of Geophysical Research: Solid Earth*. 102(B11):24931–24952. doi:10.1029/97JB01384.
- Barnes PM, de Lépinay BM, Collot J-Y, Delteil J, Audru J-C. 1998. Strain partitioning in the transition area between oblique subduction and continental collision, Hikurangi margin, New Zealand. *Tectonics*. 17(4):534–557. doi:10.1029/98TC00974.
- Barnes PM, Ghisetti FC. 2016. Structure, late Quaternary slip rate and earthquake potential of marine reverse faults along the North Westland deformation front, New Zealand. *New Zealand Journal of Geology and Geophysics*. 59(1):157–175. doi:10.1080/00288306.2015.1112816.
- Barnes P, Ghisetti F, Ellis S, Morgan J. 2018. The role of protothrusts in frontal accretion and accommodation of plate convergence, Hikurangi subduction margin, New Zealand. *Geosphere*. 14(2):440–468. doi:10.1130/GES01552.1.
- Barnes PM, Ghisetti FC, Gorman AR. 2016. New insights into the tectonic inversion of North Canterbury and the regional structural context of the 2010–2011 Canterbury earthquake sequence, New Zealand. *Geochemistry, Geophysics, Geosystems*. 17(2):324–345. doi:10.1002/2015GC006069.
- Barnes PM, Lamarche G, Bialas J, Henrys S, Pecher I, Netzeband G, Greinert J, Mountjoy J, Pedley K, Crutchley G. 2010. Tectonic and geological framework for gas hydrates and cold seeps on the Hikurangi Subduction Margin, New Zealand. *Marine Geology*. 272(1–4):26–48. doi:10.1016/j.margeo.2009.03.012.

- Barnes PM, Nicol A. 2004. Formation of an active thrust triangle zone associated with structural inversion in a subduction setting, eastern New Zealand. *Tectonics*. 23(1):TC1015. doi:10.1029/2002TC001449.
- Barnes PM, Nicol A, Harrison T. 2002b. Late Cenozoic evolution and earthquake potential of an active listric thrust complex above the Hikurangi subduction zone, New Zealand. *GSA Bulletin*. 114(11):1379–1405. doi:10.1130/0016-7606(2002)114<1379:Lceaep>2.0.Co;2.
- Barnes PM, Nodder SD, Woelz S, Orpin AR. 2019. The structure and seismic potential of the Aotea and Evans Bay faults, Wellington, New Zealand. *New Zealand Journal of Geology and Geophysics*. 62(1):46–71. doi:10.1080/00288306.2018.1520265.
- Barnes PM, Pondard N. 2010. Derivation of direct on-fault submarine paleoearthquake records from high-resolution seismic reflection profiles: Wairau Fault, New Zealand. *Geochemistry, Geophysics, Geosystems*. 11(11):Q11013. doi:10.1029/2010GC003254.
- Barnes PM, Sutherland R, Delteil J. 2005. Strike-slip structure and sedimentary basins of the southern Alpine Fault, Fiordland, New Zealand. *GSA Bulletin*. 117(3–4):411–435. doi:10.1130/b25458.1.
- Barnes PM, Wallace LM, Saffer DM, Bell RE, Underwood MB, Fagereng A, Meneghini F, Savage HM, Rabinowitz HS, Morgan JK, et al. 2020. Slow slip source characterized by lithological and geometric heterogeneity. *Science Advances*. 6(13). doi:10.1126/sciadv.aay3314.
- Barrell DJA. 2013. General distribution and characteristics of active faults and folds in the Selwyn District, North Canterbury. Dunedin (NZ): GNS Science. 53 p. Consultancy Report 2012/325. Prepared for Environment Canterbury.
- Barrell DJA. 2015. General distribution and characteristics of active faults and folds in the Kaikoura District, North Canterbury. Dunedin (NZ): GNS Science. 59 p. Consultancy Report 2014/210. Prepared for Environment Canterbury.
- Barrell DJA. 2016. General distribution and characteristics of active faults and folds in the Waimate District and Waitaki District, South Canterbury and North Otago. Dunedin (NZ): GNS Science. 124 p. + 1 DVD. Consultancy Report 2015/166. Prepared for Canterbury Regional Council (Environment Canterbury); Otago Regional Council.
- Barrell DJA. 2019a. General distribution and characteristics of active faults and folds in the Queenstown Lakes and Central Otago districts, Otago. Dunedin (NZ): GNS Science. 99 p. Consultancy Report 2018/207. Prepared for Otago Regional Council.
- Barrell DJA. 2019b. Review of active fault information for the Waimakariri District. Dunedin (NZ): GNS Science. 11 p. Consultancy Report 2019/141LR. Prepared for Environment Canterbury.
- Barrell DJA. 2021. General distribution and characteristics of active faults and folds in the Clutha and Dunedin City districts, Otago. Dunedin (NZ): GNS Science. 71 p. Consultancy Report 2020/88. Prepared for Otago Regional Council.
- Barrell DJA, Begg JG. 2013. General distribution and characteristics of active faults and folds in the Waimakariri District, North Canterbury. Dunedin (NZ): GNS Science. 53 p. Consultancy Report 2012/326. Prepared for Environment Canterbury.
- Barrell DJA, Langridge RM, Berryman KR, Lukovic B. 2004. Seismic loads on dams – Waitaki system: Dryburgh–Stonewall fault displacement characterisation. Dunedin (NZ): Institute of Geological & Nuclear Sciences. 47 p. Client Report 2004/56. Prepared for URS New Zealand Limited.
- Barrell DJA, Langridge RM, Litchfield NJ, Fraser HL, Lukovic B. 2005. Seismic loads on dams – Waitaki system: Dryburgh Fault displacement characterisation. Dunedin (NZ): Institute of Geological & Nuclear Sciences. 64 p. Client Report 2005/70. Prepared for URS New Zealand Limited.

- Barrell DJA, Litchfield NJ, Van Dissen RJ, Wang N, Taylor Silva BI, Hornblow S, Stirling MW. 2020. Investigations of past earthquakes on the Titri Fault, coastal Otago, New Zealand. Lower Hutt (NZ): GNS Science. 66 p. (GNS Science report; 2017/35).
- Barrell DJA, Read SAL, Van Dissen RJ, Macfarlane DF, Walker J, Rieser U. 2009. Aviemore: a dam of two halves. In: Turnbull IM, editor. *Geological Society of New Zealand & New Zealand Geophysical Society Joint Annual Conference, field trip guides*. 2009 Nov 23–27; Oamaru, New Zealand. Wellington (NZ): Geological Society of New Zealand. p. 30. (Miscellaneous publication; 128B).
- Barrell DJA, Stirling M, Williams J, Sauer KM, van den Berg EJ. In press. Hundalee Fault, North Canterbury, New Zealand: Late Quaternary activity and regional tectonics. *New Zealand Journal of Geology and Geophysics, Special Issue: Kaikōura earthquake 5 years on*.
- Barrell DJA, Strong DT. 2009. General distribution and characteristics of active faults and folds in the Ashburton district, mid-Canterbury. Dunedin (NZ): GNS Science. 17 p. + 1 CD. Consultancy Report 2009/227. Prepared for Environment Canterbury.
- Barrell DJA, Strong DT. 2010. General distribution and characteristics of active faults and folds in the Mackenzie District, South Canterbury. Dunedin (NZ): GNS Science. 22 p. + 1 CD. Consultancy Report 2010/147. Prepared for Environment Canterbury.
- Barrell DJA, Strong DT. 2012. Geological contours for groundwater modelling, South Canterbury. Dunedin (NZ): GNS Science. 11 p. + appendices. Consultancy Report 2012/245. Prepared for Canterbury Regional Council.
- Barrell DJA, Townsend DB. 2012. General distribution and characteristics of active faults and folds in the Hurunui District, North Canterbury. Dunedin (NZ): GNS Science. 30 p. + 1 CD. Consultancy Report 2012/113. Prepared for Environment Canterbury.
- Barrell DJA, Van Dissen RJ. 2003. Project Aqua Geotechnical Investigations: activity of geological faults in the lower Waitaki Valley. Dunedin (NZ): Institute of Geological & Nuclear Sciences. 43 p. Client Report 2003/107. Prepared for URS New Zealand Limited.
- Barrell DJA, Van Dissen RJ. 2013. Peer review of additional geotechnical investigations for the proposed Hurricane Gully dam, Waitohi River, North Canterbury. Dunedin (NZ): GNS Science. 8 p. Consultancy Report 2013/140LR. Prepared for Hurunui Water Project Limited.
- Barrell DJA, Van Dissen RJ. 2014. Assessment of active fault ground deformation hazards associated with the Ashley Fault Zone, Loburn, North Canterbury. Dunedin (NZ): GNS Science. 59 p. + 1 DVD. Consultancy Report 2013/173. Prepared for Environment Canterbury.
- Barrell DJA, Van Dissen RJ, Berryman KR, Read SAL, Wood PR, Zachariassen J, Lukovic B, Nicol A, Litchfield NJ. 2002. Seismic loads on dams: Waitaki system, Aviemore Power Station. Geological investigations for fault displacement characterisation. Dunedin (NZ): Institute of Geological & Nuclear Sciences. 2 vol. Client Report 2001/125. Prepared for URS New Zealand Limited on behalf of Meridian Energy Limited.
- Barrell DJA, Van Dissen RJ, Langridge RM, Cox SC, Wilson KJ, Rieser U, Lukovic B. 2008. Seismic loads on dams: Waitaki system – Kirkliston Fault displacement characterisation. Dunedin (NZ): GNS Science. 1 vol. Consultancy Report 2007/146. Prepared for URS New Zealand Limited on behalf of Meridian Energy Limited.
- Barth NC, Kulhanek DK, Beu AG, Murray-Wallace CV, Hayward BW, Mildenhall DC, Lee DE. 2014. New c. 270 kyr strike-slip and uplift rates for the southern Alpine Fault and implications for the New Zealand plate boundary. *Journal of Structural Geology*. 64:39–52. doi:10.1016/j.jsg.2013.08.009.

- Bartholomew TD, Little TA, Clark KJ, Van Dissen R, Barnes PM. 2014. Kinematics and paleoseismology of the Vernon Fault, Marlborough Fault System, New Zealand: implications for contractional fault bend deformation, earthquake triggering, and the record of Hikurangi subduction earthquakes. *Tectonics*. 33(7):1201–1218. doi:10.1002/2014TC003543.
- Beanland S. 1995. The North Island dextral fault belt, Hikurangi subduction margin, New Zealand [PhD thesis]. Wellington (NZ): Victoria University of Wellington. 341 p.
- Beanland S, Barrow-Hurlbert SA. 1988. The Nevis-Cardrona Fault System, Central Otago, New Zealand: Late Quaternary tectonics and structural development. *New Zealand Journal of Geology and Geophysics*. 31(3):337–352. doi:10.1080/00288306.1988.10417780.
- Beanland S, Berryman KR. 1987. Ruahine Fault reconnaissance. Lower Hutt (NZ): New Zealand Geological Survey. 15 p. Report EDS 109.
- Beanland S, Berryman KR. 1989. Style and episodicity of late Quaternary activity on the Pisa–Grandview Fault Zone, Central Otago, New Zealand. *New Zealand Journal of Geology and Geophysics*. 32(4):451–461. doi:10.1080/00288306.1989.10427553.
- Beanland S, Berryman KR. 1990. Hundalee Fault, North Canterbury. Lower Hutt (NZ): New Zealand Geological Survey. 12 p. Client Report 90/7. Prepared for Works and Development Services Corporation New Zealand Limited and Transit New Zealand.
- Beanland S, Berryman KR. 1991. Paleoseismicity studies of the Wellington Fault northeast of the Tararua Ranges. *Geological Society of New Zealand Newsletter*. 93:42–46.
- Beanland S, Berryman KR, Blick GH. 1989. Geological investigations of the 1987 Edgecumbe earthquake, New Zealand. *New Zealand Journal of Geology and Geophysics*. 32(1):73–91. doi:10.1080/00288306.1989.10421390.
- Beanland S, Blick GH, Darby DJ. 1990. Normal faulting in a back arc basin: geological and geodetic characteristics of the 1987 Edgecumbe Earthquake, New Zealand. *Journal of Geophysical Research: Solid Earth*. 95(B4):4693–4707. doi:10.1029/JB095iB04p04693.
- Beanland S, Fellows DL. 1985. Late Quaternary faulting at the Hawkdun lignite deposit, Central Otago. [Wellington] (NZ): New Zealand Geological Survey. 14 p. Immediate Report EDS 85/23.
- Beauprêtre S, Garambois S, Manighetti I, Malavieille J, Sénéchal G, Chatton M, Davies T, Larroque C, Rousset D, Cotte N, et al. 2012. Finding the buried record of past earthquakes with GPR-based palaeoseismology: a case study on the Hope fault, New Zealand. *Geophysical Journal International*. 189(1):73–100. doi:10.1111/j.1365-246X.2012.05366.x.
- Beavan J, Fielding E, Motagh M, Samsonov S, Donnelly N. 2011. Fault location and slip distribution of the 22 February 2011 Mw 6.2 Christchurch, New Zealand, earthquake from geodetic data. *Seismological Research Letters*. 82(6):789–799. doi:10.1785/gssrl.82.6.789.
- Beavan RJ, Litchfield NJ. 2012. Vertical land movement around the New Zealand coastline: implications for sea-level rise. Lower Hutt (NZ): GNS Science. 41 p. (GNS Science report; 2012/29).
- Beavan J, Tregoning P, Bevis M, Kato T, Meertens C. 2002. Motion and rigidity of the Pacific Plate and implications for plate boundary deformation. *Journal of Geophysical Research: Solid Earth*. 107(B10):2261. doi:10.1029/2001JB000282.
- Becker JA, Craw D. 2000. Structure and neotectonics on the Main Divide, upper Wilberforce valley, mid Canterbury, New Zealand. *New Zealand Journal of Geology and Geophysics*. 43(2):217–228. doi:10.1080/00288306.2000.9514882.

- Begg JG, Johnston MR. 2000. Geology of the Wellington area [map]. Lower Hutt (NZ): Institute of Geological & Nuclear Sciences. 1 sheet + 64 p., scale 1:250,000. (Institute of Geological & Nuclear Sciences geological map; 10).
- Begg JG, Mouslopoulou V. 2010. Analysis of late Holocene faulting within an active rift using lidar, Taupo Rift, New Zealand. *Journal of Volcanology and Geothermal Research*. 190(1–2):152–167. doi:10.1016/j.jvolgeores.2009.06.001.
- Begg JG, Van Dissen RJ. 1998. Whitemans Valley Fault: a newly discovered active second order fault near Wellington, New Zealand: implications for regional seismic hazard. *New Zealand Journal of Geology and Geophysics*. 41(4):441–448. doi:10.1080/00288306.1998.9514821.
- Begg JG, Villamor P, Zachariassen J, Litchfield NJ. 2001. Paleoseismic assessment of the active Masterton and Carterton faults, Wairarapa. Lower Hutt (NZ): Institute of Geological & Nuclear Sciences. 32 p. Client Report 2001/70. Prepared for Wairarapa Engineering Lifelines Association.
- Bennett ER, Youngson JH, Jackson JA, Norris RJ, Raisbeck GM, Yiou F, Fielding E. 2005. Growth of South Rough Ridge, Central Otago, New Zealand: using in situ cosmogenic isotopes and geomorphology to study an active, blind reverse fault. *Journal of Geophysical Research: Solid Earth*. 110(B2):B02404. doi:10.1029/2004JB003184.
- Benson A, Hill N, Little TA, Van Dissen RJ. 2001a. Paleoseismicity, rates of active deformation, and structure of the Lake Jasper pull-apart basin, Awatere Fault, New Zealand. Wellington (NZ): Victoria University of Wellington, School of Earth Sciences. 1 vol. Consulting Report 2001/1.
- Benson AM, Little TA, Van Dissen RJ, Hill N, Townsend DB. 2001b. Late Quaternary paleoseismic history and surface rupture characteristics of the eastern Awatere strike-slip fault, New Zealand. *Geological Society of America Bulletin*. 113(8):1079–1091. doi:10.1130/0016-7606(2001)113<1079:Lqphas>2.0.Co;2.
- Bell R, Holden C, Power W, Wang X, Downes G. 2014. Hikurangi margin tsunami earthquake generated by slow seismic rupture over a subducted seamount. *Earth and Planetary Science Letters*. 397:1–9. doi:10.1016/j.epsl.2014.04.005.
- Bell R, Sutherland R, Barker DHN, Henrys S, Bannister S, Wallace L, Beavan J. 2010. Seismic reflection character of the Hikurangi subduction interface, New Zealand, in the region of repeated Gisborne slow slip events. *Geophysical Journal International*. 180(1):34–48. doi:10.1111/j.1365-246X.2009.04401.x.
- Berryman KR. 1980. Late Quaternary movement on White Creek Fault, South Island, New Zealand. *New Zealand Journal of Geology and Geophysics*. 23(1):93–101. doi:10.1080/00288306.1980.10424194.
- Berryman KR. 1988. Late Quaternary marine terrace distribution, stratigraphy, and deformation at Mahia Peninsula, New Zealand [PhD thesis]. Wellington (NZ): Victoria University of Wellington. 169 leaves.
- Berryman KR. 1993. Age, height, and deformation of Holocene marine terraces at Mahia Peninsula, Hikurangi subduction margin, New Zealand. *Tectonics*. 12(6):1347–1364. doi:10.1029/93tc01542.
- Berryman KR, Beanland S, Cooper AF, Cutten HN, Norris RJ, Wood PR. 1992. The Alpine Fault, New Zealand: variation in Quaternary structural style and geomorphic expression. *Annales Tectonicæ*. VI(suppl):126–163.
- Berryman KR, Beanland S, Wesnousky S. 1998. Paleoseismicity of the Rotoitipakau Fault Zone, a complex normal fault in the Taupo Volcanic Zone, New Zealand. *New Zealand Journal of Geology and Geophysics*. 41(4):449–465. doi:10.1080/00288306.1998.9514822.

- Berryman KR, Cochran UA, Clark KJ, Biasi GP, Langridge RM, Villamor P. 2012a. Major earthquakes occur regularly on an isolated plate boundary fault. *Science*. 336(6089):1690–1693. doi:doi:10.1126/science.1218959.
- Berryman KR, Cooper A, Norris R, Villamor P, Sutherland R, Wright T, Schermer E, Langridge RM, Biasi G. 2012b. Late Holocene rupture history of the Alpine Fault in South Westland, New Zealand. *Bulletin of the Seismological Society of America*. 102(2):620–638. doi:10.1785/0120110177.
- Berryman KR, Marden M, Palmer A, Litchfield NJ. 2009. Holocene rupture of the Repongaere Fault, Gisborne: implications for Raukumara Peninsula deformation and impact on the Waipaoa Sedimentary System. *New Zealand Journal of Geology and Geophysics*. 52(4):335–347. doi:10.1080/00288306.2009.9518462.
- Berryman KR, Ota Y, Miyauchi T, Hull A, Clark KJ, Ishibashi K, Iso N, Litchfield NJ. 2011. Holocene paleoseismic history of upper-plate faults in the southern Hikurangi subduction margin, New Zealand, deduced from marine terrace records. *Bulletin of the Seismological Society of America*. 101(5):2064–2087. doi:10.1785/0120100282.
- Berryman KR, Van Dissen RJ, Mouslopoulou V. 2002. Recent rupture of the Tararua section of the Wellington Fault and relationships to other fault sections and rupture segments. Lower Hutt (NZ): Institute of Geological & Nuclear Sciences. 22 p. EQC Research Report 97/248.
- Berryman KR, Villamor P. 2004. Surface rupture of the Poulter Fault in the 1929 March 9 Arthur's Pass earthquake, and redefinition of the Kakapo Fault, New Zealand. *New Zealand Journal of Geology and Geophysics*. 47(2):341–351. doi:10.1080/00288306.2004.9515060.
- Berryman KR, Villamor P, Litchfield NJ. 2001a. Waikato seismic loads task 4: review of faulting hazard. Lower Hutt (NZ): Institute of Geological & Nuclear Sciences. 31 p. + map. Client Report 2001/69. Prepared for URS & Mighty River Power.
- Berryman KR, Villamor P, Nairn IA, Van Dissen RJ, Begg JG, Lee JM. 2008. Late Pleistocene surface rupture history of the Paeroa Fault, Taupo Rift, New Zealand. *New Zealand Journal of Geology and Geophysics*. 51(2):135–158. doi:10.1080/00288300809509855.
- Berryman KR, Webb TH, Hill N, Stirling MW, Rhoades DA, Beavan RJ, Darby DJ. 2001b. Seismic loads on dams – Waitaki system: earthquake source characterisation. Lower Hutt (NZ): Institute of Geological & Nuclear Sciences. 80 p. + appendices. Client Report 2001/129. Prepared for URS (NZ) Limited on behalf of Meridian Energy Limited.
- Bishop DG. 1971. Farewell–Collingwood [map]. 1<sup>st</sup> ed. Wellington (NZ): Department of Scientific & Industrial Research. 1 fold. map + 1 booklet. (Geological map of New Zealand 1:63,360; S1, S3 & pt S4).
- Bishop DG. 1979. Ranfurly [map]. 1<sup>st</sup> ed. Wellington (NZ): Department of Scientific & Industrial Research. 1 fold. map + 1 booklet. (Geological map of New Zealand 1:63,360; sheet S135).
- Bland KJ, Uruski CI, Isaac MJ. 2015. Pegasus Basin, eastern New Zealand: a stratigraphic record of subsidence and subduction, ancient and modern. *New Zealand Journal of Geology and Geophysics*. 58(4):319–343. doi:10.1080/00288306.2015.1076862.
- Brough T, Nicol A, Stahl T, Pettinga JR, Van Dissen R, Clark D, Khajavi N, Pedley K, Langridge R, Wang N. 2021. Paleoseismicity of the western Humps fault on the Emu Plain, North Canterbury, New Zealand. *New Zealand Journal of Geology and Geophysics*. doi:10.1080/00288306.2021.1986727.

- Bull JM, Barnes PM, Lamarche G, Sanderson DJ, Cowie PA, Taylor SK, Dix JK. 2006. High-resolution record of displacement accumulation on an active normal fault: implications for models of slip accumulation during repeated earthquakes. *Journal of Structural Geology*. 28(7):1146–1166. doi:10.1016/j.jsg.2006.03.006.
- Buxton R, Langridge RM. 2017. Seismic design spectra for the Martha Hill Mine with rock ground conditions. Lower Hutt (NZ): GNS Science. 23 p. Consultancy Report 2017/177. Prepared for Engineering Geology Ltd.
- Buxton R, Langridge RM. 2019. Site specific seismic hazard study for the Mangahao substation site. Lower Hutt (NZ): GNS Science. 73 p. Consultancy Report 2019/36. Prepared for Mitton Electronet Limited.
- Cameron H. 2017. Evolution of a normal fault system, Northern Graben, Taranaki Basin, New Zealand. Wellington (NZ): Ministry of Business, Innovation & Employment. 158 p. New Zealand Unpublished Petroleum Report 5479.
- Canora-Catalán C, Villamor P, Berryman K, Martínez-Díaz JJ, Raen T. 2008. Rupture history of the Whirinaki fault, an active normal fault in the Taupo rift, New Zealand. *New Zealand Journal of Geology and Geophysics*. 51(4):277–293. doi:10.1080/00288300809509866.
- Carne RC, Little TA, Rieser U. 2011. Using displaced river terraces to determine Late Quaternary slip rate for the central Wairarapa Fault at Waiohine River, New Zealand. *New Zealand Journal of Geology and Geophysics*. 54(2):217–236. doi:10.1080/00288306.2010.532224.
- Carter RM, Norris RJ. 2005. The geology of the Blackmount district, Te Anau and Waiiau Basins, western Southland. Institute of Geological & Nuclear Sciences. 97 p. + 1 CD. (Institute of Geological & Nuclear Sciences science report; 2004/23).
- Chamberlain CJ, Frank WB, Lanza F, Townend J, Warren-Smith E. 2021. Illuminating the pre-, co-, and post-seismic phases of the 2016 M7.8 Kaikōura earthquake with 10 Years of seismicity. *Journal of Geophysical Research: Solid Earth*. 126(8):e2021JB022304. doi:10.1029/2021JB022304.
- Chan C-H, Ma K-F, Shyu JBH, Lee Y-T, Wang Y-J, Gao J-C, Yen Y-T, Rau R-J. 2020. Probabilistic seismic hazard assessment for Taiwan: TEM PSHA2020. *Earthquake Spectra*. 36(1\_suppl):137–159. doi:10.1177/8755293020951587.
- Chandler-Yates N. 2016. Active tectonic and paleoseismic investigation of the Lower Miconui Valley in Westland, New Zealand [MSc thesis]. Christchurch (NZ): University of Canterbury. 97 p.
- Chick LM, De Lange WP, Healy TR. 2001. Potential tsunami hazard associated with the Kerepehi Fault, Firth of Thames, New Zealand. *Natural Hazards*. 24(3):309–318. doi:10.1023/A:1012210314609.
- Clark KJ, Villamor P, Lee JM. 2019. Bay of Plenty regional active fault mapping for growth areas. Lower Hutt (NZ): GNS Science. 44 p. + appendices. Consultancy Report 2018/143. Prepared for Bay of Plenty Regional Council.
- Collot J-Y, Davy B. 1998. Forearc structures and tectonic regimes at the oblique subduction zone between the Hikurangi Plateau and the southern Kermadec margin. *Journal of Geophysical Research: Solid Earth*. 103(B1):623–650. doi:10.1029/97JB02474.
- Collot J-Y, Lamarche G, Wood RA, Delteil J, Sosson M, Lebrun J-Fdr, Coffin MF. 1995. Morphostructure of an incipient subduction zone along a transform plate boundary: Puysegur Ridge and Trench. *Geology*. 23(6):519–522. doi:10.1130/0091-7613(1995)023<0519:Moaisz>2.3.Co;2.

- Collot J-Y, Lewis K, Lamarche G, Lallemand S. 2001. The giant Ruatoria debris avalanche on the northern Hikurangi margin, New Zealand: Result of oblique seamount subduction. *Journal of Geophysical Research: Solid Earth*. 106(B9):19271–19297. doi:10.1029/2001JB900004.
- Cowan HA. 1990. Late Quaternary displacements on the Hope Fault at Glynn Wye, North Canterbury. *New Zealand Journal of Geology and Geophysics*. 33(2):285–293. doi:10.1080/00288306.1990.10425686.
- Cowan HA. 1991. The North Canterbury earthquake of September 1, 1888. *Journal of the Royal Society of New Zealand*. 21(1):1–12. doi:10.1080/03036758.1991.10416105.
- Cowan HA, McGlone MS. 1991. Late Holocene displacements and characteristic earthquakes on the Hope River segment of the Hope Fault, New Zealand. *Journal of the Royal Society of New Zealand*. 21(4):373–384. doi:10.1080/03036758.1991.10420834.
- Cowan H, Nicol A, Tonkin P. 1996. A comparison of historical and paleoseismicity in a newly formed fault zone and a mature fault zone, North Canterbury, New Zealand. *Journal of Geophysical Research: Solid Earth*. 101(B3):6021–6036. doi:10.1029/95JB01588.
- Cox SC, Barrell DJA. 2007. Geology of the Aoraki area [map]. Lower Hutt (NZ): GNS Science. 1 folded map + 71 p., scale 1:250,000. (Institute of Geological & Nuclear Sciences 1:250,000 geological map; 15).
- Cox SC, Stirling MW, Herman F, Gerstenberger M, Ristau J. 2012. Potentially active faults in the rapidly eroding landscape adjacent to the Alpine Fault, central Southern Alps, New Zealand. *Tectonics*. 31(2):TC2011. doi:10.1029/2011TC003038.
- Craw D, Parvizi E, Read S, Fraser CI, Waters JM. 2021. Late Holocene uplift of a coastal terrace near the Akatore Fault, southern New Zealand. *New Zealand Journal of Geology and Geophysics*. 64(4):542–557. doi:10.1080/00288306.2020.1828940.
- Crutchley GJ, Klaeschen D, Henrys SA, Pecher IA, Mountjoy JJ, Woelz S. 2020. Subducted sediments, upper-plate deformation and dewatering at New Zealand's southern Hikurangi subduction margin. *Earth and Planetary Science Letters*. 530:115945. doi:10.1016/j.epsl.2019.115945.
- Cutten HNC, Beanland S, Berryman KR. 1988. The Rangiora Fault, an active structure in Hawkes Bay. In: *Research notes 1988*. Lower Hutt (NZ): New Zealand Geological Survey. p. 65–72. (New Zealand Geological Survey record; 35).
- Davidson SR, Barnes PM, Pettinga JR, Nicol A, Mountjoy JJ, Henrys SA. 2020. Conjugate strike-slip faulting across a subduction front driven by incipient seamount subduction. *Geology*. 48(5):493–498. doi:10.1130/g47154.1.
- Davy BW, Caldwell TG. 1998. Gravity, magnetic and seismic surveys of the caldera complex, Lake Taupo, North Island, New Zealand. *Journal of Volcanology and Geothermal Research*. 8(1–2):69–89. doi:10.1016/S0377-0273(97)00074-7.
- Davy B, Hoernle K, Werner R. 2008. Hikurangi Plateau: crustal structure, rifted formation, and Gondwana subduction history. *Geochemistry, Geophysics, Geosystems*. 9(7):Q07004. doi:10.1029/2007GC001855.
- De Pascale GP, Chandler-Yates N, Dela Pena F, Wilson P, May E, Twiss A, Cheng C. 2016. Active tectonics west of New Zealand's Alpine Fault: South Westland Fault Zone activity shows Australian Plate instability. *Geophysical Research Letters*. 43(7):3120–3125. doi:10.1002/2016GL068233.
- De Pascale GP, Quigley MC, Davies TRH. 2014. Lidar reveals uniform Alpine fault offsets and bimodal plate boundary rupture behavior, New Zealand. *Geology*. 42(5):411–414. doi:10.1130/g35100.1.

- Delteil J, Herzer RH, Sosson M, Lebrun J-Fdr, Collot J-Y, Wood RA. 1996. Influence of preexisting backstop structure on oblique tectonic accretion: the Fiordland margin (southwestern New Zealand). *Geology*. 24(11):1045–1048. doi:10.1130/0091-7613(1996)024<1045:lopbs>2.3.Co;2.
- Dorn C, Green AG, Jongens R, Carpentier S, Kaiser AE, Campbell F, Horstmeyer H, Campbell J, Finnemore M, Pettinga J. 2010. High-resolution seismic images of potentially seismogenic structures beneath the northwest Canterbury Plains, New Zealand. *Journal of Geophysical Research: Solid Earth*. 115(B11):B11303. doi:10.1029/2010JB007459.
- Eberhart-Phillips D, Bannister S, Reyners M, Henrys S. 2020. New Zealand wide model 2.2 seismic velocity and Qs and Qp models for New Zealand [dataset]. Genève (CH): Zenodo; [accessed 2022 May]. <http://doi.org/10.5281/zenodo.3779523>
- Edbrooke SW, compiler. 2001. Geology of the Auckland area [map]. Lower Hutt (NZ): Institute of Geological & Nuclear Sciences. 1 map + 74 p., scale 1:250,000. (Institute of Geological & Nuclear Sciences 1:250,000 geological map; 3).
- Edbrooke SW, Heron DW, Forsyth PJ, Jongens R, compilers. 2014. Geological map of New Zealand 1:1,000,000: digital vector data 2014. Lower Hutt (NZ): GNS Science. 1 DVD-ROM. (GNS Science geological map; 2).
- Ellis SM, Bannister S, Van Dissen RJ, Eberhart-Phillips D, Boulton C, Reyners ME, Funnell R, Mortimer N, Upton P. 2021. New Zealand Fault-Rupture Depth Model v1.0: a provisional estimate of the maximum depth of seismic rupture on New Zealand's active faults. Lower Hutt (NZ): GNS Science. 47 p. (GNS Science report; 2021/08).
- Estrada BE. 2003. Seismic hazard associated with the Springbank Fault, North Canterbury Plains [MSc thesis]. Christchurch (NZ): University of Canterbury. 193 p. + 2 maps.
- Eusden JD, Upton P, Eichelberger N, Pettinga JR. 2012. The Dillon and Acheron sinistral faults, Marlborough Fault System, New Zealand: field studies and mechanical modelling. *New Zealand Journal of Geology and Geophysics*. 55(2):91–102. doi:10.1080/00288306.2011.627564.
- Field EH, Arrowsmith RJ, Biasi GP, Bird P, Dawson TE, Felzer KR, Jackson DD, Johnson KM, Jordan TH, Madden C, et al. 2014. Uniform California earthquake rupture forecast, version 3 (UCERF3) – the time-independent model. *Bulletin of the Seismological Society of America*. 104(3):1122–1180. doi:10.1785/0120130164.
- Field EH, Jordan TH, Cornell CA. 2003. OpenSHA: a developing community-modeling environment for seismic hazard analysis. *Seismological Research Letters*. 74(4):406–419. doi:10.1785/gssrl.74.4.406.
- Finnemore M. 2004. The application of seismic reflection surveying to the characterisation of aquifer geometry and related active tectonic deformation, North Canterbury [PhD thesis]. Christchurch (NZ): University of Canterbury. 300 p.
- Formento-Trigilio ML, Burbank DW, Nicol A, Shulmeister J, Rieser U. 2003. River response to an active fold-and-thrust belt in a convergent margin setting, North Island, New Zealand. *Geomorphology*. 49(1–2):125–152. doi:10.1016/S0169-555X(02)00167-8.
- Forsyth PJ, Barrell DJA, Jongens R. 2008. Geology of the Christchurch area [map]. Lower Hutt (NZ): GNS Science. 1 folded map + 67 p., scale 1:250,000. (Institute of Geological & Nuclear Sciences 1:250,000 geological map; 16).
- Fougere SR. 2002. Paleoseismicity and active earth deformation, Lake Rotoiti to west Wairau Valley section of the Alpine Fault. Christchurch (NZ): University of Canterbury. 134 p. + appendices.

- Fraser JG, Nicol A, Pettinga JR, Johnston MR. 2006. Paleoearthquake investigation of the Waimea-Flaxmore fault system, Nelson, New Zealand. In: *Earthquakes and urban development: New Zealand Geotechnical Society 2006 Symposium*; 2006 Feb; Nelson, New Zealand. Wellington (NZ): Institution of Professional Engineers. p. 59–67. (Proceedings of technical groups; 31).
- Freund R. 1971. The Hope fault: a strike slip fault in New Zealand. Wellington (NZ): Department of Scientific & Industrial Research. 49 p. (New Zealand Geological Survey bulletin; 86).
- Fujiwara H, Kawai S, Aoi S, Morikawa N, Senna S, Kudo N, Ooi M, Hao KX-S, Wakamatsu K, Ishikawa Y, et al. 2009. Technical reports on national seismic hazard maps for Japan. Tsukuba (JP): National Research Institute for Earth Science and Disaster Prevention. 44 p. + appendices. Technical Note of the National Research Institute for Earth Science and Disaster Prevention 336.
- Gase AC, Van Avendonk HJA, Bangs NL, Luckie TW, Barker DHN, Henrys SA, Bassett D, Okaya DA, Jacobs KM, Kodaira S, et al. 2019. Seismic evidence of magmatic rifting in the offshore Taupo Volcanic Zone, New Zealand. *Geophysical Research Letters*. 46(22):12949–12957. doi:10.1029/2019GL085269.
- Ghisetti FC, Barnes PM, Ellis S, Plaza-Faverola AA, Barker DHN. 2016a. The last 2 Myr of accretionary wedge construction in the central Hikurangi margin (North Island, New Zealand): insights from structural modeling. *Geochemistry, Geophysics, Geosystems*. 17(7):2661–2686. doi:10.1002/2016GC006341.
- Ghisetti FC, Barnes PM, Sibson RH. 2014. Deformation of the Top Basement Unconformity west of the Alpine Fault (South Island, New Zealand): seismotectonic implications. *New Zealand Journal of Geology and Geophysics*. 57(3):271–294. doi:10.1080/00288306.2013.876433.
- Ghisetti FC, Johnston MR, Wopereis P. 2020. Structural evolution of the active Waimea-Flaxmore Fault System in the Nelson-Richmond urban area, South Island, New Zealand. *New Zealand Journal of Geology and Geophysics*. 63(2):168–189. doi:10.1080/00288306.2019.1651346.
- Ghisetti FC, Johnston MR, Wopereis P, Sibson RH. 2018. Structural and morpho-tectonic evidence of Quaternary faulting within the Moutere Depression, South Island, New Zealand. *New Zealand Journal of Geology and Geophysics*. 61(4):461–479. doi:10.1080/00288306.2018.1502673.
- Ghisetti FC, Sibson RH. 2006. Accommodation of compressional inversion in north-western South Island (New Zealand): old faults versus new? *Journal of Structural Geology*. 28(11):1994–2010. doi:10.1016/j.jsg.2006.06.010.
- Ghisetti F, Sibson RH, Hamling I. 2016b. Deformed Neogene basins, active faulting and topography in Westland: distributed crustal mobility west of the Alpine Fault transpressive plate boundary (South Island, New Zealand). *Tectonophysics*. 693:340–362. doi:10.1016/j.tecto.2016.03.024.
- Giba M, Nicol A, Walsh JJ. 2010. Evolution of faulting and volcanism in a back-arc basin and its implications for subduction processes. *Tectonics*. 29(4):TC4020. doi:10.1029/2009TC002634.
- Goded T, Gerstenberger MC, Litchfield NJ, McVerry GH, Lukovic B, Van Dissen RJ, Rhoades DA, Holden C, Langridge RM, Christophersen A, et al. 2018a. Seismic hazard analysis for State Highway 1 and an alternative route following the 2016 Kaikoura earthquake (revised). Lower Hutt (NZ): GNS Science 83 p. + 240 maps. Consultancy Report 2018/114. Prepared for North Canterbury Transport Infrastructure Recovery.
- Goded T, McVerry GH, Litchfield NJ, Langridge RM, Bruce ZR. 2019. Probabilistic seismic hazard analysis for Evans Bay Wharf, Port of Timaru. Lower Hutt (NZ): GNS Science. 154 p. Consultancy Report 2019/79. Prepared for PrimePort Timaru Ltd.

- Goded T, McVerry GH, Villamor P, Bruce ZR, Perrin ND. 2018b. Seismic design study for State Highway 1, Cambridge. Lower Hutt (NZ): GNS Science. 90 p. Consultancy Report 2017/234. Prepared for Opus International Consultants Ltd.
- Gómez-Vasconcelos MG, Villamor P, Cronin SJ, Procter J, Kereszturi G, Palmer A, Townsend DB, Leonard GS, Berryman KR, Ashraf S. 2016. Earthquake history at the eastern boundary of the South Taupo Volcanic Zone, New Zealand. *New Zealand Journal of Geology and Geophysics*. 59(4):522–543. doi:10.1080/00288306.2016.1195757.
- Gómez-Vasconcelos MG, Villamor P, Cronin S, Procter J, Palmer A, Townsend DB, Leonard GS. 2017. Crustal extension in the Tongariro graben, New Zealand: insights into volcano-tectonic interactions and active deformation in a young continental rift. *Geological Society of America Bulletin*. 129(9–10):1085–1099. doi:10.1130/b31657.1.
- Gómez-Vasconcelos MG, Villamor P, Procter J, Palmer A, Cronin S, Wallace C, Townsend DB, Leonard GS. 2019. Characterisation of faults as earthquake sources from geomorphic data in the Tongariro Volcanic Complex, New Zealand. *New Zealand Journal of Geology and Geophysics*. 62(1):131–142. doi:10.1080/00288306.2018.1548495.
- Gore ES. 2015. Tectonic geomorphology and paleoseismology of the Lees Valley fault zone, South Island [MSc thesis]. Christchurch (NZ): University of Canterbury. 152 p.
- Grapes R, Downes G. 1997. The 1855 Wairarapa, New Zealand, earthquake: analysis of historical data. *Bulletin of the New Zealand National Society for Earthquake Engineering*. 30(4):271–368. doi:10.5459/bnzsee.30.4.271-368.
- Grapes RH, Little TA, Browne GH, Rait GJ. 1997. Ngapotiki Thrust, White Rock and Te Kaukau Point, southeast Wairarapa: active and inactive structures of the Hikurangi Forearc. In: Campbell HJ, Grapes RH, editors. *Geological Society of New Zealand Inc 1997 Annual Conference: field trip guides*; 1997 Nov 25–27; Wellington, New Zealand. Wellington (NZ): Geological Society of New Zealand. 22 p. (GSNZ miscellaneous publication; 95B).
- Grapes R, Little T, Downes G. 1998. Rupturing of the Awatere Fault during the 1848 October 16 Marlborough earthquake, New Zealand: historical and present day evidence. *New Zealand Journal of Geology and Geophysics*. 41(4):387–399. doi:10.1080/00288306.1998.9514818.
- Grapes RH, Wellman HW. 1988. The Wairarapa Fault. Wellington (NZ): Victoria University of Wellington. 55 p. (Geology Board of Studies publication; 4).
- Grindley GW. 1960. Geological map of New Zealand: sheet 8 Taupo [map]. 1<sup>st</sup> ed. Wellington (NZ): Department of Scientific and Industrial Research. 1 folded map, scale 1:250,000. (Geological map of New Zealand 1:250,000; 8).
- Grindley GW. 1980. Cobb [map]. 1<sup>st</sup> ed. Wellington (NZ): Department of Scientific & Industrial Research. 1 fold. map + 1 booklet. (Geological map of New Zealand 1:63,360; sheet S13 ).
- Halliday S. 2003. The tectonic geomorphology and paleoseismology of the Patoka Fault, North Island Dextral Fault Belt, New Zealand [BSc(Hons) thesis]. Wellington (NZ): Victoria University of Wellington. 77 p.
- Hanson JA. 1998. The neotectonics of the Wellington and Ruahine faults between the Manawatu Gorge and Puketitiri, North Island, New Zealand [PhD thesis]. Palmerston North (NZ): Massey University. 2 vol.
- Hatem AE, Dolan JF, Zinke RW, Langridge RM, McGuire CP, Rhodes EJ, Brown N, Van Dissen RJ. 2020. Holocene to latest Pleistocene incremental slip rates from the east-central Hope fault (Conway segment) at Hossack Station, Marlborough fault system, South Island, New Zealand: towards a dated path of earthquake slip along a plate boundary fault. *Geosphere*. 16(6):1558–1584. doi:10.1130/ges02263.1.

- Hatem AE, Dolan JF, Zinke RW, Van Dissen RJ, McGuire CM, Rhodes EJ. 2019. A 2000 Yr Paleoearthquake Record along the Conway Segment of the Hope Fault: Implications for Patterns of Earthquake Occurrence in Northern South Island and Southern North Island, New Zealand. *Bulletin of the Seismological Society of America*. 109(6):2216–2239. doi:10.1785/0120180313.
- Hayes G. 2018. Slab2 – a comprehensive subduction zone geometry model. Reston (VA): U.S. Geological Survey; [accessed 2022 May]. <https://doi.org/10.5066/F7PV6JNV>
- Hayes GP, Furlong KP. 2010. Quantifying potential tsunami hazard in the Puysegur subduction zone, south of New Zealand. *Geophysical Journal International*. 183(3):1512–1524. doi:10.1111/j.1365-246X.2010.04808.x.
- Henderson J. 1933. The geological aspects of the Hawke's Bay earthquakes. *New Zealand Journal of Science and Technology*. 15(1):38–75.
- Henderson J. 1937. The West Nelson earthquakes of 1929. *New Zealand Journal of Science and Technology*. 19:65–144.
- Henne A, Craw D, MacKenzie D. 2011. Structure of the Blue Lake Fault Zone, Otago Schist, New Zealand. *New Zealand Journal of Geology and Geophysics*. 54(3):311–328. doi:10.1080/00288306.2011.577080.
- Henrys S, Wech A, Sutherland R, Stern T, Savage M, Sato H, Mochizuki K, Iwasaki T, Okaya D, Seward A, et al. 2013. SAHKE geophysical transect reveals crustal and subduction zone structure at the southern Hikurangi margin, New Zealand. *Geochemistry, Geophysics, Geosystems*. 14(7):2063–2083. doi:10.1002/ggge.20136.
- Heron DW, custodian. 2020. Geological map of New Zealand 1:250,000: digital vector data [map]. 3<sup>rd</sup> ed. Lower Hutt (NZ): GNS Science. 1 USB. (GNS Science geological map; 1).
- Heron DW, Van Dissen RJ, Sawa M. 1998. Late Quaternary movement on the Ohariu Fault, Tongue Point to MacKays Crossing, North Island, New Zealand. *New Zealand Journal of Geology and Geophysics*. 41(4):419–439. doi:10.1080/00288306.1998.9514820.
- Holt A. 2017. Acoustic investigations of geological hazards and seismic processing off the coast of Otago, New Zealand [MSc thesis]. Dunedin (NZ): University of Otago. 205 leaves.
- Hornblow S, Quigley M, Nicol A, Van Dissen R, Wang N. 2014. Paleoseismology of the 2010  $M_w$  7.1 Darfield (Canterbury) earthquake source, Greendale Fault, New Zealand. *Tectonophysics*. 637:178–190. doi:10.1016/j.tecto.2014.10.004.
- Howard M, Nicol A, Campbell J, Pettinga JR. 2005. Holocene paleoearthquakes on the strike-slip Porters Pass Fault, Canterbury, New Zealand. *New Zealand Journal of Geology and Geophysics*. 48(1):59–74. doi:10.1080/00288306.2005.9515098.
- Howarth JD, Barth NC, Fitzsimons SJ, Richards-Dinger K, Clark KJ, Biasi GP, Cochran UA, Langridge RM, Berryman KR, Sutherland R. 2021. Spatiotemporal clustering of great earthquakes on a transform fault controlled by geometry. *Nature Geoscience*. 14(5):314–320. doi:10.1038/s41561-021-00721-4.
- Howarth JD, Cochran UA, Langridge RM, Clark KJ, Fitzsimons SJ, Berryman KR, Villamor P, Strong DT. 2018. Past large earthquakes on the Alpine Fault: paleoseismological progress and future directions. *New Zealand Journal of Geology and Geophysics*. 61(3):309–328. doi:10.1080/00288306.2018.1464658.
- Howell A, Nissen E, Stahl T, Clark K, Kears J, Van Dissen R, Villamor P, Langridge R, Jones K. 2020. Three-dimensional surface displacements during the 2016  $M_w$  7.8 Kaikōura earthquake (New Zealand) from photogrammetry-derived point clouds. *Journal of Geophysical Research: Solid Earth*. 125(1):e2019JB018739. doi:10.1029/2019JB018739.

- Hull AG. 1990. Tectonics of the 1931 Hawke's Bay earthquake. *New Zealand Journal of Geology and Geophysics*. 33(2):309–320. doi:10.1080/00288306.1990.10425689.
- Hull AG. 1994. Past earthquake timing and magnitude along the Inglewood fault, Taranaki, New Zealand. *Bulletin of the New Zealand Society for Earthquake Engineering*. 27(2):155–162. doi:10.5459/bnzsee.27.2.155-162.
- Hull AG. 1996. Earthquake and volcanic hazards in Taranaki: potential threats to oil and gas production and distribution infrastructure. In: *1996 New Zealand Petroleum Conference proceedings: confronting the issues 1996: an international perspective*; Wellington, New Zealand. Wellington (NZ): Ministry of Commerce. p. 261–271.
- Hull AG, Dowrick DJ, Latter JH, Zhao J. 1992. Reassessment of potential earthquake losses in Taranaki. Lower Hutt (NZ): Institute of Geological & Nuclear Sciences. 22 p. Client Report 1992/101. Prepared for Fletcher Challenge Methanol.
- Johnson KM, Wallace LM, Maurer J, Hamling IJ, Williams CA, Rollins C, Gerstenberger MC, Van Dissen RJ. Forthcoming 2022. Geodetic deformation model for the 2022 update of the New Zealand National Seismic Hazard Model. Lower Hutt (NZ): GNS Science. (GNS Science report; 2021/37).
- Jongens R, Barrell DJA, Campbell JK, Pettinga JR. 2012. Faulting and folding beneath the Canterbury Plains identified prior to the 2010 emergence of the Greendale Fault. *New Zealand Journal of Geology and Geophysics*. 55(3):169–176. doi:10.1080/00288306.2012.674050.
- Kearse J, Little TA, Van Dissen RJ, Barnes PM, Langridge R, Mountjoy J, Ries W, Villamor P, Clark KJ, Benson A, et al. 2018. Onshore to offshore ground-surface and seabed rupture of the Jordan–Kekerengu–Needles fault network during the 2016 Mw 7.8 Kaikōura earthquake, New Zealand. *Bulletin of the Seismological Society of America*. 108(3B):1573–1595. doi:10.1785/0120170304.
- Kelsey HM, Cashman SM, Beanland S, Berryman KR. 1995. Structural evolution along the inner forearc of the obliquely convergent Hikurangi margin, New Zealand. *Tectonics*. 14(1):1–18. doi:10.1029/94TC01506.
- Kelsey HM, Hull AG, Cashman SM, Berryman KR, Cashman PH, Trexler JH, Jr., Begg JG. 1998. Paleoseismology of an active reverse fault in a forearc setting: the Poukawa fault zone, Hikurangi forearc, New Zealand. *GSA Bulletin*. 110(9):1123–1148. doi:10.1130/0016-7606(1998)110<1123:Poaarf>2.3.Co;2.
- Khajavi N, Langridge RM, Quigley MC, Smart C, Rezanejad A, Martin-Gonzalez F. 2016. Late Holocene rupture behavior and earthquake chronology on the Hope fault, New Zealand. *Geological Society of America Bulletin*. 128(11–12):1736–1761. doi:10.1130/b31199.1.
- Khajavi N, Nicol A, Quigley MC, Langridge RM. 2018. Temporal slip-rate stability and variations on the Hope Fault, New Zealand, during the late Quaternary. *Tectonophysics*. 738–739:112–123. doi:10.1016/j.tecto.2018.05.001.
- Kieckhefer RM. 1979. Sheets M31D, N31A, N31C and parts M32A and M32B, Leader Dale, Sheets N31B and N31D, Dillon, Sheets O30C and O31A, Lake McRae. Wellington (NZ): Department of Scientific & Industrial Research. 27 p. Late Quaternary tectonic map of New Zealand 1:50,000.
- Klos PZ. 2009. The Ruataniwha Fault: neotectonic evaluation and seismic hazard, Dannevirke Region, New Zealand [thesis]. Colorado Springs (CO): Colorado College Department of Geology. 86 p.

- Knuepfer PLK. 1984. Tectonic geomorphology and present-day tectonics of the Alpine shear system, South Island, New Zealand (neotectonics, faults) [PhD thesis]. Arizona (TX): University of Arizona. 488 p.
- Knuepfer PLK. 1988. Estimating ages of late Quaternary stream terraces from analysis of weathering rinds and soils. *GSA Bulletin*. 100(8):1224–1236. doi:10.1130/0016-7606(1988)100<1224: Eaolqs>2.3.Co;2.
- Knuepfer PLK. 1992. Temporal variations in latest Quaternary slip across the Australian-Pacific Plate Boundary, northeastern South Island, New Zealand. *Tectonics*. 11(3):449–464. doi:10.1029/91TC02890.
- Lamarche G, Barnes P. 2005. Fault characterisation and earthquake source identification in the offshore Bay of Plenty. Wellington (NZ): National Institute of Water & Atmospheric Research Ltd (NIWA). 63 p. NIWA Client Report WLG2005-51. Prepared for Environment Bay of Plenty Regional Council.
- Lamarche G, Barnes PM, Bull JM. 2006. Faulting and extension rates over the last 20,000 years in the offshore Whakatane Graben, New Zealand continental shelf. *Tectonics*. 25(4):TC4005. doi:10.1029/2005tc001886.
- Lamarche G, Lebrun J-F. 2000. Transition from strike-slip faulting to oblique subduction: active tectonics at the Puysegur Margin, South New Zealand. *Tectonophysics*. 316(1):67–89. doi:10.1016/S0040-1951(99)00232-2.
- Lamarche G, Proust J-N, Nodder SD. 2005. Long-term slip rates and fault interactions under low contractional strain, Wanganui Basin, New Zealand. *Tectonics*. 24(4):TC4004. doi:10.1029/2004TC001699.
- Lamb SH, Vella P. 1987. The last million years of deformation in part of the New Zealand plate-boundary zone. *Journal of Structural Geology*. 9(7):877–891. doi:10.1016/0191-8141(87)90088-5.
- Langridge RM. 2004. How is tectonic slip partitioned from the Alpine Fault to the Marlborough Fault System? Results from the Hope Fault. Lower Hutt (NZ): Institute of Geological & Nuclear Sciences. 29 p. (Institute of Geological & Nuclear Sciences science report; 2004/32).
- Langridge RM, Almond PC, Duncan RP. 2013. Timing of late Holocene paleoearthquakes on the Hurunui segment of the Hope fault: implications for plate boundary strain release through South Island, New Zealand. *Geological Society of America Bulletin*. 125(5–6):756–776. doi:10.1130/b30674.1.
- Langridge RM, Berryman KR. 2005. Morphology and slip rates of the Hurunui section of the Hope Fault, South Island, New Zealand. *New Zealand Journal of Geology and Geophysics*. 48(1):43–57. doi:10.1080/00288306.2005.9515097.
- Langridge RM, Berryman KR, Van Dissen RJ. 2005a. Defining the geometric segmentation and Holocene slip rate of the Wellington Fault, New Zealand: the Pahiatua section. *New Zealand Journal of Geology and Geophysics*. 48(4):591–607. doi:10.1080/00288306.2005.9515136.
- Langridge RM, Berryman KR, Van Dissen RJ. 2007. Late Holocene paleoseismicity of the Pahiatua section of the Wellington Fault, New Zealand. *New Zealand Journal of Geology and Geophysics*. 50(3):205–226. doi:10.1080/00288300709509832.
- Langridge R, Campbell J, Hill N, Pere V, Pope J, Pettinga J, Estrada B, Berryman K. 2003a. Paleoseismology and slip rate of the Conway Segment of the Hope Fault at Greenburn Stream, South Island, New Zealand. *Annals of Geophysics*. 46(5):1119–1139. doi:10.4401/ag-3449.

- Langridge RM, Hemphill-Haley M, Ries W. 2008. Active fault mapping and rupture avoidance at Queen Mary Hospital, Hanmer Springs. Lower Hutt (NZ): GNS Science. 52 p. Consultancy Report 2008/113. Prepared for Tonkin & Taylor Ltd.
- Langridge RM, Howarth JD, Carey JM, Zondervan A, Strong DT. 2017a. Reconnaissance geology of Lake McRae, Marlborough: landslides, lake sediments and paleo-earthquakes. Lower Hutt (NZ): GNS Science. 55 p. (GNS Science report; 2015/27).
- Langridge RM, Morgenstern R. 2019. Active fault mapping and fault avoidance zones for Horowhenua District and Palmerston North City. Lower Hutt (NZ): GNS Science. 72 p. Consultancy Report 2018/75. Prepared for Horizons Regional Council.
- Langridge RM, Morgenstern R. 2020a. Active fault mapping and fault avoidance zones for the Manawatū District. Lower Hutt (NZ): GNS Science. 69 p. Consultancy Report 2019/123. Prepared for Horizons Regional Council.
- Langridge RM, Morgenstern R. 2020b. Active fault mapping and fault avoidance zones for the Rangitikei District. Lower Hutt (NZ): GNS Science. 66 p. Consultancy Report 2019/168. Prepared for Horizons Regional Council.
- Langridge RM, Ries WF. 2014. Active fault mapping and fault avoidance zones for Central Hawke's Bay District: 2013 update. Lower Hutt (NZ): GNS Science. 50 p. + 1 CD. Consultancy Report 2013/151. Prepared for Hawke's Bay Regional Council.
- Langridge RM, Ries WF. 2015. Active fault mapping and fault avoidance zones for Hastings District and environs. Lower Hutt (NZ): GNS Science. 50 p. + 1 DVD. Consultancy Report 2015/112. Prepared for Hawke's Bay Regional Council.
- Langridge RM, Ries WF, Dolan JF, Schermer ER, Siddoway C. 2017b. Slip rate estimates and slip gradient for the Alpine Fault at Calf Paddock, Maruia River, New Zealand. *New Zealand Journal of Geology and Geophysics*. 60(2):73–88. doi:10.1080/00288306.2016.1275707.
- Langridge RM, Ries WF, Litchfield NJ, Villamor P, Van Dissen RJ, Barrell DJA, Rattenbury MS, Heron DW, Haubrock S, Townsend DB, et al. 2016. The New Zealand Active Faults Database. *New Zealand Journal of Geology and Geophysics*. 59(1):86–96. doi:10.1080/00288306.2015.1112818.
- Langridge RM, Rowland J, Villamor P, Mountjoy J, Townsend DB, Nissen E, Madugo C, Ries WF, Gasston C, Canva A, et al. 2018. Coseismic rupture and preliminary slip estimates for the Papatea Fault and its role in the 2016 Mw 7.8 Kaikōura, New Zealand, earthquake. *Bulletin of the Seismological Society of America*. 108(3B):1596–1622. doi:10.1785/0120170336.
- Langridge RM, Townsend DB, Persaud M. 2003b. Paleoseismic assessment of the active Mokonui Fault, Wairarapa. Lower Hutt (NZ): Institute of Geological & Nuclear Sciences. 35 p. Client Report 2003/68. Prepared for Wairarapa Engineering Lifelines Association.
- Langridge RM, Van Dissen RJ, Cochran UA, Litchfield NJ, Berryman KR, Begg JG, Villamor P, Heron DW, Nicol A, Townsend DB. 2005b. Active faulting and paleoearthquakes in the Wairarapa and Wellington regions. In: Townend J, Langridge RM, Jones A, editors. *The 1855 Wairarapa Earthquake Symposium: 150 years of thinking about magnitude 8+ earthquakes and seismic hazard in New Zealand: proceedings volume*; 2005 Sep 8–10; Wellington, New Zealand. Wellington (NZ): Greater Wellington Regional Council. p. 49–65.
- Langridge RM, Van Dissen RJ, Rhoades DA, Villamor P, Little T, Litchfield NJ, Clark KJ, Clark D. 2011a. Five thousand years of surface ruptures on the Wellington Fault, New Zealand: implications for recurrence and fault segmentation. *Bulletin of the Seismological Society of America*. 101(5):2088–2107. doi:10.1785/0120100340.

- Langridge RM, Van Dissen RJ, Villamor P, Little TA. 2009. It's Our Fault: Wellington Fault paleo-earthquake investigations: final report. Lower Hutt (NZ): GNS Science. 45 p. Consultancy Report 2008/344. Prepared for EQC, ACC and Wellington City Council.
- Langridge RM, Villamor P, Basili R, Almond P, Martinez-Diaz JJ, Canora C. 2010. Revised slip rates for the Alpine Fault at Inchbonnie: implications for plate boundary kinematics of South Island, New Zealand. *Lithosphere*. 2(3):139–152. doi:10.1130/l88.1.
- Langridge RM, Villamor P, McVerry GH, Cabeza M. 2011b. A7 Makaroro River dam site, phase 1B: updated active fault and surface rupture displacement hazard and acceleration response spectra reassessment. Lower Hutt (NZ): GNS Science. 60 p. Consultancy Report 2011/300. Prepared for Hawke's Bay Regional Council.
- Langridge RM, Villamor P, Townsend DB. 2006. Paleoseismicity of the Wellington Fault at Putara: implications for fault segmentation and earthquake timing. Lower Hutt (NZ): GNS Science. 66 p. Consultancy Report 2005/116. Prepared for the Earthquake Commission.
- Lebrun J-F, Lamarche G, Collot J-Y, Delteil J. 2000. Abrupt strike-slip fault to subduction transition: the Alpine Fault-Puysegur Trench connection, New Zealand. *Tectonics*. 19(4):688–706. doi:10.1029/2000TC900008.
- Lee JM, Begg JG, compilers. 2002. Geology of the Wairarapa area [map]. Lower Hutt (NZ): Institute of Geological & Nuclear Sciences. 1 fold. map + 66 p., scale 1:250,000. (Institute of Geological & Nuclear Sciences 1:250,000 geological map; 11).
- Lee JM, Begg JG, Bland KJ. 2020. Geological map of the Napier-Hastings urban area [map]. Lower Hutt (NZ): GNS Science. 1 map, scale 1:75,000. (GNS Science geological map; 7a).
- Lee JM, Bland KJ, Townsend DB, Kamp PJJ, compilers. 2011. Geology of the Hawke's Bay area [map]. Lower Hutt (NZ): GNS Science. 1 fold. map + 93 p., scale 1:250,000. (Institute of Geological & Nuclear Sciences 1:250,000 geological map; 8).
- Lensen GJ. 1968. Analysis of progressive fault displacement during downcutting at the Branch River terraces, South Island, New Zealand. *GSA Bulletin*. 79(5):545–556. doi:10.1130/0016-7606(1968)79[545:Aopfdd]2.0.Co;2.
- Lensen GJ. 1976. Sheets N28D, O28C & N29B Hillersden and sheets O28D, P28A & P28C Renwick. Wellington (NZ): Department of Scientific & Industrial Research. 19 p. (Late Quaternary tectonic map of New Zealand 1:50,000).
- Lensen GJ, Otway PM. 1971. Earthshift and post-earthshift deformation associated with the May 1968 Inangahua earthquake, New Zealand. In: Collins BW, Fraser R, editors. *Recent crustal movements*. Wellington (NZ): Royal Society of New Zealand. p. 107–116. (Royal Society of New Zealand bulletin; 9).
- Lensen GJ, Suggate RP. 1968. 2. Inangahua earthquake – preliminary account of the geology. In: Adams RD, Eiby GA, Lowry MA, Lensen GJ, Suggate RP, Stephenson WR, editors. *Preliminary reports on the Inangahua earthquake, New Zealand, May 1968*. Wellington (NZ): Department of Scientific & Industrial Research. p. 17–36. (DSIR Bulletin; 193).
- Lewis KB, Collot J-Y, Davy BW, Delteil J, Lallemand SE, Uruski C. 1997. North Hikurangi GeodyNZ swath maps: depths, texture and geological interpretation [chart]. Wellington (NZ): National Institute of Water & Atmospheric Research. Map 9342, scale 1:500,000. (NIWA miscellaneous series; 72).
- Lewis KB, Pantin HM. 1984. Intersection of a marginal basin with a continent: structure and sediments of the Bay of Plenty, New Zealand. *Geological Society, London, Special Publications*. 16:121–135. doi:10.1144/GSL.SP.1984.016.01.09.

- Lewis KB, Pettinga JR. 1993. The emerging, imbricate frontal wedge of the Hikurangi margin. *Sedimentary Basins of the World*. 2:225–250.
- Litchfield NJ. 2001. The Titri Fault System: Quaternary-active faults near the leading edge of the Otago reverse fault province. *New Zealand Journal of Geology and Geophysics*. 44(4):517–534. doi:10.1080/00288306.2001.9514953.
- Litchfield NJ, Bland KJ, Hayward B, Page MJ, Langridge RM. 2005. New Zealand Friends of the Quaternary fieldtrip, Hawke's Bay, 1–3 July, 2005. Wellington (NZ): Geological Society of New Zealand; [accessed 2022 May]. [https://www.gns.cri.nz/static/nzpaoclimate/images/2005\\_foq\\_guide.pdf](https://www.gns.cri.nz/static/nzpaoclimate/images/2005_foq_guide.pdf)
- Litchfield NJ, Campbell JK, Nicol A. 2003. Recognition of active reverse faults and folds in North Canterbury, New Zealand, using structural mapping and geomorphic analysis. *New Zealand Journal of Geology and Geophysics*. 46(4):563–579. doi:10.1080/00288306.2003.9515030.
- Litchfield NJ, Clark KJ. 2015. Fluvial terrace formation in the lower Awhea and Pahaoa River valleys, New Zealand: implications for tectonic and sea-level controls. *Geomorphology*. 231:212–228. doi:10.1016/j.geomorph.2014.12.009.
- Litchfield NJ, Clark KJ, Cochran UA, Palmer AS, Mountjoy J, Mueller C, Morgenstern R, Berryman KR, McFadgen BG, Steele R, et al. 2020a. Marine terraces reveal complex near-shore upper-plate faulting in the northern Hikurangi margin, New Zealand. *Bulletin of the Seismological Society of America*. 110(2):825–849. doi:10.1785/0120190208.
- Litchfield NJ, Humphrey J, Morgenstern R, Langridge RM, Coffey G, Van Dissen RJ. Forthcoming 2022. New Zealand Paleoseismic Site Database: design and overview of version 1.0. Lower Hutt (NZ): GNS Science. (GNS Science report; 2021/52).
- Litchfield NJ, Morgenstern R, Villamor P, Van Dissen RJ, Townsend DB, Kelly SD. 2020b. Active fault hazards in the Taupō District. Lower Hutt (NZ): GNS Science. 114 p. Consultancy Report 2020/31. Prepared for Taupō District Council.
- Litchfield NJ, Norris RJ. 2000. Holocene motion on the Akatore Fault, south Otago coast, New Zealand. *New Zealand Journal of Geology and Geophysics*. 43(3):405–418. doi:10.1080/00288306.2000.9514897.
- Litchfield NJ, Van Dissen RJ, Hemphill-Haley M, Townsend DB, Heron DW. 2010. Post c. 300 year rupture of the Ohariu Fault in Ohariu Valley, New Zealand. *New Zealand Journal of Geology and Geophysics*. 53(1):43–56. doi:10.1080/00288301003631780.
- Litchfield NJ, Van Dissen RJ, Heron DW, Rhoades DA. 2006. Constraints on the timing of the three most recent surface rupture events and recurrence interval for the Ohariu Fault: trenching results from MacKays Crossing, Wellington, New Zealand. *New Zealand Journal of Geology and Geophysics*. 49(1):57–61. doi:10.1080/00288306.2006.9515147.
- Litchfield NJ, Van Dissen RJ, Langridge RM, Heron DW, Prentice C. 2004. Timing of the most recent surface rupture event on the Ohariu Fault near Paraparaumu, New Zealand: short communication. *New Zealand Journal of Geology and Geophysics*. 47(1):123–127. doi:10.1080/00288306.2004.9515041.
- Litchfield NJ, Van Dissen RJ, Nicol A. 2007. Reassessment of slip rate and implications for surface rupture hazard of the Martinborough Fault, south Wairarapa, New Zealand. *New Zealand Journal of Geology and Geophysics*. 50(3):239–243. doi:10.1080/00288300709509834.
- Litchfield NJ, Van Dissen RJ, Sutherland R, Barnes PM, Cox SC, Norris RJ, Beavan RJ, Langridge RM, Villamor P, Berryman KR, et al. 2013. A model of active faulting in New Zealand: fault zone parameter descriptions. Lower Hutt (NZ): GNS Science. 120 p. (GNS Science report; 2012/19).

- Litchfield NJ, Van Dissen RJ, Sutherland R, Barnes PM, Cox SC, Norris R, Beavan RJ, Langridge RM, Villamor P, Berryman KR, et al. 2014. A model of active faulting in New Zealand. *New Zealand Journal of Geology and Geophysics*. 57(1):32–56. doi:10.1080/00288306.2013.854256.
- Litchfield NJ, Villamor P, Dissen RJV, Nicol A, Barnes PM, A. Barrell DJ, Pettinga JR, Langridge RM, Little TA, Mountjoy JJ, et al. 2018. Surface rupture of multiple crustal faults in the 2016 Mw 7.8 Kaikōura, New Zealand, earthquake. *Bulletin of the Seismological Society of America*. 108(3B):1496–1520. doi:10.1785/0120170300.
- Little T, Begg JG. 2005. 1855 Wairarapa Earthquake Symposium: all-day field-trip to the Wairarapa Fault and 1855 rupture sites. In: *1855 Wairarapa Earthquake Symposium*; 2005 September 8–10; Wellington, New Zealand. Wellington (NZ): Greater Wellington Regional Council. 28 p.
- Little TA, Grapes R, Berger GW. 1998. Late Quaternary strike slip on the eastern part of the Awatere fault, South Island, New Zealand. *Geological Society of America Bulletin*. 110(2):127–148. doi:10.1130/0016-7606(1998)110<0127:LQSSOT>2.3.CO;2.
- Little T, Van Dissen R, Kearse J, Norton K, Benson A, Wang N. 2018. Kekerengu Fault, New Zealand: timing and size of late Holocene surface ruptures. *Bulletin of the Seismological Society of America*. 108(3B):1556–1572. doi:10.1785/0120170152.
- Little TA, Van Dissen RJ, Rieser U, Smith EGC, Langridge RM. 2010. Coseismic strike slip at a point during the last four earthquakes on the Wellington Fault near Wellington, New Zealand. *Journal of Geophysical Research: Solid Earth*. 115(B5):B05403. doi:10.1029/2009jb006589.
- Little T, Van Dissen R, Schermer E, Carne R. 2009. Late Holocene surface ruptures on the southern Wairarapa fault, New Zealand: link between earthquakes and the uplifting of beach ridges on a rocky coast. *Lithosphere*. 1(1):4–28. doi:10.1130/L7.1.
- Manighetti I, Perrin C, Dominguez S, Garambois S, Gaudemer Y, Malavieille J, Matteo L, Delor E, Vitard C, Beauprêtre S. 2015. Recovering paleoearthquake slip record in a highly dynamic alluvial and tectonic region (Hope Fault, New Zealand) from airborne lidar. *Journal of Geophysical Research: Solid Earth*. 120(6):4484–4509. doi:10.1002/2014JB011787.
- Marden M, Neall VE. 1990. Dated Ohakean terraces offset by the Wellington Fault, near Woodville, New Zealand. *New Zealand Journal of Geology and Geophysics*. 33(3):449–453. doi:10.1080/00288306.1990.10425700.
- Markley M, Norris RJ. 1999. Structure and neotectonics of the Blackstone Hill Antiform, Central Otago, New Zealand. *New Zealand Journal of Geology and Geophysics*. 42(2):205–218. doi:10.1080/00288306.1999.9514840.
- Markley M, Tikoff B. 2003. Geometry of the folded Otago penepplain surface beneath Ida valley, Central Otago, New Zealand, from gravity observations. *New Zealand Journal of Geology and Geophysics*. 46(3):449–456. doi:10.1080/00288306.2003.9515020.
- Mason DPM, Little TA. 2006. Refined slip distribution and moment magnitude of the 1848 Marlborough earthquake, Awatere Fault, New Zealand. *New Zealand Journal of Geology and Geophysics*. 49(3):375–382. doi:10.1080/00288306.2006.9515174.
- Mason DPM, Little TA, Van Dissen RJ. 2006. Refinements to the paleoseismic chronology of the eastern Awatere Fault from trenches near Upcot Saddle, Marlborough, New Zealand. *New Zealand Journal of Geology and Geophysics*. 49(3):383–397. doi:10.1080/00288306.2006.9515175.
- Mazengarb C, Speden IG. 2000. Geology of the Raukumara area [map]. Lower Hutt (NZ): Institute of Geological & Nuclear Sciences Limited. 1 fold. map + 60 p., scale 1:250,000. (Institute of Geological & Nuclear Sciences 1:250,000 geological map; 6).

- McCalpin JP. 1992. Glacial and postglacial geology near Lake Tennyson, Clarence River, New Zealand. *New Zealand Journal of Geology and Geophysics*. 35(2):201–210. doi:10.1080/00288306.1992.9514514.
- McCalpin JP. 1996. Tectonic geomorphology and Holocene paleoseismicity of the Molesworth section of the Awatere Fault, South Island, New Zealand. *New Zealand Journal of Geology and Geophysics*. 39(1):33–50. doi:10.1080/00288306.1996.9514693.
- McClymont AF, Villamor P, Green AG. 2009. Fault displacement accumulation and slip rate variability within the Taupo Rift (New Zealand) based on trench and 3-D ground-penetrating radar data. *Tectonics*. 28:TC4005. doi:10.1029/2008tc002334.
- McKay A. 1890. On the earthquakes of September, 1888, in the Amuri and Marlborough districts of the South Island. *Reports of geological explorations*. 20:1–16.
- McNamara DD, Milicich SD, Massiot C, Villamor P, McLean K, Sépulveda F, Ries WF. 2019. Tectonic controls on Taupo Volcanic Zone geothermal expression: insights From Te Mihi, Wairakei Geothermal Field. *Tectonics*. 38(8):3011–3033. doi:10.1029/2018tc005296.
- McVerry GH, Barrell DJA, Abbott ER. 2017. Seismic hazard assessment for the Klondyke Storage Pond. Lower Hutt (NZ): GNS Science. 39 p. Consultancy Report 2017/160. Prepared for Rangitata Diversion Race Management Group.
- McVerry GH, Stirling MW, Nicol A. 2005. Kupe Development Project: seismic hazard study. Lower Hutt (NZ): Institute of Geological & Nuclear Sciences. 40 p. Client Report 2005/14. Prepared for Beca International Limited on behalf of Worley Parsons Pty Limited.
- Meade BJ. 2007. Algorithms for the calculation of exact displacements, strains, and stresses for triangular dislocation elements in a uniform elastic half space. *Computers & Geosciences*. 33(8):1064–1075. doi:10.1016/j.cageo.2006.12.003.
- Melhuish A, Sutherland R, Davey FJ, Lamarche G. 1999. Crustal structure and neotectonics of the Puysegur oblique subduction zone, New Zealand. *Tectonophysics*. 313(4):335–362. doi:10.1016/S0040-1951(99)00212-7.
- Micallef A, Mountjoy JJ, Barnes PM, Canals M, Lastras G. 2014. Geomorphic response of submarine canyons to tectonic activity: Insights from the Cook Strait canyon system, New Zealand. *Geosphere*. 10(5):905–929. doi:10.1130/ges01040.1.
- Mittelstaedt J. 2011. Southward propagation of the Marlborough Fault System: fault linkage and blind faults in North Canterbury [MSc thesis]. Christchurch (NZ): University of Canterbury. 131 p.
- Miyoshi M, Heron DW, Berryman KR. 1987. Active faults and associated hazards in the Pauatahanui-Waikanae area, northwest Wellington. 39 p. Report R26/72.
- Morris P, Little T, Van Dissen RJ, Hill MP, Hemphill-Haley M, Kearse J, Norton K. 2021. Evaluating 9 m of near-surface transpressional displacement during the Mw 7.8 2016 Kaikoura earthquake: re-excavation of a pre-earthquake paleoseismic trench, Kekerengu Fault, New Zealand. *New Zealand Journal of Geology and Geophysics*. doi:10.1080/00288306.2021.1954958.
- Mountjoy JJ, Barnes PM. 2011. Active upper plate thrust faulting in regions of low plate interface coupling, repeated slow slip events, and coastal uplift: Example from the Hikurangi Margin, New Zealand. *Geochemistry, Geophysics, Geosystems*. 12(1):Q01005. doi:10.1029/2010gc003326.
- Mountjoy JJ, Barnes PM, Pettinga JR. 2009. Morphostructure and evolution of submarine canyons across an active margin: Cook Strait sector of the Hikurangi Margin, New Zealand. *Marine Geology*. 260(1–4):45–68. doi:10.1016/j.margeo.2009.01.006.

- Mouslopoulou V. 2006. Quaternary geometry, kinematics and paleoearthquake history at the intersection of the strike-slip North Island Fault System and Taupo Rift, New Zealand [PhD thesis]. Wellington (NZ): Victoria University of Wellington. 437 p.
- Mouslopoulou V, Nicol A, Little TA, Begg JG. 2009. Palaeoearthquake surface rupture in a transition zone from strike-slip to oblique-normal slip and its implications to seismic hazard, North Island Fault System, New Zealand. In: Reicherter K, Michetti AM, Silva PG, editors. *Palaeoseismology: historical and prehistorical records of earthquake ground effects for seismic hazard assessment*. London (GB): Geological Society. p. 269–292. (Geological Society special publication; 316).
- Mouslopoulou V, Nicol A, Little TA, Walsh JJ. 2007. Terminations of large strike-slip faults: an alternative model from New Zealand. In: Cunningham WD, Mann P, editors. *Tectonics of strike-slip restraining and releasing bends*. London (GB): Geological Society of London. p. 387–415. (Geological Society special publication; 290).
- Mouslopoulou V, Nicol A, Walsh JJ, Beetham D, Stagpoole V. 2008. Quaternary temporal stability of a regional strike-slip and rift fault intersection. *Journal of Structural Geology*. 30(4):451–463. doi:10.1016/j.jsg.2007.12.005.
- Mouslopoulou V, Saltogianni V, Nicol A, Oncken O, Begg J, Babeyko A, Cesca S, Moreno M. 2019. Breaking a subduction-termination from top to bottom: the large 2016 Kaikōura Earthquake, New Zealand. *Earth and Planetary Science Letters*. 506:221–230. doi:10.1016/j.epsl.2018.10.020.
- Nairn IA, Hedenquist JW, Villamor P, Berryman KR, Shane PA. 2005. The ~AD1315 Tarawera and Waiotapu eruptions, New Zealand: contemporaneous rhyolite and hydrothermal eruptions driven by an arrested basalt dike system? *Bulletin of Volcanology*. 67(2):186–193. doi:10.1007/s00445-004-0373-7.
- Nathan S, Rattenbury MS, Suggate RP, compilers. 2002. Geology of the Greymouth area [map]. Lower Hutt (NZ): Institute of Geological & Nuclear Sciences. 1 folded map + 58 p., scale 1:250,000. (Institute of Geological & Nuclear Sciences 1:250,000 geological map; 12).
- Nicholson C, Plesch A, Shaw JH. 2017. Community Fault Model Version 5.2: updating & expanding the CFM 3D fault set and its associated fault database [poster]. In: *2017 SCEC Annual Meeting*; 2017 Sep 9–13; Palm Springs, California. Los Angeles (CA): Southern California Earthquake Center. Poster 234. (SCEC contribution; 7735).
- Nicol A. 1993. Haumurian (c. 66–80 Ma) half-graben development and deformation, mid Waipara, North Canterbury, New Zealand. *New Zealand Journal of Geology and Geophysics*. 36(1):127–130. doi:10.1080/00288306.1993.9514560.
- Nicol A, Alloway BV, Tonkin PJ. 1994. Rates of deformation, uplift, and landscape development associated with active folding in the Waipara area of North Canterbury, New Zealand. *Tectonics*. 13(6):1327–1344.
- Nicol A, Campbell JK. 2001. The impact of episodic fault-related folding on late Holocene degradation terraces along Waipara River, New Zealand. *New Zealand Journal of Geology and Geophysics*. 44(1):145–156. doi:10.1080/00288306.2001.9514931.
- Nicol A, Khajavi N, Pettinga JR, Fenton C, Stahl T, Bannister S, Pedley K, Hyland-Brook N, Bushell T, Hamling I, et al. 2018. Preliminary geometry, displacement, and kinematics of fault ruptures in the epicentral region of the 2016 Mw 7.8 Kaikōura, New Zealand, earthquake. *Bulletin of the Seismological Society of America*. 108(3B):1521–1539. doi:10.1785/0120170329.

- Nicol A, Langridge RM, Van Dissen RJ. 2011. Wairau Fault Late Quaternary displacements and paleoearthquakes. In: Clark KJ, Litchfield NJ, editors. *Geoscience Society of New Zealand 2011 conference: field trip guide*. Wellington (NZ): Geoscience Society of New Zealand. p. 2–33. (Geoscience Society of New Zealand miscellaneous publication; 130B).
- Nicol A, Robinson R, Van Dissen RJ, Harvison A. 2016. Variability of recurrence interval and single-event slip for surface-rupturing earthquakes in New Zealand. *New Zealand Journal of Geology and Geophysics*. 59(1):97–116. doi:10.1080/00288306.2015.1127822.
- Nicol A, Van Dissen RJ. 1997. A reassessment of abruptly fanning bed dips on the northwestern limb of the Huangarua Syncline, Wairarapa, New Zealand. *New Zealand Journal of Geology and Geophysics*. 40(2):257–260. doi:10.1080/00288306.1997.9514757.
- Nicol A, Van Dissen RJ. 2002. Up-dip partitioning of displacement components on the oblique-slip Clarence Fault, New Zealand. *Journal of Structural Geology*. 24:1521–1535. doi:10.1016/S0191-8141(01)00141-9.
- Nicol A, Van Dissen RJ. 2018. A 6000-year record of surface-rupturing paleoearthquakes on the Wairau Fault, New Zealand. *New Zealand Journal of Geology and Geophysics*. 61(3):341–358. doi:10.1080/00288306.2018.1498360.
- Nicol A, Van Dissen RJ, Stirling MW, Gerstenberger MC. 2016. Completeness of the paleoseismic active-fault record in New Zealand. *Seismological Research Letters*. 87(6):1299–1310. doi:10.1785/0220160088.
- Nicol A, Van Dissen RJ, Vella P, Alloway BV, Melhuish A. 2002. Growth of contractional structures during the last 10 m.y. at the southern end of the emergent Hikurangi forearc basin, New Zealand. *New Zealand Journal of Geology and Geophysics*. 45(3):365–385. doi:10.1080/00288306.2002.9514979.
- Ninis D, Little TA, Van Dissen RJ, Litchfield NJ, Smith EGC, Wang N, Rieser U, Henderson CM. 2013. Slip rate on the Wellington fault, New Zealand, during the Late Quaternary: evidence for variable slip during the Holocene. *Bulletin of the Seismological Society of America*. 103(1):559–579. doi:10.1785/0120120162.
- Noble DP. 2011. Tectonic geomorphology and paleoseismicity of the Northern Esk Fault, North Canterbury, New Zealand [MSc thesis]. Christchurch (NZ): University of Canterbury. 169 p.
- Nodder SD. 1994. Characterizing potential offshore seismic sources using high-resolution geophysical and seafloor sampling programs: an example from Cape Egmont fault zone, Taranaki shelf, New Zealand. *Tectonics*. 13(3):641–658. doi:10.1029/94TC00296.
- Nodder S, Lamarche G, Proust J-N, Stirling M. 2007. Characterizing earthquake recurrence parameters for offshore faults in the low-strain, compressional Kapiti-Manawatu Fault System, New Zealand. *Journal of Geophysical Research: Solid Earth*. 112:B12102. doi:10.1029/2007JB005019.
- Norris RJ, Cooper AF. 2001. Late Quaternary slip rates and slip partitioning on the Alpine Fault, New Zealand. *Journal of Structural Geology*. 23(2):507–520. doi:10.1016/S0191-8141(00)00122-X.
- Oakley DOS, Fisher DM, Gardner TW, Stewart MK. 2018. Uplift rates of marine terraces as a constraint on fault-propagation fold kinematics: examples from the Hawkswood and Kate anticlines, North Canterbury, New Zealand. *Tectonophysics*. 724–725:195–219. doi:10.1016/j.tecto.2017.12.021.

- Oakley DOS, Kaufman DS, Gardner TW, Fisher DM, VanderLeest RA. 2017. Quaternary marine terrace chronology, North Canterbury, New Zealand, using amino acid racemization and infrared-stimulated luminescence. *Quaternary Research*. 87(1):151–167. doi:10.1017/qua.2016.9.
- Oliver PJ, Keene HW. 1990. Geological map of New Zealand 1:50,000 Sheet J36 BD and part Sheet J35 Clearwater [map]. Lower Hutt (NZ): New Zealand Geological Survey. 1 fold. map + 1 booklet.
- Ota Y, Beanland S, Berryman KR, Nairn IA. 1988a. The Matata Fault: active faulting at the north-western margin of the Whakatane graben, eastern Bay of Plenty. In: Survey NZG, editor. *Research notes 1988*. Lower Hutt (NZ): New Zealand Geological Survey. p. 6–13. (New Zealand Geological Survey record; 35).
- Ota Y, Berryman KR, Hull AG, Miyauchi T, Iso N. 1988b. Age and height distribution of Holocene transgressive deposits in eastern North Island, New Zealand. *Palaeogeography, Palaeoclimatology, Palaeoecology*. 68(2–4):135–151. doi:10.1016/0031-0182(88)90036-3.
- Ota Y, Hull AG, Berryman KR. 1991. Coseismic uplift of Holocene marine terraces in the Pakarua River area, Eastern North Island, New Zealand. *Quaternary Research*. 35(3 – Part1):331–346. doi:10.1016/0033-5894(91)90049-B.
- Ota Y, Pillans B, Berryman K, Beu A, Fujimori T, Miyauchi T, Berger G, Beu AG, Climo FM. 1996. Pleistocene coastal terraces of Kaikoura Peninsula and the Marlborough coast, South Island, New Zealand. *New Zealand Journal of Geology and Geophysics*. 39(1):51–73. doi:10.1080/00288306.1996.9514694.
- Pace B, Stirling MW, Litchfield NJ, Rieser U. 2005. New active fault data and seismic hazard estimates for west Otago, New Zealand. *New Zealand Journal of Geology and Geophysics*. 48(1):75–83. doi:10.1080/00288306.2005.9515099.
- Palmer A, Van Dissen RJ. 2002. Northern Ohariu Fault: earthquake hazard assessment of a newly discovered active strike-slip fault in Horowhenua. Wellington (NZ): Earthquake Commission Research Foundation. 52 p.
- Paquet F, Proust J-N, Barnes PM, Pettinga JR. 2011. Controls on active forearc basin stratigraphy and sediment fluxes: the Pleistocene of Hawke Bay, New Zealand. *GSA Bulletin*. 123(5–6):1074–1096. doi:10.1130/b30243.1.
- Pedley K, Barnes P, Pettinga J, Lewis K. 2010. Seafloor structural geomorphic evolution of the accretionary frontal wedge in response to seamount subduction, Poverty Indentation, New Zealand. *Marine Geology*. 270:119–138. doi:10.1016/j.margeo.2009.11.006.
- Persaud M, Villamor P, Berryman KR, Ries W, Cousins WJ, Litchfield NJ, Alloway BV. 2016. The Kerepehi Fault, Hauraki Rift, North Island, New Zealand: active fault characterisation and hazard. *New Zealand Journal of Geology and Geophysics*. 59(1):117–135. doi:10.1080/00288306.2015.1127826.
- Pettinga JR, Yetton MD, Dissen RJ, Downes G. 2001. Earthquake source identification and characterisation for the Canterbury Region, South Island, New Zealand. *Bulletin of the New Zealand Society for Earthquake Engineering*. 34(4):282–317. doi:10.5459/bnzsee.34.4.282-317.
- Pillans B. 1990. Vertical displacement rates on Quaternary faults, Wanganui Basin. *New Zealand Journal of Geology and Geophysics*. 33(2):271–275. doi:10.1080/00288306.1990.10425684.
- Plaza-Faverola A, Henrys S, Pecher I, Wallace L, Klaeschen D. 2016. Splay fault branching from the Hikurangi subduction shear zone: Implications for slow slip and fluid flow. *Geochemistry, Geophysics, Geosystems*. 17(12):5009–5023. doi:10.1002/2016GC006563.

- Plaza-Faverola A, Klaeschen D, Barnes P, Pecher I, Henrys S, Mountjoy J. 2012. Evolution of fluid expulsion and concentrated hydrate zones across the southern Hikurangi subduction margin, New Zealand: an analysis from depth migrated seismic data. *Geochemistry, Geophysics, Geosystems*. 13(8):Q08018. doi:10.1029/2012GC004228.
- Plaza-Faverola A, Pecher I, Crutchley G, Barnes PM, Bünz S, Golding T, Klaeschen D, Papenberg C, Bialas J. 2014. Submarine gas seepage in a mixed contractional and shear deformation regime: cases from the Hikurangi oblique-subduction margin. *Geochemistry, Geophysics, Geosystems*. 15(2):416–433. doi:10.1002/2013GC005082.
- Plesch A, Nicholson C, Sorlien CC, Shaw JH, Hauksson E. 2016. CFM Version 5.1: new and revised 3D fault representations and an improved database [poster]. In: *2016 SCEC Annual Meeting*; 2016 Sep 10–14; Palm Springs, California. Los Angeles (CA): Southern California Earthquake Center. Poster 003. (SCEC contribution; 6768).
- Plesch A, Shaw JH, Benson C, Bryant WA, Carena S, Cooke M, Dolan J, Fuis G, Gath E, Grant L, et al. 2007. Community Fault Model (CFM) for Southern California. *Bulletin of the Seismological Society of America*. 97(6):1793–1802. doi:10.1785/0120050211.
- Plesch A, Shaw JH, Ross ZE, Hauksson E. 2020. Detailed 3D fault representations for the 2019 Ridgecrest, California, earthquake sequence. *Bulletin of the Seismological Society of America*. 110(4):1818–1831. doi:10.1785/0120200053.
- Pondard N, Barnes PM. 2010. Structure and paleoearthquake records of active submarine faults, Cook Strait, New Zealand: implications for fault interactions, stress loading, and seismic hazard. *Journal of Geophysical Research: Solid Earth*. 115(B12):B12320. doi:10.1029/2010JB007781.
- Putnam AE, Schaefer JM, Denton GH, Barrell DJA, Andersen BG, Koffman TNB, Rowan AV, Finkel RC, Rood DH, Schwartz R, et al. 2013. Warming and glacier recession in the Rakaia valley, Southern Alps of New Zealand, during Heinrich Stadial 1. *Earth and Planetary Science Letters*. 382:98–110. doi:10.1016/j.epsl.2013.09.005.
- Quigley M, Van Dissen RJ, Litchfield NJ, Villamor P, Duffy B, Barrell DJA, Furlong K, Stahl T, Bilderback E, Noble D. 2012. Surface rupture during the 2010  $M_w$  7.1 Darfield (Canterbury) earthquake: implications for fault rupture dynamics and seismic-hazard analysis. *Geology*. 40(1):55–58. doi:10.1130/g32528.1.
- Rattenbury MS. 2020. The New Zealand Community Fault Model: information management principles and processes. Lower Hutt (NZ): GNS Science. 9 p. (GNS Science report; 2020/08).
- Rattenbury MS. 2022. Regional fault orientation and length analysis, Aotearoa New Zealand. Lower Hutt (NZ): GNS Science. 49 p. (GNS Science report; 2022/13).
- Rattenbury MS, Cooper RA, Johnston MR. 1998. Geology of the Nelson area [map]. Lower Hutt (NZ): Institute of Geological & Nuclear Sciences. 1 fold map + 67 p., scale 1:250,000. (Institute of Geological & Nuclear Sciences geological map; 9).
- Rattenbury MS, Isaac MJ. 2012. The QMAP 1:250 000 Geological Map of New Zealand project. *New Zealand Journal of Geology and Geophysics*. 55(4):393–405. doi:10.1080/00288306.2012.725417.
- Rattenbury MS, Jongens R, Cox SC, compilers. 2010. Geology of the Haast area [map]. Lower Hutt (NZ): GNS Science. 1 fold. map + 58 p., scale 1:250,000. (GNS Science 1:250,000 geological map; 14).
- Rattenbury MS, Townsend DB, Johnston MR. 2006. Geology of the Kaikoura area [map]. Lower Hutt (NZ): GNS Science. 1 map + 70 p., scale 1:250,000. (Institute of Geological & Nuclear Sciences 1:250,000 geological map; 13).

- Raub ML. 1985. The Neotectonic evolution of the Wakarara area, southern Hawke's Bay, New Zealand [MPhil thesis]. Auckland (NZ): University of Auckland. 117 leaves.
- Retallack GJ, Ryburn RJ. 1982. Middle Triassic deltaic deposits in Long Gully, near Otematata, north Otago, New Zealand. *Journal of the Royal Society of New Zealand*. 12(3):207–220. doi:10.1080/03036758.1982.10415345.
- Reyners ME, Eberhart-Phillips D, Bannister S. 2011. Tracking repeated subduction of the Hikurangi Plateau beneath New Zealand. *Earth and Planetary Science Letters*. 311(1/2):165–171. doi:10.1016/j.epsl.2011.09.011.
- Reyners M, Eberhart-Phillips D, Stuart G, Nishimura Y. 2006. Imaging subduction from the trench to 300 km depth beneath the central North Island, New Zealand, with  $V_p$  and  $V_p/V_s$ . *Geophysical Journal International*. 165(2):565–583. doi:10.1111/j.1365-246X.2006.02897.x.
- Reyners M, Robinson R, Pancha A, McGinty P. 2002. Stresses and strains in a twisted subduction zone – Fiordland, New Zealand. *Geophysical Journal International*. 148(3):637–648. doi:10.1046/j.1365-246X.2002.01611.x.
- Richards-Dinger K, Dieterich JH. 2012. RSQSim earthquake simulator. *Seismological Research Letters*. 83(6):983–990. doi:10.1785/0220120105.
- Ristau J. 2008. Implementation of routine regional moment tensor analysis in New Zealand. *Seismological Research Letters*. 79(3):400–415. doi:10.1785/gssrl.79.3.400.
- Ristau J, Holden C, Kaiser A, Williams C, Bannister S, Fry B. 2013. The Pegasus Bay aftershock sequence of the Mw 7.1 Darfield (Canterbury), New Zealand earthquake. *Geophysical Journal International*. 195(1):444–459. doi:10.1093/gji/ggt222.
- Robinson R, Van Dissen R, Litchfield N. 2011. Using synthetic seismicity to evaluate seismic hazard in the Wellington region, New Zealand. *Geophysical Journal International*. 187(1):510–528. doi:10.1111/j.1365-246X.2011.05161.x.
- Rodgers DW, Little TA. 2006. World's largest coseismic strike-slip offset: the 1855 rupture of the Wairarapa Fault, New Zealand, and implications for displacement/length scaling of continental earthquakes. *Journal of Geophysical Research: Solid Earth*. 111(B12):B12408. doi:10.1029/2005jb004065.
- Saul G. 1994. The basin development and deformation associated with the Kongahu (Lower Buller) fault zone over the last 12 Ma, Mokihinui River, West Coast, South Island, New Zealand. *Journal of the Royal Society of New Zealand*. 24(3):277–288. doi:10.1080/03014223.1994.9517472.
- Schermer ER, Little TA, Rieser U. 2009. Quaternary deformation along the Wharekauhau fault system, North Island, New Zealand: implications for an unstable linkage between active strike-slip and thrust faults. *Tectonics*. 28(6):TC6008. doi:10.1029/2008tc002426.
- Schermer E, Van Dissen RJ, Berryman KR. 1998. In search of the source of the 1934 Pahiataua earthquake. Lower Hutt (NZ): Institute of Geological & Nuclear Sciences. 53 leaves.
- Schermer ER, Van Dissen R, Berryman KR, Kelsey HM, Cashman SM. 2004. Active faults, paleoseismology, and historical fault rupture in northern Wairarapa, North Island, New Zealand. *New Zealand Journal of Geology and Geophysics*. 47(1):101–122. doi:10.1080/00288306.2004.9515040.
- Seebeck H, Thrasher GP, Viskovic GPD, Macklin C, Bull S, Wang X, Nicol A, Holden C, Kaneko Y, Mouslopoulou V, et al. 2021. Geologic, earthquake and tsunami modelling of the active Cape Egmont Fault Zone. Lower Hutt (NZ): GNS Science. 370 p. (GNS Science report; 2021/06).

- Shuck B, Van Avendonk H, Gulick SPS, Gurnis M, Sutherland R, Stock J, Patel J, Hightower E, Saustrup S, Hess T. 2021. Strike-slip enables subduction initiation beneath a failed rift: new seismic constraints from Puysegur Margin, New Zealand. *Tectonics*. 40(5):e2020TC006436. doi:10.1029/2020TC006436.
- Silva V, Crowley H, Pagani M, Monelli D, Pinho R. 2014. Development of the OpenQuake engine, the Global Earthquake Model's open-source software for seismic risk assessment. *Natural Hazards*. 72(3):1409–1427. doi:10.1007/s11069-013-0618-x.
- Sisson RJ, Campbell J, Pettinga J, Milner D. 2001. Paleoseismicity of the Ashley and Loburn faults, North Canterbury, New Zealand. Wellington (NZ): Earthquake Commission Research Foundation. 31 p. EQC Research Report 97/237.
- Stahl T, Quigley MC, Bebbington MS. 2016a. Tectonic geomorphology of the Fox Peak and Forest Creek Faults, South Canterbury, New Zealand: slip rates, segmentation and earthquake magnitudes. *New Zealand Journal of Geology and Geophysics*. 59(4):568–591. doi:10.1080/00288306.2016.1212908.
- Stahl T, Quigley MC, McGill A, Bebbington MS. 2016b. Modeling earthquake moment magnitudes on imbricate reverse faults from paleoseismic data: Fox Peak and Forest Creek Faults, South Island, New Zealand. *Bulletin of the Seismological Society of America*. 106(5):2345–2363. doi:10.1785/0120150215.
- Stirling MW. 1992. Late Holocene beach ridges displaced by the Wellington Fault in the Lower Hutt area, New Zealand. *New Zealand Journal of Geology and Geophysics*. 35(4):447–453. doi:10.1080/00288306.1992.9514539.
- Stirling MW, Abbott ER, Rood DH, McVerry GH, Abrahamson NA, Barrell DJA, Huso R, Litchfield NJ, Luna L, Rhoades DA, et al. 2021. First use of fragile geologic features to set the design motions for a major existing engineered structure. *Bulletin of the Seismological Society of America*. 111(5):2673–2695. doi:10.1785/0120210026.
- Stirling M, McVerry G, Gerstenberger M, Litchfield N, Van Dissen RJ, Berryman K, Barnes P, Wallace L, Villamor P, Langridge R, et al. 2012. National Seismic Hazard Model for New Zealand: 2010 update. *Bulletin of the Seismological Society of America*. 102(4):1514–1542. doi:10.1785/0120110170.
- Stratford WR, Chamberlain C, Sutherland R, Stern T. 2020. Crustal structure and subduction geometry in southern South Island, New Zealand. In: Bassett KN, Nichols ARL, Fenton CH, editors. *Geoscience Society of New Zealand annual conference 2020: abstract volume*. 2020 Nov 22–25; Christchurch, New Zealand. Wellington (NZ): Geoscience Society of New Zealand. p. 279. (Miscellaneous publication; 157A).
- Sutherland R. 1995. Late Cenozoic tectonics of the southwest Pacific, and the development of the Alpine Fault through southern South Island, New Zealand [PhD thesis]. Dunedin (NZ): University of Otago. 1 vol.
- Sutherland R, Barnes P, Uruski C. 2006a. Miocene-Recent deformation, surface elevation, and volcanic intrusion of the overriding plate during subduction initiation, offshore southern Fiordland, Puysegur margin, southwest New Zealand. *New Zealand Journal of Geology and Geophysics*. 49(1):131–149. doi:10.1080/00288306.2006.9515154.
- Sutherland R, Berryman KR, Norris R. 2006b. Quaternary slip rate and geomorphology of the Alpine Fault: implications for kinematics and seismic hazard in southwest New Zealand. *Geological Society of America Bulletin*. 118(3–4):464–474. doi:10.1130/B25627.1.

- Sutherland R, Gurnis M, Kamp PJJ, House MA. 2009a. Regional exhumation history of brittle crust during subduction initiation, Fiordland, southwest New Zealand, and implications for thermochronologic sampling and analysis strategies. *Geosphere*. 5(5):409–425. doi:10.1130/ges00225.1.
- Sutherland R, Kim KJ, Zondervan A, McSaveney MJ. 2007. Orbital forcing of mid-latitude Southern Hemisphere glaciation since 100 ka inferred from cosmogenic nuclide ages of moraine boulders from the Cascade Plateau, southwest New Zealand. *Geological Society of America Bulletin*. 119(3–4):443–451. doi:10.1130/b25852.1.
- Sutherland R, Nathan S, Turnbull IM, Beu AG. 1995. Pliocene-Quaternary sedimentation and Alpine Fault related tectonics in the lower Cascade valley, South Westland, New Zealand. *New Zealand Journal of Geology and Geophysics*. 38(4):431–450. doi:10.1080/00288306.1995.9514670.
- Sutherland R, Norris RJ. 1995. Late Quaternary displacement rate, paleoseismicity, and geomorphic evolution of the Alpine Fault: evidence from Hokuri Creek, South Westland, New Zealand. *New Zealand Journal of Geology and Geophysics*. 38(4):419–430. doi:10.1080/00288306.1995.9514669.
- Sutherland R, Stagpoole V, Uruski C, Kennedy C, Bassett D, Henrys S, Scherwath M, Kopp H, Field B, Toulmin S, et al. 2009b. Reactivation of tectonics, crustal underplating, and uplift after 60 Myr of passive subsidence, Raukumara Basin, Hikurangi-Kermadec fore arc, New Zealand: Implications for global growth and recycling of continents. *Tectonics*. 28:TC5017. doi:10.1029/2008tc002356.
- Taylor-Silva BI, Stirling MW, Litchfield NJ, Griffin JD, van den Berg EJ, Wang N. 2020. Paleoseismology of the Akatore Fault, Otago, New Zealand. *New Zealand Journal of Geology and Geophysics*. 63(2):151–167. doi:10.1080/00288306.2019.1645706.
- Thingbaijam KKS, Martin Mai P, Goda K. 2017. New empirical earthquake source-scaling laws. *Bulletin of the Seismological Society of America*. 107(5):2225–2246. doi:10.1785/0120170017.
- Thrasher GP. 1986. Basement structure and sediment thickness beneath the continental shelf of the Hauraki Gulf and offshore Coromandel region, New Zealand. *New Zealand Journal of Geology and Geophysics*. 29(1):41–50. doi:10.1080/00288306.1986.10427521.
- Thrasher GP. 1988. Subsurface geology of the continental shelf, Bay of Plenty to the Three Kings Islands, New Zealand. Lower Hutt (NZ): Department of Scientific & Industrial Research. 13 p. New Zealand Geological Survey Report G 133.
- Townsend DB, Begg JG, Villamor P, Lukovic B. 2002. Late Quaternary displacement of the Mokonui Fault, Wairarapa, New Zealand: a preliminary assessment of earthquake generating potential. Lower Hutt (NZ): Institute of Geological & Nuclear Sciences. 30 p. + 2 maps. Client Report 2002/58. Prepared for Wairarapa Engineering Lifelines Association.
- Townsend DB, Little TA. 1998. Pliocene-Quaternary deformation and mechanisms of near-surface strain close to the eastern tip of the Clarence Fault, northeast Marlborough, New Zealand. *New Zealand Journal of Geology and Geophysics*. 41(4):401–417. doi:10.1080/00288306.1998.9514819.
- Townsend DB, Nicol A, Mouslopoulou V, Begg JG, Beetham RD, Clark D, Giba M, Heron DW, Lukovic B, McPherson A, et al. 2010. Palaeoearthquake histories across a normal fault system in the southwest Taranaki Peninsula, New Zealand. *New Zealand Journal of Geology and Geophysics*. 53(4):375–394. doi:10.1080/00288306.2010.526547.

- Townsend T. 1998. Paleoseismology of the Waverley Fault Zone and implications for earthquake hazard in South Taranaki, New Zealand. *New Zealand Journal of Geology and Geophysics*. 41(4):467–474. doi:10.1080/00288306.1998.9514823.
- Turnbull IM. 2000. Geology of the Wakatipu area [map]. Lower Hutt (NZ): Institute of Geological and Nuclear Sciences. 1 fold. map + 72 p., scale 1:250,000. (Institute of Geological & Nuclear Sciences 1:250,000 geological map; 18).
- Turnbull IM, Allibone AH. 2003. Geology of the Murihiku area [map]. Lower Hutt (NZ): Institute of Geological & Nuclear Sciences. 1 fold. map + 74 p., scale 1:250,000. (Institute of Geological & Nuclear Sciences 1:250,000 geological map; 20).
- Turnbull IM, Allibone AH, Jongens R, compilers. 2010. Geology of the Fiordland area [map]. Lower Hutt (NZ): GNS Science. 1 fold. map + 97 p., scale 1:250,000. (Institute of Geological & Nuclear Sciences 1:250,000 geological map; 17).
- Turnbull IM, Uruski CI, Anderson HJ, Lindqvist JK, Scott GH, Morgans HEG, Hoskins RH, Raine JI, Mildenhall DC, Pocknall DT, et al. 1993. Cretaceous and Cenozoic sedimentary basins of western Southland, South Island, New Zealand. Lower Hutt (NZ): Institute of Geological & Nuclear Sciences. 86 p. (Institute of Geological & Nuclear Sciences monograph; 1).
- Van Avendonk HJA, Davis JK, Harding JL, Lawver LA. 2017. Decrease in oceanic crustal thickness since the breakup of Pangaea. *Nature Geoscience*. 10(1):58–61. doi:10.1038/ngeo2849.
- van den Berg E. 2020. Paleoseismology of the NW Cardrona Fault, Central Otago [MGeol thesis]. Dunedin (NZ): University of Otago. 141 p. + appendices.
- Van Dissen RJ. 1989. Late Quaternary faulting in the Kaikoura region, southeastern Marlborough, New Zealand [MSc thesis]. Corvallis (OR): Oregon State University. 72 p.
- Van Dissen RJ, Barrell DJA, Langridge RM, Litchfield NJ, Villamor P, Tonkin P. 2007. Reassessment of seismic hazard at Clyde Dam, Central Otago: earthquake geology field investigations and determination of Dunstan Fault rupture characteristics. Lower Hutt (NZ): GNS Science. 2 vol. + appendices. Consultancy Report 2006/147. Prepared for Contact Energy Limited.
- Van Dissen RJ, Barrell DJA, Litchfield NJ, Villamor P, Quigley M, King AB, Furlong K, Begg JG, Townsend DB, Mackenzie H, et al. 2011. Surface rupture displacement on the Greendale Fault during the  $M_w$  7.1 Darfield (Canterbury) Earthquake, New Zealand, and its impact on man-made structures. In: *Proceedings of the Ninth Pacific Conference on Earthquake Engineering: building an earthquake resilient society*; 2011 Apr 14–16; Auckland, New Zealand. Auckland (NZ): 9PCEE. Paper 186.
- Van Dissen RJ, Begg JG, Palmer A, Nicol A, Darby DJ, Reyners ME. 1998. Newly discovered active faults in the Wellington region, New Zealand. In: *New Zealand National Society for Earthquake Engineering Technical Conference and AGM*; 1998 Mar 27–29; Taupō, New Zealand. [Wellington] (NZ): New Zealand National Society for Earthquake Engineering. 7 p.
- Van Dissen RJ, Begg JG, Robinson R. 2001. The Akatarawa Fault: a newly discovered active fault in the Wellington region, and implications for increased hazard on the Wellington fault. In: *New Zealand Society for Earthquake Engineering Inc Technical Conference and AGM*; 2001 Mar 23–25; Taupō, New Zealand. [Wellington] (NZ): New Zealand Society of Earthquake Engineering. 8 p.
- Van Dissen RJ, Berryman KR. 1996. Surface rupture earthquakes over the last ~1000 years in the Wellington region, New Zealand, and implications for ground shaking hazard. *Journal of Geophysical Research: Solid Earth*. 101(B3):5999–6019. doi:10.1029/95JB02391.

- Van Dissen RJ, Berryman KR, Pettinga JR, Hill NL. 1992. Paleoseismicity of the Wellington – Hutt Valley segment of the Wellington Fault, North Island, New Zealand. *New Zealand Journal of Geology and Geophysics*. 35(2):165–176. doi:10.1080/00288306.1992.9514511.
- Van Dissen RJ, Heron DW. 2003. Earthquake fault trace survey, Kapiti Coast District. Lower Hutt (NZ): Institute of Geological & Nuclear Sciences. 45 p. Client Report 2003/77. Prepared for Kāpiti Coast District Council.
- Van Dissen RJ, Hull AG, Read SAL. 1994. Timing of some large Holocene earthquakes on the Ostler Fault, New Zealand. In: *Proceedings of the Eighth International Symposium on Recent Crustal Movements (CRCM '93)*; 1993 Dec 6–11; Kobe, Japan. [Tokyo] (JP): Geodetic Society of Japan. p. 381–386.
- Van Dissen RJ, Little TA, Burke RM, Tonkin PJ, Norton KP, Bacon SN, Bowers R, Goldstein HL, Redwine JR, Sutherland DG, et al. 2016. Late Quaternary dextral slip rate of the Kekerengu Fault: New Zealand's third fastest on-land fault. In: White JDL, Smillie RW, editors. *Geosciences 2016: Annual Conference of the Geoscience Society of New Zealand: abstract volume*; 2016 Nov 28 – Dec 1; Wānaka, New Zealand. [Wellington] (NZ): Geoscience Society of New Zealand. p. 89. (Miscellaneous publication; 145A).
- Van Dissen RJ, Little T, Nicol A. 2005. Field trip 4: faults of eastern Marlborough: Picton, Awatere and Kekerengu. In: Pettinga JR, Wandres AM, editors. *Geological Society of New Zealand 50<sup>th</sup> annual conference: Kaikoura: field trip guides*; 2005 Nov 28 – Dec 1; Kaikōura, New Zealand. [Wellington] (NZ): Geological Society of New Zealand. p. 85–110. (Miscellaneous publication; 119B).
- Van Dissen RJ, Nicol A. 2009. Mid-Late Holocene paleoseismicity of the eastern Clarence Fault, Marlborough, New Zealand. *New Zealand Journal of Geology and Geophysics*. 52(3):195–208. doi:10.1080/00288300909509886.
- Van Dissen R, Yeats RS. 1991. Hope fault, Jordan thrust, and uplift of the Seaward Kaikoura Range, New Zealand. *Geology*. 19(4):393–396. doi:10.1130/0091-7613(1991)019<0393:Hfjtau>2.3.Co;2.
- Vandergoes MJ, Hogg AG, Lowe DJ, Newnham RM, Denton GH, Southon J, Barrell DJA, Wilson CJN, McGlone MS, Allan ASR, et al. 2013. A revised age for the Kawakawa/Oruanui tephra, a key marker for the Last Glacial Maximum in New Zealand. *Quaternary Science Reviews*. 74:195–201. doi:10.1016/j.quascirev.2012.11.006.
- VanderLeest RA. 2015. Investigation of fold growth in North Canterbury, South Island, New Zealand [MSc thesis]. University Park (PA): Pennsylvania State University. 78 p.
- Vermeer JL, Quigley MC, Duffy BG, Langridge RM, Pettinga JR. 2021. Structure and kinematics of active faulting in the Hope-Kelly and Alpine Fault intersection zone, South Island, New Zealand. *Tectonophysics*. 813:article 228928. doi:10.1016/j.tecto.2021.228928.
- Villamor P, Barrell DJA, Gorman A, Davy BW, Hreinsdottir S, Hamling IJ, Stirling MW, Cox SC, Litchfield NJ, Holt A, et al. 2018. Unknown faults under cities. Lower Hutt (NZ): GNS Science. 71 p. (GNS Science miscellaneous series; 124).
- Villamor P, Berryman KR. 2001. A late Quaternary extension rate in the Taupo Volcanic Zone, New Zealand, derived from fault slip data. *New Zealand Journal of Geology and Geophysics*. 44(2):243–269. doi:10.1080/00288306.2001.9514937.
- Villamor P, Berryman KR. 2006a. Evolution of the southern termination of the Taupo Rift, New Zealand. *New Zealand Journal of Geology and Geophysics*. 49(1):23–37. doi:10.1080/00288306.2006.9515145.

- Villamor P, Berryman KR. 2006b. Late Quaternary geometry and kinematics of faults at the southern termination of the Taupo Volcanic Zone, New Zealand. *New Zealand Journal of Geology and Geophysics*. 49(1):1–21. doi:10.1080/00288306.2006.9515144.
- Villamor P, Berryman KR, Ellis SM, Schreurs G, Wallace LM, Leonard GS, Langridge RM, Ries WF. 2017. Rapid evolution of subduction-related continental intraarc rifts: the Taupo Rift, New Zealand. *Tectonics*. 36(10):2250–2272. doi:10.1002/2017tc004715.
- Villamor P, Berryman KR, Nairn IA, Wilson KJ, Litchfield NJ, Ries W. 2011. Associations between volcanic eruptions from Okataina Volcanic Center and surface rupture of nearby active faults, Taupo rift, New Zealand: insights into the nature of volcano-tectonic interactions. *Geological Society of America Bulletin*. 123(7–8):1383–1405. doi:10.1130/b30184.1.
- Villamor P, Berryman KR, Webb TH, Stirling MW, McGinty PJ, Downes GL, Harris JS, Litchfield NJ. 2001. Waikato seismic loads – Task 2.1 revision of seismic source characterisation. Lower Hutt (NZ): Institute of Geological & Nuclear Sciences. 109 p. Client Report 2001/59. Prepared for URS & Mighty River Power.
- Villamor P, Clark KJ, Watson M, Rosenberg MD, Lukovic B, Ries W, Gonzalez A, Milicich SD, McNamara DD, Pummer B, et al. 2015. New Zealand geothermal power plants as critical facilities: an active fault avoidance study in the Wairakei Geothermal Field, New Zealand. In: Horne R, Boyd T, editors. *Proceedings, World Geothermal Congress 19–24 April 2015, Australia-New Zealand*. Bochum (DE): International Geothermal Association. 12 p.
- Villamor P, Langridge RM, Ries W, Carne R, Wilson KJ, Seebeck H, Cowan L. 2008. It's Our Fault, Wairarapa Fault slip rate investigations task: completion report, is the Wairarapa Fault slip rate decreasing to the north? Lower Hutt (NZ): GNS Science. 53 p. Consultancy Report 2008/170. Prepared for the Earthquake Commission.
- Villamor P, Litchfield NJ, Gomez D, Martin-González F, Alloway B, Berryman K, Clark K, Ries W, Howell A, Ansell IA. 2022. Fault ruptures triggered by large rhyolitic eruptions at the boundary between tectonic and magmatic rift segments: the Manawahe Fault, Taupō Rift, New Zealand. *Journal of Volcanology and Geothermal Research*. doi:10.1016/j.jvolgeores.2022.107478.
- Villamor P, Van Dissen RJ, Alloway B, Palmer A, Litchfield N. 2004. The Rangipo (Desert Road) Fault: the most hazardous fault in the Taupo Volcanic Zone? Lower Hutt (NZ): Institute of Geological & Nuclear Sciences. 73 p. Client Report 2004/34. Prepared for Earthquake Commission.
- Villamor P, Van Dissen RJ, Alloway BV, Palmer AS, Litchfield NJ. 2007. The Rangipo Fault, Taupo rift, New Zealand: an example of temporal slip-rate and single-event displacement variability in a volcanic environment. *Geological Society of America Bulletin*. 119(5–6):529–547. doi:10.1130/b26000.1.
- Wallace LM. 2020. Slow slip events in New Zealand. *Annual Review of Earth and Planetary Sciences*. 48:175–203. doi:10.1146/annurev-earth-071719-055104.
- Wallace LM, Barnes P, Beavan J, Van Dissen R, Litchfield N, Mountjoy J, Langridge R, Lamarche G, Pondard N. 2012. The kinematics of a transition from subduction to strike-slip: an example from the central New Zealand plate boundary. *Journal of Geophysical Research: Solid Earth*. 117(B2):B02405. doi:10.1029/2011jb008640.
- Wallace LM, Beavan J, McCaffrey R, Berryman K, Denys P. 2007. Balancing the plate motion budget in the South Island, New Zealand using GPS, geological and seismological data. *Geophysical Journal International*. 168(1):332–352. doi:10.1111/j.1365-246X.2006.03183.x.
- Wang N, Grapes R. 2008. Infrared-stimulated luminescence dating of Late Quaternary aggradation surfaces and their deformation along an active fault, southern North Island of New Zealand. *Geomorphology*. 96(1–2):86–104. doi:10.1016/j.geomorph.2007.07.016.

- Wellman HW. 1953. The geology of the Geraldine subdivision sheet district. Wellington: Department of Scientific & Industrial Research. 72 p. (New Zealand Geological Survey bulletin; 50).
- Williams CA, Eberhart-Phillips D, Bannister S, Barker DHN, Henrys S, Reyners M, Sutherland R. 2013. Revised interface geometry for the Hikurangi subduction zone, New Zealand. *Seismological Research Letters*. 84(6):1066–1073. doi:10.1785/0220130035.
- Williams J, Barrell D, Stirling M, Sauer K, Duke G, Hao K. 2018. Surface rupture of the Hundalee Fault during the 2016 Mw 7.8 Kaikōura earthquake. *Bulletin of the Seismological Society of America*. 108(3B):1540–1555. doi:10.1785/0120170291.
- Wilson KJ, Berryman KR, Litchfield NJ, Little T. 2006. A revision of mid-late Holocene marine terrace distribution and chronology at the Pakarae River mouth, North Island, New Zealand. *New Zealand Journal of Geology and Geophysics*. 49(4):477–489. doi:10.1080/00288306.2006.9515182.
- Wise DJ, Cassidy J, Locke CA. 2003. Geophysical imaging of the Quaternary Wairoa North Fault, New Zealand: a case study. *Journal of Applied Geophysics*. 53(1):1–16. doi:10.1016/S0926-9851(03)00013-2.
- Wood RA, Pettinga JR, Bannister S, Lamarche G, McMorran TJ. 1994. Structure of the Hanmer strike-slip basin, Hope fault, New Zealand. *GSA Bulletin*. 106(11):1459–1473. doi:10.1130/0016-7606(1994)106<1459:Sothss>2.3.Co;2.
- Wright IC. 1990. Late Quaternary faulting of the offshore Whakatane Graben, Taupo Volcanic Zone, New Zealand. *New Zealand Journal of Geology and Geophysics*. 33(2):245–256. doi:10.1080/00288306.1990.10425682.
- Yang JS. 1991. The Kakapo Fault – a major active dextral fault in the central North Canterbury – Buller regions of New Zealand. *New Zealand Journal of Geology and Geophysics*. 34(2):137–143. doi:10.1080/00288306.1991.9514451.
- Yang JS. 1992. Landslide mapping and major earthquakes on the Kakapo Fault, South Island, New Zealand. *Journal of the Royal Society of New Zealand*. 22(3):205–212. doi:10.1080/03036758.1992.10426557.
- Yeats RS. 2000. The 1968 Inangahua, New Zealand, and 1994 Northridge, California, earthquakes: Implications for northwest Nelson. *New Zealand Journal of Geology and Geophysics*. 43(4):587–599. doi:10.1080/00288306.2000.9514911.
- Yetton MD. 1998. Progress in understanding the paleoseismicity of the central and northern Alpine Fault, Westland, New Zealand. *New Zealand Journal of Geology and Geophysics*. 41(4):475–483. doi:10.1080/00288306.1998.9514824.
- Yetton MD. 2002. Paleoseismic investigation of the north and west Wairau sections of the Alpine Fault, South Island, New Zealand. Christchurch (NZ): Geotech Consulting Ltd. 96 p. Earthquake Commission Research Report 99/353. Prepared for the Earthquake Commission Research Foundation.
- Zachariassen J, Berryman K, Langridge R, Prentice C, Rymer M, Stirling M, Villamor P. 2006. Timing of late Holocene surface rupture of the Wairau Fault, Marlborough, New Zealand. *New Zealand Journal of Geology and Geophysics*. 49(1):159–174. doi:10.1080/00288306.2006.9515156.
- Zachariassen J, Van Dissen RJ. 2001. Paleoseismicity of the northern Horohoro Fault, Taupo Volcanic Zone, New Zealand. *New Zealand Journal of Geology and Geophysics*. 44(3):391–401. doi:10.1080/00288306.2001.9514946.

- Zachariassen J, Villamor P, Lee JM, Lukovic B, Begg JG. 2000. Late Quaternary faulting of the Masterton and Carterton faults, Wairarapa, New Zealand. Lower Hutt (NZ): Institute of Geological & Nuclear Sciences. 36 p. Client Report 2000/71. Prepared for Wairarapa Engineering Lifelines Association.
- Zinke R, Dolan JF, Rhodes EJ, Van Dissen RJ, Hatem AE, McGuire CP, Brown ND, Grenader JR. 2021. Latest Pleistocene–Holocene incremental slip rates of the Wairau Fault: implications for long-distance and long-term coordination of faulting between North and South Island, New Zealand. *Geochemistry, Geophysics, Geosystems*. 22(9):e2021GC009656. doi:10.1029/2021GC009656.
- Zinke R, Dolan JF, Rhodes EJ, Van Dissen RJ, McGuire CP. 2017. Highly variable latest Pleistocene–Holocene incremental slip rates on the Awatere fault at Saxton River, South Island, New Zealand, revealed by lidar mapping and luminescence dating. *Geophysical Research Letters*. 44(22):11301–11310. doi:10.1002/2017gl075048.
- Zinke R, Hollingsworth J, Dolan JF, Van Dissen R. 2019. Three-dimensional surface deformation in the 2016  $M_w$  7.8 Kaikōura, New Zealand, earthquake from optical image correlation: implications for strain localization and long-term evolution of the Pacific-Australian Plate boundary. *Geochemistry, Geophysics, Geosystems*. 20(3):1609–1628. doi:10.1029/2018GC007951.

## APPENDICES

This page left intentionally blank.

## APPENDIX 1 NZ CFM V1.0

This appendix (attached as an Excel spreadsheet) contains a tabulation of all faults in NZ CFM v1.0 and their attributes, derived from the 2D component of the model in an ArcGIS database. The index map (Figure A1.1) provides a key to a set of overlapping maps that show all faults and fault segments in NZ CFM v1.0 (Figures A1.2–A1.11). The numbers associated with each fault in Figures A1.2–A1.11 relate to the Fault\_ID detailed in the attribute table.

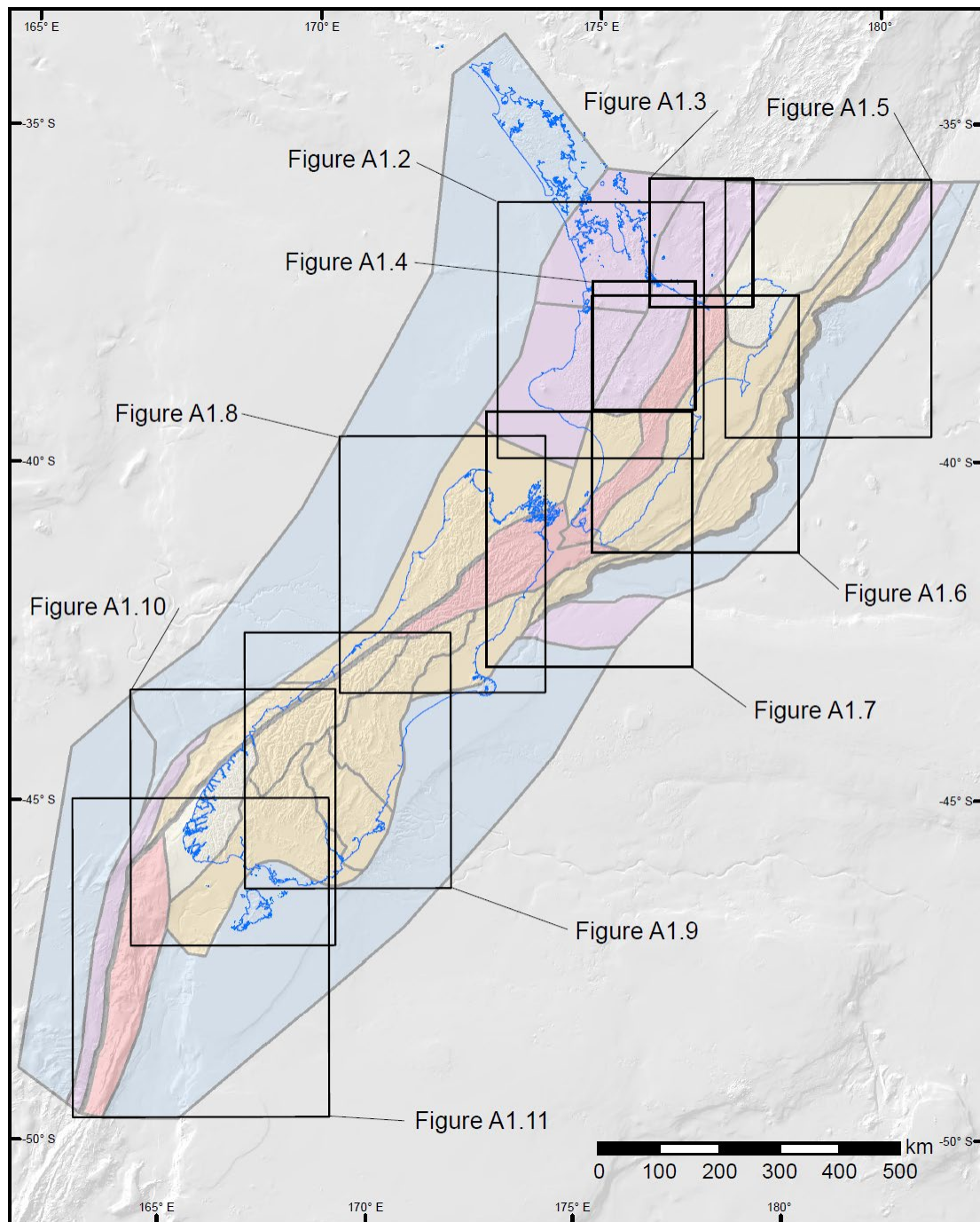


Figure A1.1 Map extent showing regions of the New Zealand Community Fault Model. Location of Figures A1.2–A1.11. Neotectonic domains (coloured polygons) in Figure 3.3 are shown for context.

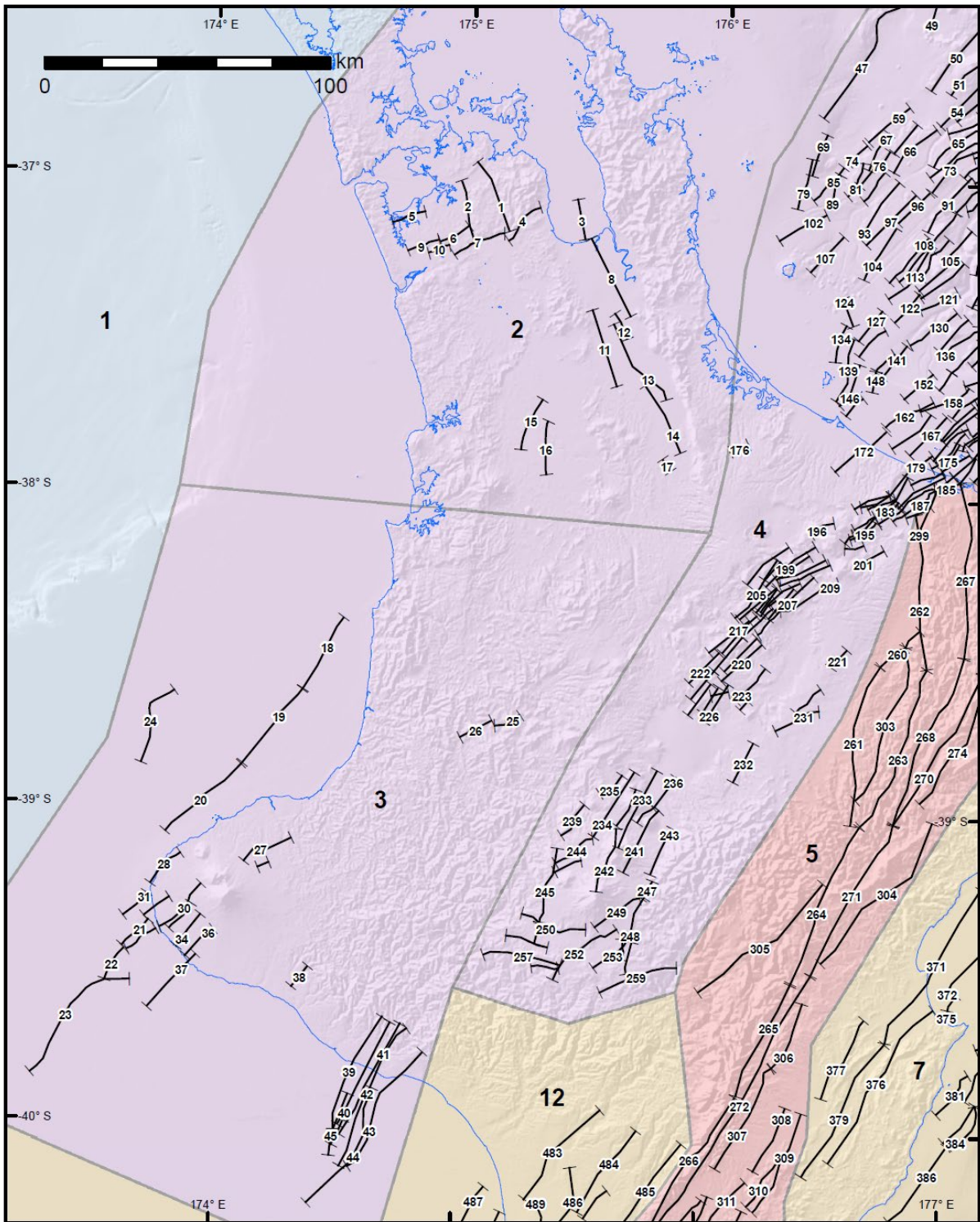


Figure A1.2 Western North Island. Fault ID (numbers with white outline) is shown for each fault or fault segment in NZ CFM v1.0. The extent of each fault or fault segment is shown by a marker line. Neotectonic domains (coloured polygons) in Figure 3.3 are shown for context. A description of the neotectonic domains (large bold numbers) is provided in Table 3.1.

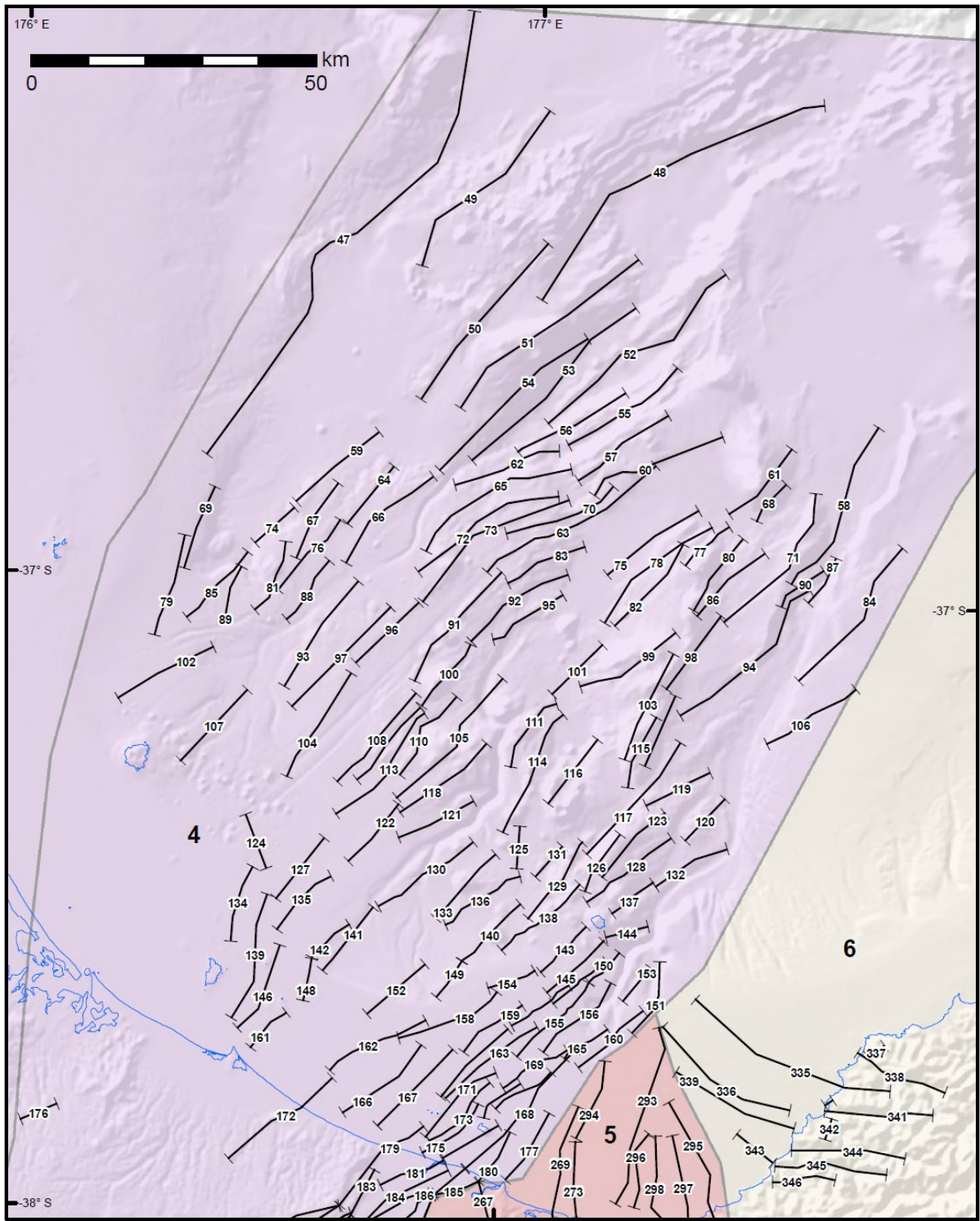


Figure A1.3 Bay of Plenty. Fault ID (numbers with white outline) is shown for each fault or fault segment in NZ CFM v1.0. The extent of each fault or fault segment is shown by a marker line. Neotectonic domains (coloured polygons) in Figure 3.3 are shown for context. A description of the neotectonic domains (large bold numbers) is provided in Table 3.1.



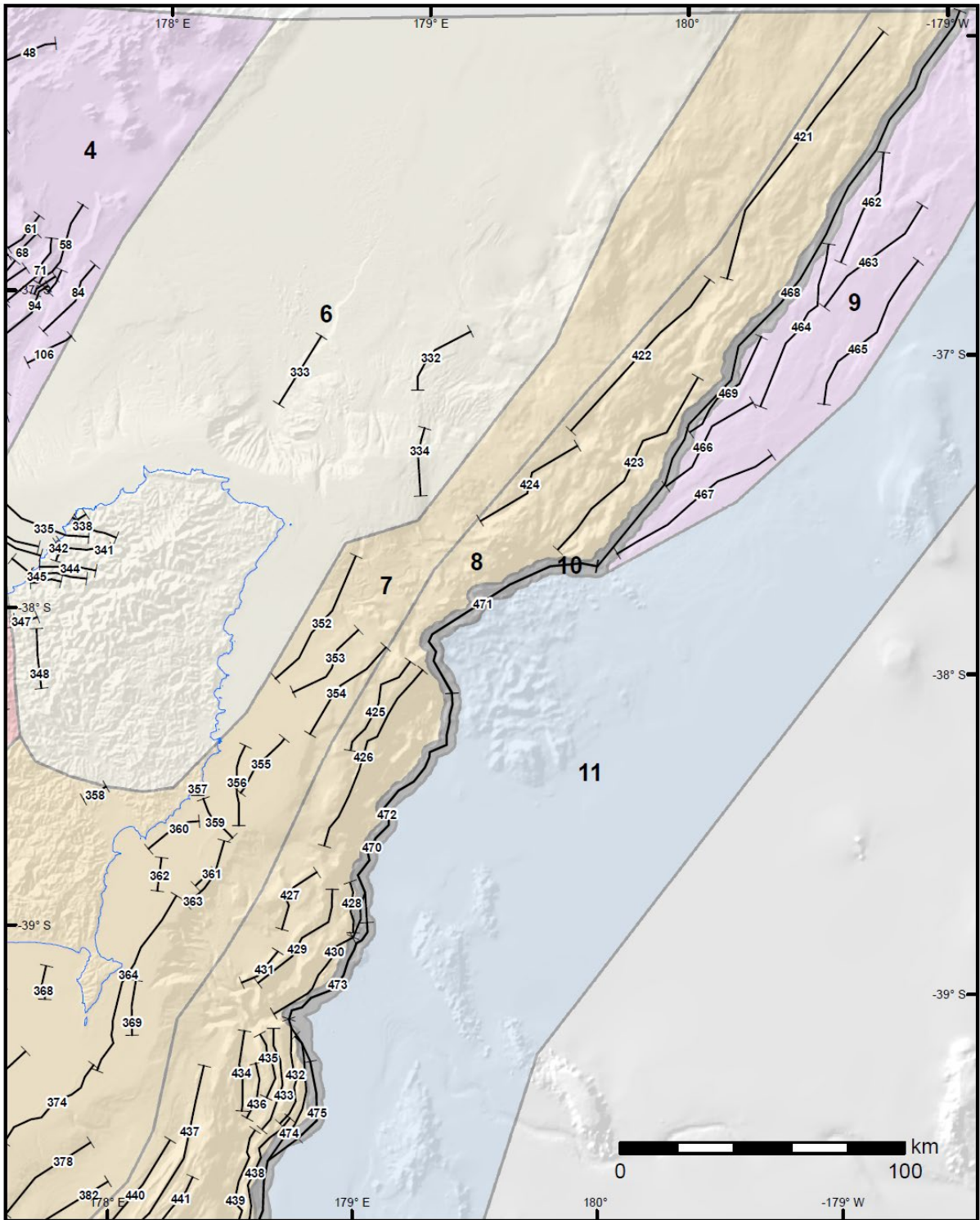


Figure A1.5 Northern Hikurangi and southern Kermadec margins. Fault ID (numbers with white outline) is shown for each fault or fault segment in NZ CFM v1.0. The extent of each fault or fault segment is shown by a marker line. Neotectonic domains (coloured polygons) in Figure 3.3 are shown for context. A description of the neotectonic domains (large bold numbers) is provided in Table 3.1.





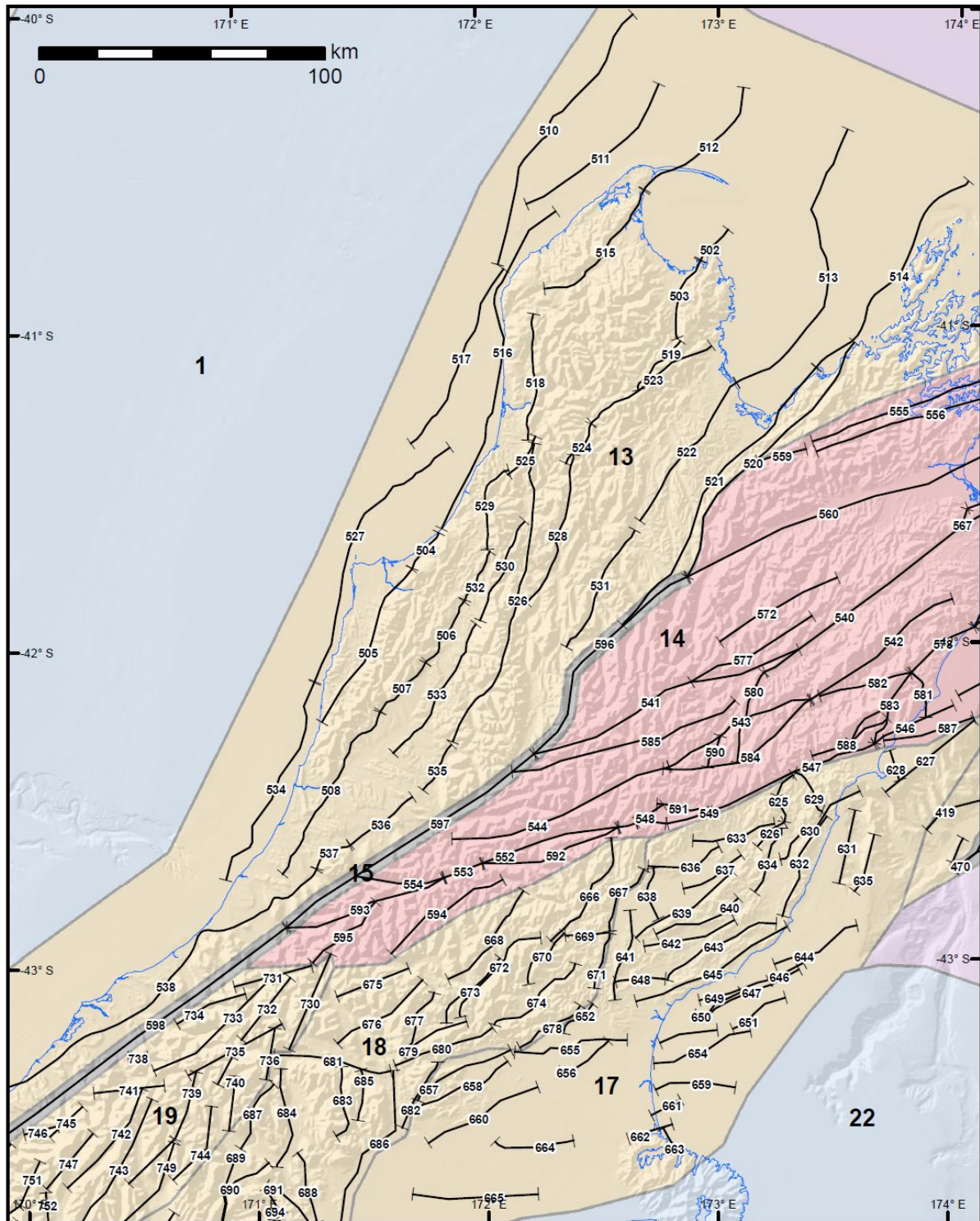


Figure A1.8 Western and central South Island. Fault ID (numbers with white outline) is shown for each fault or fault segment in NZ CFM v1.0. The extent of each fault or fault segment is shown by a marker line. Neotectonic domains (coloured polygons) in Figure 3.3 are shown for context. A description of the neotectonic domains (large bold numbers) is provided in Table 3.1.

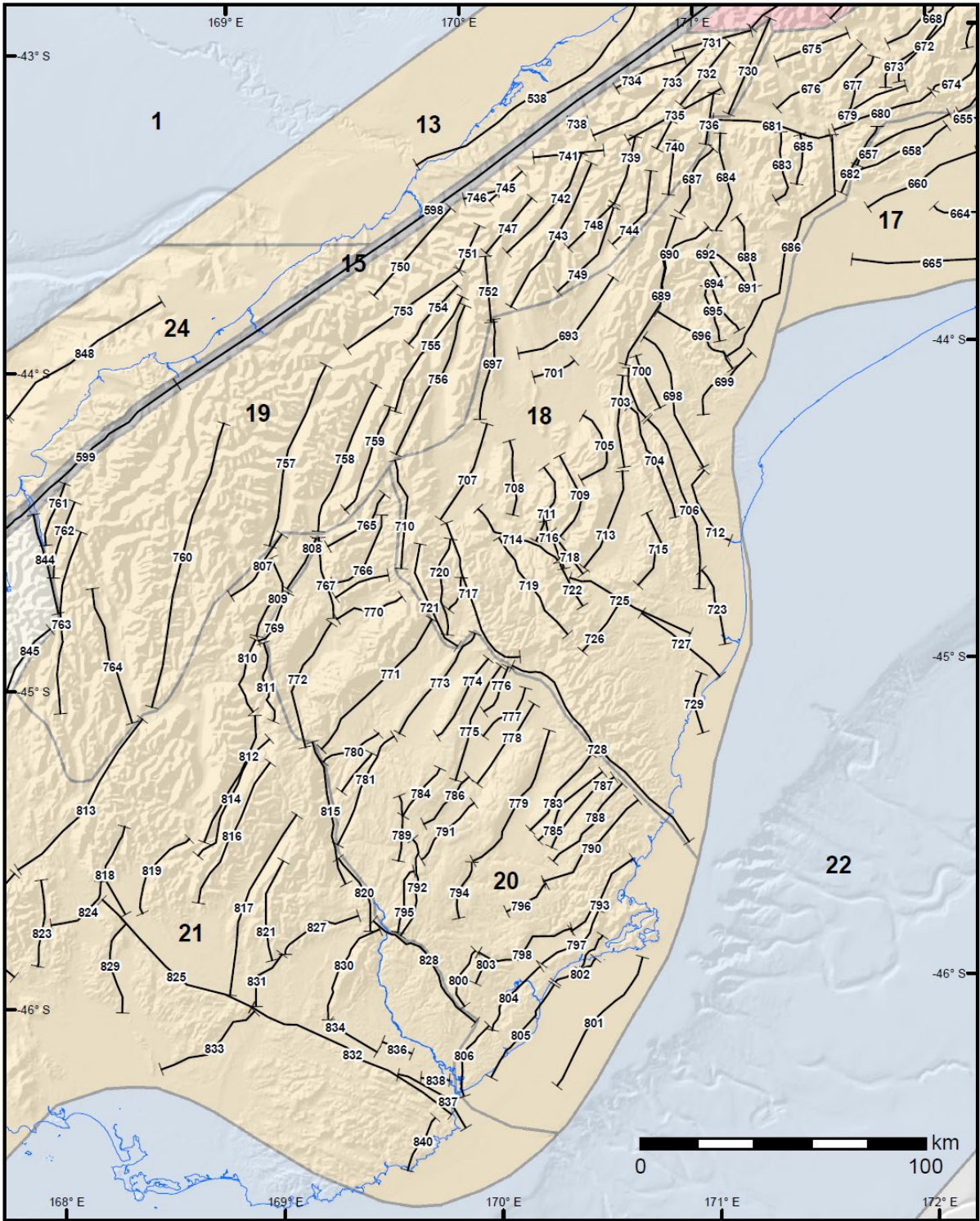


Figure A1.9 Southeastern South Island. Fault ID (numbers with white outline) is shown for each fault or fault segment in NZ CFM v1.0. The extent of each fault or fault segment is shown by a marker line. Neotectonic domains (coloured polygons) in Figure 3.3 are shown for context. A description of the neotectonic domains (large bold numbers) is provided in Table 3.1.

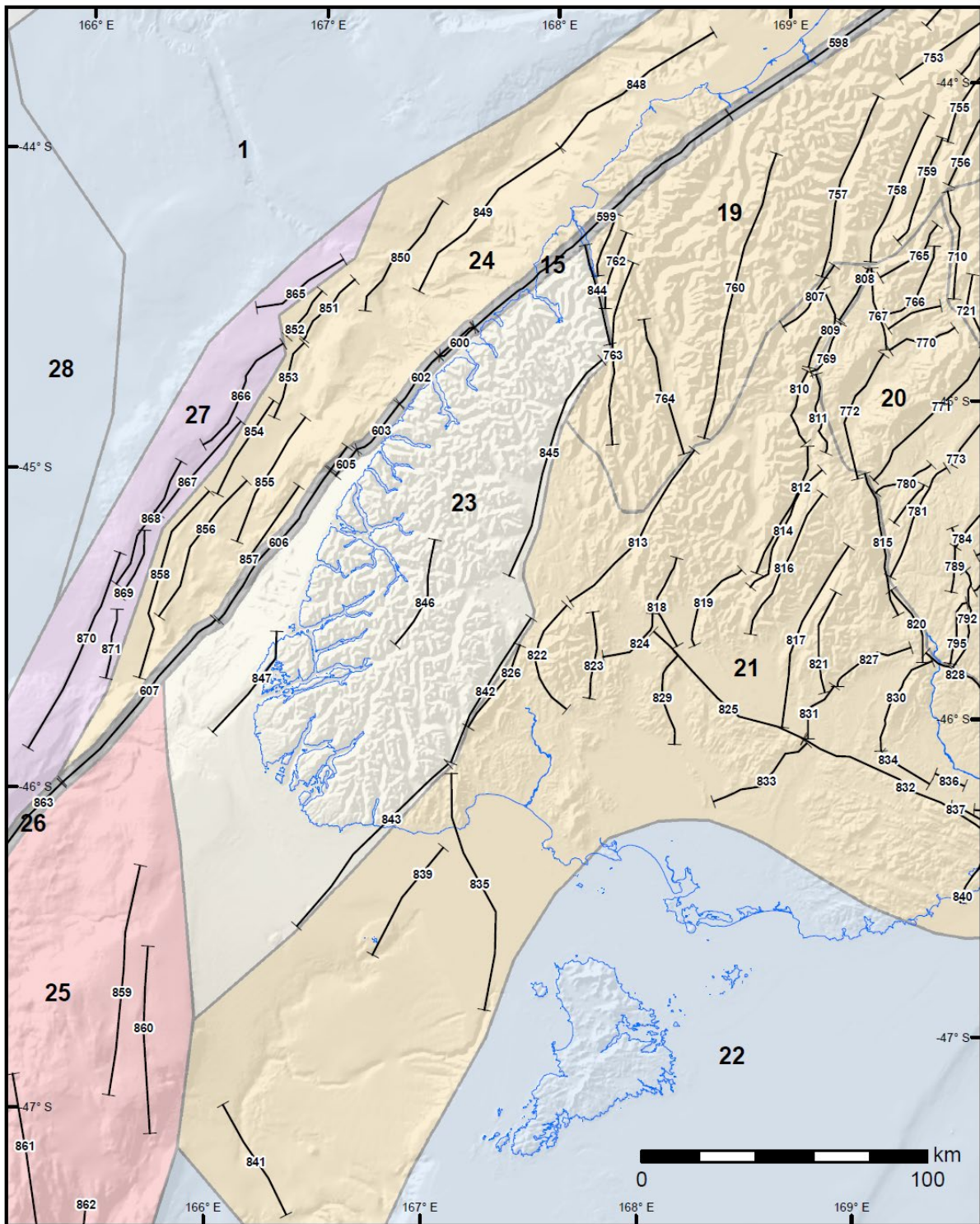


Figure A1.10 Fiordland margin and southern South Island. Fault ID (numbers with white outline) is shown for each fault or fault segment in NZ CFM v1.0. The extent of each fault or fault segment is shown by a marker line. Neotectonic domains (coloured polygons) in Figure 3.3 are shown for context. A description of the neotectonic domains (large bold numbers) is provided in Table 3.1.



## APPENDIX 2 GNS SCIENCE DATASET CATALOGUE METADATA RECORD

The following is an exported version of the metadata record relating to the New Zealand Community Fault Model held in GNS Science's Dataset Catalogue:

<http://data.gns.cri.nz/metadata>

### New Zealand Community Fault Model v1.0

The New Zealand Community Fault Model (NZ CFM) is a community-driven project led by GNS Science that pools the collective knowledge of the earth science community to develop a fault model for New Zealand that is open, updatable and publicly available.

NZ CFM v1.0 is a 2D and 3D geometrical representation of active and seismogenically capable fault zones. Each fault zone in the model is associated with available kinematic information such as sense of slip, slip-rake angle and slip rate, along with geometric parameters such as dip angle and depth of the fault plane.

Geologists and geophysicists from several organisations collaborated to define the model, including uncertainties and limitations, and ensure that it is fit-for-purpose for multiple needs. The NZ CFM and associated data are of value to a range of kinematic, active-fault and seismic-hazard studies.

DOI: <https://doi.org/10.21420/NMSX-WP67>

Cite as:

GNS Science. 2022. New Zealand Community Fault Model [dataset]. Lower Hutt (NZ): GNS Science.  
<https://doi.org/10.21420/NMSX-WP67>

### Download and Links

General web access to the Community Fault Model:

<https://www.gns.cri.nz/Home/Our-Science/Natural-Hazards-and-Risks/Earthquakes/Community-Fault-Model>

### About this Resource

Categories: Geoscientific information

Keywords: Active fault, Community Fault Model, New Zealand, sense of movement, dip, dip direction, rake, slip rate, kinematics, plate boundary, tectonic domain

Language: English

Classification: Unclassified

Legal constraints:

(C) Institute of Geological and Nuclear Sciences Limited.

This material is licensed under a Creative Commons Attribution International 4.0 (CC BY 4.0) Licence. For more details, visit <https://creativecommons.org/licenses/by/4.0/>. Where the data are used in a figure, GNS Science requests attribution in the following manner: (C) GNS Science.

Where reference to the data is to be included in a reference list, the following citation is suggested:

Seebeck H, Van Dissen RJ, Litchfield NJ, Barnes P, Nicol A, Langridge RM, Barrel DJA, Villamor P, Ellis SM, Rattenbury MS, et al. 2022. New Zealand Community Fault Model – version 1.0. Lower Hutt (NZ): GNS Science. 95 p. (GNS Science report; 2021/57). doi:10.21420/GA7S-BS61.

## Resource Constraints

The NZ CFM is owned by GNS Science and is based on the model explained in:

Seebeck H, Van Dissen RJ, Litchfield NJ, Barnes P, Nicol A, Langridge RM, Barrel DJA, Villamor P, Ellis SM, Rattenbury MS, et al. 2022. New Zealand Community Fault Model – version 1.0. Lower Hutt (NZ): GNS Science. 95 p. (GNS Science report; 2021/57). doi:10.21420/GA7S-BS61.

That report carries the following limitation, which also applies to this dataset:

*“The Institute of Geological and Nuclear Sciences Limited (GNS Science) and its funders give no warranties of any kind concerning the accuracy, completeness, timeliness or fitness for purpose of the contents of this report. GNS Science accepts no responsibility for any actions taken based on, or reliance placed on the contents of this report and GNS Science and its funders exclude to the full extent permitted by law liability for any loss, damage or expense, direct or indirect, and however caused, whether through negligence or otherwise, resulting from any person’s or organisation’s use of, or reliance on, the contents of this report.”*

Contact for the resource: GNS Science

Point of contact: [NZCFM\\_data@gns.cri.nz](mailto:NZCFM_data@gns.cri.nz)

Status: Ongoing

## Technical Information

Update frequency: [‘Not planned’, ‘As needed’]

Format: ESRI shapefile GOCAD ASCII (t-surf)

Lineage:

GNS Science has long maintained products such as the National Seismic Hazard Model’s active fault earthquake source model (Stirling et al. 2012); New Zealand Active Faults Database (Langridge et al. 2016), Active Fault Model of New Zealand (Litchfield et al. 2014) and national 1:1,000,000- and 1:250,000-scale digital geological maps, which provide a significant amount of basic fault information across onshore and offshore New Zealand. To date, however, a 3D model of active fault zones that represents New Zealand’s collective scientific knowledge that can be easily used or adapted for multiple scientific and practical uses has not been available.

The NZ CFM has been compiled as part of a multi-organisational project led by GNS Science. Important input data sources have been GNS Science’s New Zealand Active Faults Database (Langridge et al. 2016) and the 1:250,000 Geological Map of New Zealand (Heron 2020). Fault zone representations in NZ CFM v1.0 are defined by many types of constraints, including

surface traces (e.g. Langridge et al. 2016), earthquake focal mechanisms and hypocentre distributions (e.g. Williams et al. 2013), geodetic inversions (Beavan et al. 2011), seismic reflection profiles (e.g. Lamarche and Barnes 2005; Barnes and Ghisetti 2016; Seebeck et al. 2021), geologic cross-sections (e.g. Ghisetti et al. 2016b) and combinations thereof (Williams et al. 2013). NZ CFM v1.0 also builds on the 2D Active Fault Model of New Zealand (Litchfield et al. 2013, 2014) and updates that model as a 2D dataset through scientific community engagement and input. NZ CFM v1.0 also extends the updated fault zones from the surface to seismogenic depths using 3D modelling software. The 3D model NZ CFM dataset is a single, expert-led, explicit model representation of active and potentially seismogenic fault zones and does not yet incorporate alternative interpretations. The modelled fault zone surfaces are provided in GOCAD ACSII t-surf format in New Zealand Transverse Mercator projection. The NZ CFM project has developed 2D and 3D representations of important fault zones (primarily, but not exclusively, active fault zones) across New Zealand to support downstream applications such as seismic hazard and synthetic seismicity modelling.

### **Other Resources**

New Zealand Active Fault Model (associated resource).

### **Metadata Information**

Contact: GNS Science

Point of contact: [datamanagement@gns.cri.nz](mailto:datamanagement@gns.cri.nz)

Metadata language: English

Identifier: 9a074db9-a887-4dac-aef4-84eabaeda732

### APPENDIX 3 PUYSEGUR

The Puysegur Subduction Margin is associated with the highly oblique eastward subduction of Australian Plate oceanic crust beneath the continental crust of the Pacific Plate of the Solander Basin and southwestern South Island. Further to the south, subduction of oceanic Australian Plate occurs along the Puysegur Ridge: deformed oceanic crust of the Emerald Basin.

The geometry of the Puysegur Subduction Margin at depth is generally poorly constrained. The sparse data coverage along strike and down dip has resulted in a number of different plate interface geometries being published.

It is noted that outer-rise normal faults of the Caswell High indicate flexure of the incoming oceanic crust adjacent to Fiordland. This flexure of the Australian Plate may be related to the curvature of a continuous subducted plate to depths of 150 km or loading by overthrusting of the Pacific plate.

Lebrun et al. (2000) interpreted seismic reflection data and structural cross-sections that show the Alpine Fault truncating the down-going slab towards the north from the latitude of the southern-most Fiordland coastline.

Based on a catalogue of relocated earthquakes and focal mechanisms, Reyners et al. (2002) interpreted a 'ploughshare' geometry along the Fiordland section of the margin with smoothly curving plate from the deformation front to depth.

Wallace et al. (2007) show a continuous 'ploughshare' geometry with a more steeply dipping plate interface from the deformation front.

Hayes and Furlong (2010) use a global catalogue of relocated earthquakes and associated focal mechanisms to interpret a shallow-dipping slab along the Puysegur margin truncated by the Alpine Fault.

Hayes (2018) geometry differs significantly from Hayes and Furlong (2010) and is much more consistent with the more steeply dipping Reyners et al. (2002) plate interface. The Hayes (2018) plate interface does not extend to the western limit of the deformation front.

Stratford et al. (2020) present a preliminary seismic refraction line indicating a strong refraction from a shallow-dipping isovelocity surface beneath the Solander Basin. The geometry of the refractor is consistent with the location of the plate interface of Hayes and Furlong (2010).

Most recently, Shuck et al. (2021) present depth-converted seismic reflection lines indicating that the plate interface dips approximately 15–20° from the trench to depths of 20–25 km along the Puysegur margin.

To reconcile these different data sources and interpretations, sections presented in each of the above publications were georeferenced into ArcGIS and MOVE and displayed relative to plate interface surfaces interpretations (Wallace et al. 2007; Hayes and Furlong 2010; Hayes 2018), the faults of NZ CFM v1.0 and a relocated catalogue of earthquakes from Reyners et al. (2011). The Reyners et al. (2011) earthquake catalogue contains a subset of well-constrained GeoNet earthquakes from 2001 to 2010. As such, it provides little detail on the geometry of the slab along the Puysegur Subduction Margin due to the limited number of earthquakes of sufficient quality. Figure A3.1 shows the locations of sections used to reconcile the different plate interface interpretations.

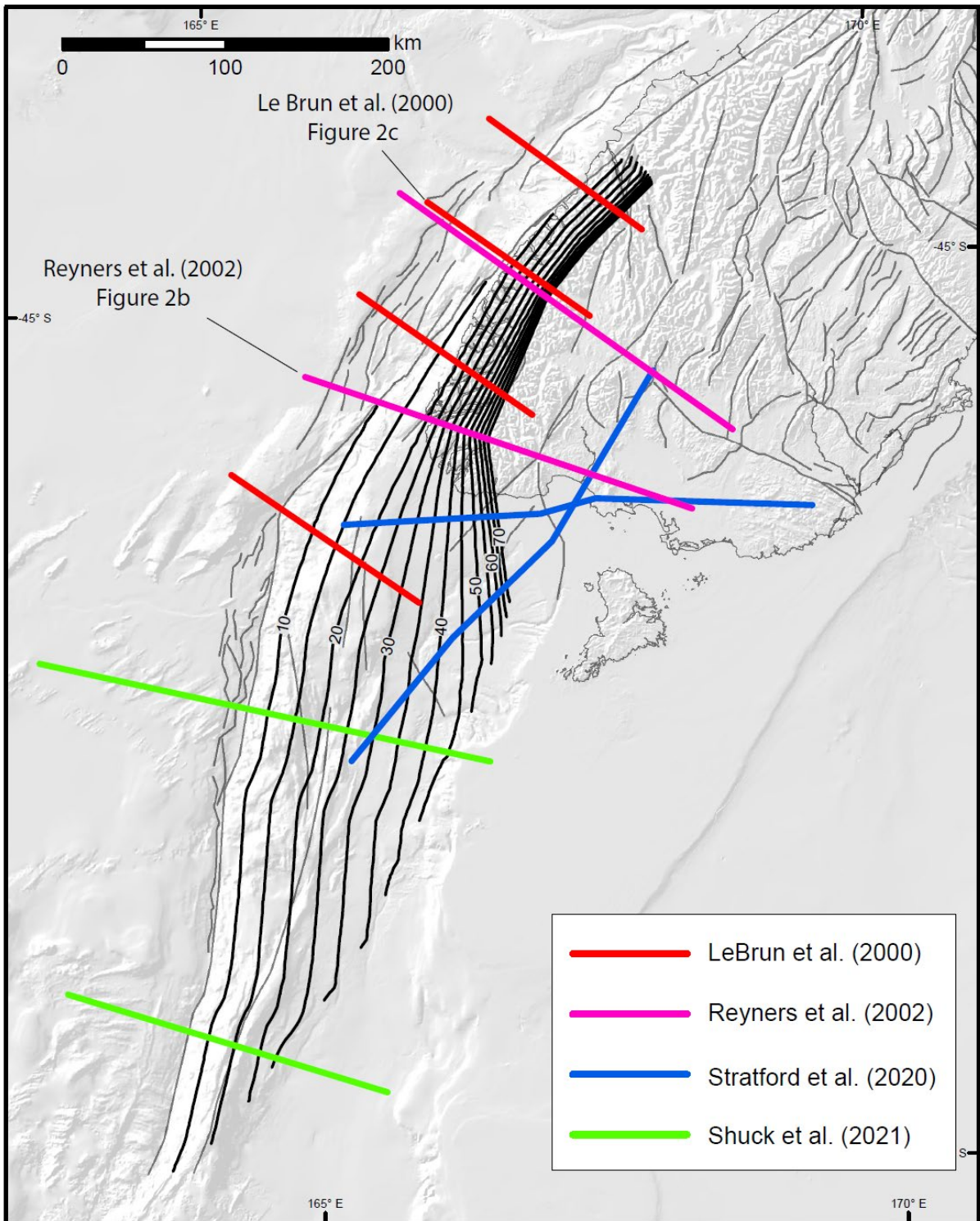


Figure A3.1 Puysegur Subduction Margin. Contours on the new plate interface geometry in 5 km intervals. Faults of NZ CFM v1.0 shown by grey lines.

Due to the similarities between the Hayes (2018) and Reyners et al. (2002) plate interface geometries beneath the Puysegur Subduction Margin, an interface surface geometry was generated that linked the two interpreted cross-sections of Reyners et al. (2002), effectively smoothing out perturbations in the Hayes (2018) surface. This surface was extended northwards beyond the limit of Hayes (2018) to the northern-most limit of deep intermediate depth seismicity observed in the Reyners et al. (2011) catalogue.

The geometry of the plate interface along the Puysegur Subduction Margin was constrained by the depth-converted seismic reflection profiles of Shuck et al. (2021) and the seismic refraction profiles of Stratford et al. (2020) to dip 17° to a depth of c. 50 km.

The geometry of the plate interface between the more steeply dipping northern section and shallow-dipping southern section of the margin was interpolated by hand to produce a continuous smoothly varying surface. The geometry between the contrasting dips of the northern and southern sections of the margin is largely unconstrained. Some earthquakes within the Reyners et al. (2011) catalogue are inconsistent with the modelled geometry. Further studies will be required to properly constrain the plate interface to depth along the Puysegur Subduction Margin. Figure A3.1 shows contours for the Puysegur subduction interface developed for this study.

Examining sections of Lebrun et al. (2000) offshore Fiordland with relocated earthquakes suggests that the Alpine Fault has significant influence on the geometry of the plate interface (Figure A3.2). As in previous studies, we adopt a subduction interface that is truncated by the Alpine Fault. To the west along the Fiordland margin, the subduction thrust is represented by shallow-dipping reverse Central and South Wedge faults.

While the interpretation of Reyners et al. (2002) and Hayes (2018) follow a smooth curve with dips increasing with depth, sections show that a more planar shallow geometry, such as the Wallace et al. (2007) model, may be more appropriate along the Fiordland section of the margin.

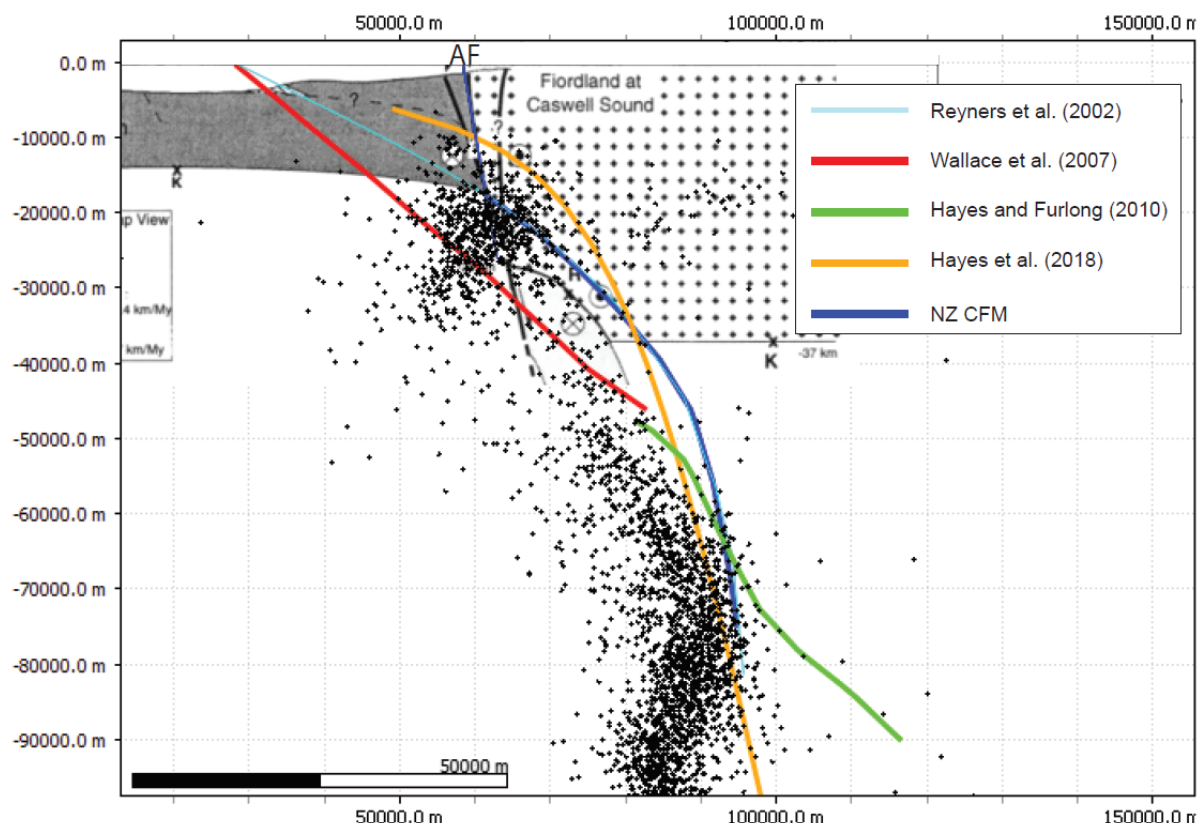


Figure A3.2 Northern Fiordland margin cross-section. Cross-section through the Fiordland margin collocated with Figure 2c of Lebrun et al. (2000; background image). The intersection of 3D plate interface surfaces with the cross-section is shown by coloured lines. Relocated earthquakes (small black crosses) within 20 km are projected onto plane of section. Reverse faults of the NZ CFM (not shown here) west of the Alpine Fault (AF) will represent the plate interface, while a surface east of the Alpine Fault is continuous towards the south and the Puysegur margin.

To the south, a section through Reyners et al. (2002; Figure A3.3) highlights the sparse relocated earthquake coverage in this region. The conformance between Hayes (2018) and Reyners et al. (2002) is noted between 30 and 90 km. In both Figure A3.2 and Figure A3.3, the Hayes and Furlong (2010) plate interface geometry does not conform well to the relocated earthquakes of Reyners et al. (2011) in these locations.

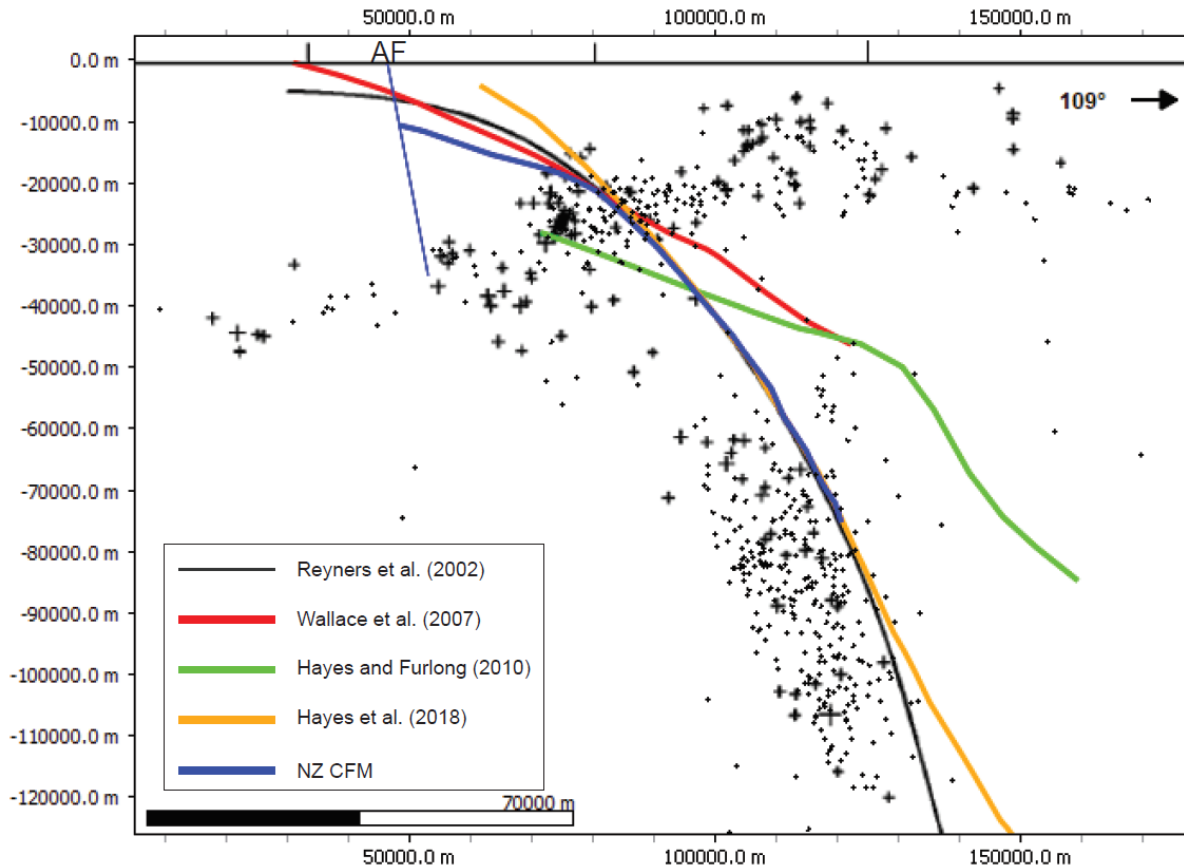


Figure A3.3 Southern Fiordland margin cross-section. Cross-section through the Fiordland margin collocated with Figure 2b of Reyners et al. (2002; background image). The intersection of 3D plate interface surfaces with the cross-section is shown by coloured lines. Relocated earthquakes (small black crosses) within 20 km are projected onto plane of section. Earthquakes from the original study shown by larger black crosses.

An alternative representation of the Puysegur subduction interface is also included that considers the plate interface as a continuous surface extending to the west along the Fiordland region. This interface geometry, named Puysegur–Fiordland, is similar to that presented by Wallace et al. (2007). In this Puysegur–Fiordland subduction interface, surface will cross-cut the Alpine Fault, resulting in a shallowing of its maximum down-dip depth towards the south, where the subduction interface shallows to 6 km depth. Users should carefully consider the implication of using either Puysegur subduction interface interpretation for their downstream application.

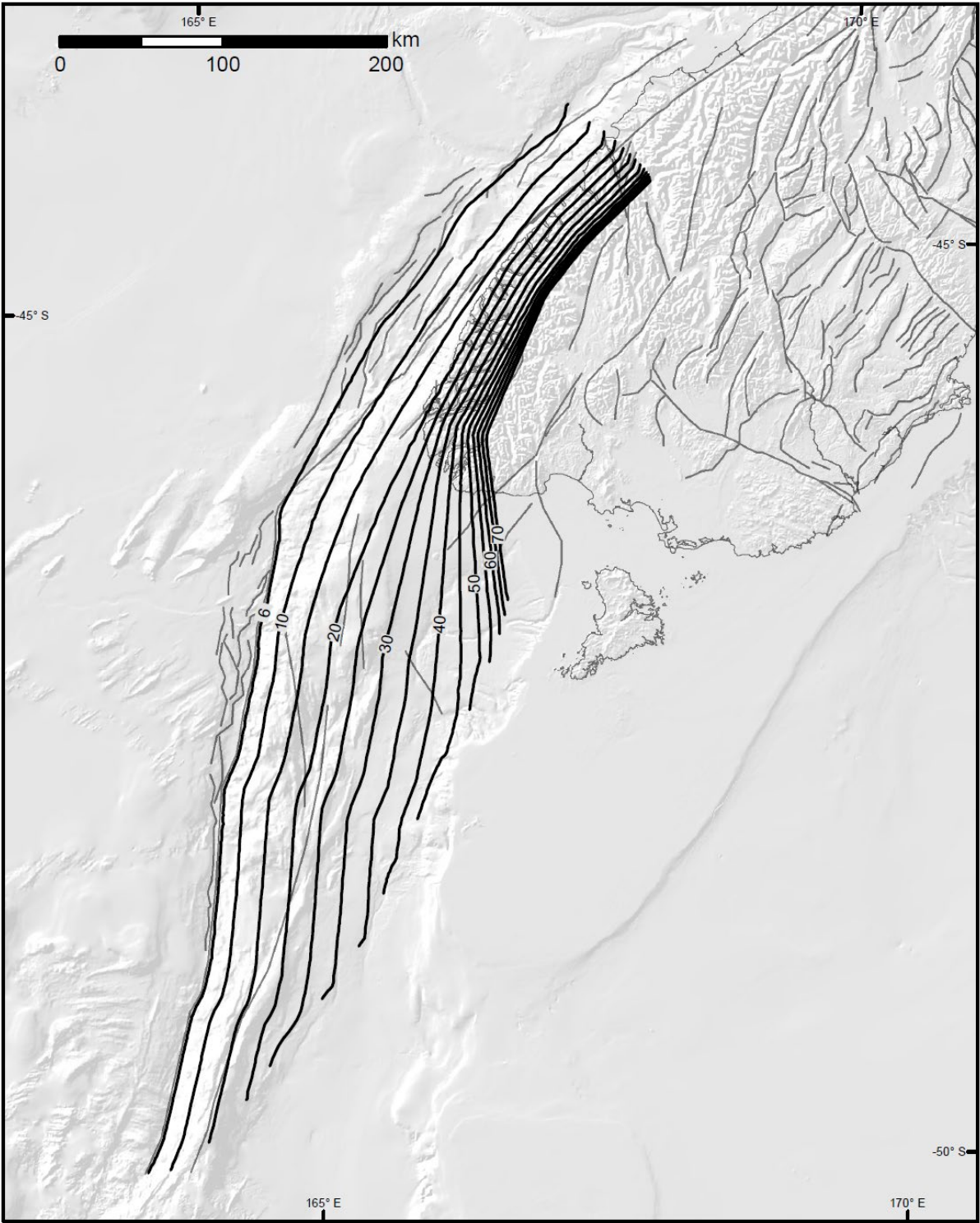


Figure A3.4 Alternative Puysegur–Fiordland subduction interface surface.



[www.gns.cri.nz](http://www.gns.cri.nz)

#### Principal Location

1 Fairway Drive, Avalon  
Lower Hutt 5010  
PO Box 30368  
Lower Hutt 5040  
New Zealand  
T +64-4-570 1444  
F +64-4-570 4600

#### Other Locations

Dunedin Research Centre  
764 Cumberland Street  
Private Bag 1930  
Dunedin 9054  
New Zealand  
T +64-3-477 4050  
F +64-3-477 5232

Wairakei Research Centre  
114 Karetoto Road  
Private Bag 2000  
Taupo 3352  
New Zealand  
T +64-7-374 8211  
F +64-7-374 8199

National Isotope Centre  
30 Gracefield Road  
PO Box 30368  
Lower Hutt 5040  
New Zealand  
T +64-4-570 1444  
F +64-4-570 4657